2009

Peptide Targeting of Platinum Anti-Cancer Drug and Synthesis of Water Soluble Monofunctional Pt(II) Complexes Useful for Biological Labeling

Margaret W. Ndinguri
Louisiana State University and Agricultural and Mechanical College

PEPTIDE TARGETING OF PLATINUM ANTI-CANCER DRUG AND SYNTHESIS OF WATER SOLUBLE MONOFUNCTIONAL Pt (II) COMPLEXES USEFUL FOR BIOLOGICAL LABELING

A Dissertation
Submitted to the Graduate Faculty of the
Louisiana State University and
Agricultural and Mechanical College
in partial fulfillment of the
requirements for the degree of
Doctor of Philosophy

in

The Department of Chemistry.

By
Margaret W. Ndinguri
B. S., Jomo Kenyatta University of Agriculture and Technology, 2001
August, 2009

DEDICATION

To my parents Simon and Phyllis Ndinguri, my husband Anthony Ndirangu and children Chealsea and Chris Gachagua

ACKNOWLEDGEMENTS

I wish to express my gratitude to the following people who have been instrumental in the completion of this work.

I thank the almighty **God** for his faithfulness, mercy and grace. I have drawn strength and inspiration from Psalms 23

My advisor, **Dr. Robert Hammer** for his mentorship advice, patience and support through out this project. He made my research experience challenging and rewarding.

Committee members **Dr. William Crowe, Dr. Brian Hales, Dr. Bin Chen**, and external representative **Dr. Inder Sehgal**.

Dr. Sita Aggarwal from Pennington Biomedical Research Institute, **Martha Juban** of protein facility and **Dr. Azeem Hasaan** of mass spectrometry for their help in their respective facilities.

Dr. Isaah Warner, Dr. Alfonso Davila, Dr. Steve Watkins and **Sheridan Wilkes** for their special help and guidance whenever I was in need. You were God sent to me in times of need and I will always be grateful for your kind deeds.

Dr. Hammer's group for their support and friendship. Special thanks to **Cyrus** and **Marcus**.

My mother **Phyllis Ndinguri** and father **Simon Ndinguri** for their unconditional love, confidence in me, prayers, encouragement, and unwavering support during my years of study. To you I will always be indebted.

My mother in law **Virginia Ndirangu** and my mom for the great help in taking care of the little ones Chealsea and Chris while I was in school. Your love and support are priceless.

To my sibling, **Elizabeth Ndinguri, Monicah Ndinguri, Leah Ndinguri**, and **Erastus Ndinguri** for their words of encouragement.

Last but not least, an immeasurable amount of gratitude to my husband, **Anthony Ndirangu** for his love, sacrifice and constant support. My children **Chealsea** and **Chris Gachagua**, who are two bundles of joy, that give me a reason to live and to forget my worries. They are the best thing that happened to me in graduate school!

To all my friends and relatives who have supported me all the way. Thank you!

TABLE OF CONTENTS

LIST OF ABBREVIATIONS

Atfcdien	*N*′-[7-(acetamido)-4-(trifluoromethyl)coumarin] diethylenetriamine
acdien	2-(bis(2-aminoethyl)amino)acetic acid
atfc	7-amino-4-(trifluoromethyl)coumarin
Arg	arginine
Asn	asparagine
Acm	acetamidomethyl
$AgNO_3$	silver nitrate
Bocdien	*N*,*N*″-bis(tert-butyloxycarbonyl)diethylenetriamine
Bocdienatfc	*N*,*N*″-bis(tert-butyloxycarbonyl)diethylenetriaminly-N′-[7-(acetamido)-4-(trifluoromethyl)coumarin]
Bocdienac	*N*,*N*″-bis(tert-butyloxycarbonyl)diethylenetriaminly-N′-glycine
Cys	cysteine
Dien	diethyltriamine
DBU	1,8-diazobicyclo[4.50] undec-7-ene
DIPEA	diisopropylethylamine
DMF	dimethylformamide

Et_2O	diethyl ether
EtOH	ethanol
Fmoc	9-fluorenylmethoxycarbonyl
Gly	glycine
HPLC	high performance liquid chromatography
NaH	sodium hydride
NMR	nuclear magnetic resonance
Pbf	2,2,4,6,7-pentamethyldihydrobenzofuran-5-sulfonyl
mPEG	oligoethylene glycol group
PYAOP	7-azabenzotriazolyoxytris(pyrrolidino) phosphonium hexafluorophosphate.
TFA	trifluoroacetic acid
THF	tetrahydrofuran
Trt	trityl
m	multiplet
MALDI	matrix assisted laser desorption ionization
min	minute
µM	micromolar

mM	millimolar
mmol	millimole
MTT	3-(4,5-dimethylthiazol-2-yl)-2,5-diphenyltetrazolium bromide
NaOH	sodium hydroxide
NMR	nuclear magnetic resonance
MeCN	acetonitile
PDT	photodynamic therapy
Pip	piperidine
PyAOP	7-azabenzotriazol-1-yloxy)tripyrrolidinophosphonium hexafluorophosphate
TIPS	triisopropylsilane
TMS	tetramethylsilane

ABSTRACT

Platinum has been used as an inorganic medicinal agent with various applications such as anti cancer agents. Several new targeted Pt(II) conjugates were synthesized having the NGR and LHRH targeting motif. The platinum conjugates bearing the NGR motif revealed selective delivery and destruction of cancer cells that had CD13 receptors compared to untargeted carboplatin drug. The development of targeted chemotherapeutic has opened a new approach for efficient delivery of antitumor toxins with minimal exposure to normal cells. Several peptide sequences are known to have the ability to target tumors, for instance NGR motif which home specifically in solid tumors and has receptors aminopeptidase N (APN), also referred to as CD13 which binds specifically to NGR peptides. Luteinizing hormone-releasing hormone (LHRH), another targeting moiety, has been found to be more prevalent in tumor cells than normal cells and has receptors. LHRH sequence was used in the synthesis of targeted curcumin, phthalocyanine and platinum conjugate.

Another set of platinum complexes synthesized are monofuctional platinum (II) complexes. The monofuctional platinum complexes are useful in understanding the chemistry of cisplatin which is bifunctional and forms various adducts on interaction with DNA which are not well understood. To monitor and understand the interaction of nucleotide with platinum complexes, complexes with only one reactive sight were synthesized. The tridentate ligands were characterized by X-ray crystallography, fluorescence and NMR spectroscopy. Interaction of platinum complexes and nucleotide (5′-GMP) was monitored by NMR to reveal different rate of rotation about the Pt–N(7) bond depending on the platinum complex studied. These new complexes have desirable features for assessing the potential of tridentate platinum complexes for investigating selective monocoordination of metal complexes to DNA and peptides.

CHAPTER 1. INTRODUCTION

Cancer is a disease where a group of cells divide beyond the normal limits. From American Cancer Society, cancer statistics in 2008 revealed that cancer is the second highest cause of death exceeded only by heart diseases. Various organic and inorganic compounds have been found to have anticancer activity. Platinum (II) complexes are examples of inorganic compounds that are know to have anti- tumor effects. These compounds are known to have severe side effects and establishing a way to reduce the side effect, understanding and improve the drug efficacy of some of these drugs has been partially addressed in this work.

1.1 Platinum Complexes

A number of platinum containing drugs have been extensively studied with cisplatin having remarkable activity against mutants. Cisplatin (Figure 1.1) is used to treat a various cancers, such as lung, neck, head, and bladder.[1, 2] The drug is administered to patient intravenously in sterile brine solution which helps to reduce hydrolysis and retain the cisplatin intact due to high concentration of chloride ions. Once the neutral cisplatin enters the cell, it undergoes hydrolysis and the chloro ligands are displaced by water forming positively charged species. This is made possible by the low concentration of chloride ions in the cell. Cisplatin has various possible targets in the cell, with include DNA, RNA, enzymes and mitochondria.[3, 4] The effects of cisplatin on RNA and DNA have been extensively studied and established that the main target is N7 atom of purines.[5-7] Once bound to the purines, it affects the replication and transcription of DNA leading to eventual cell death.

Carboplatin, an analogue of cisplatin, has been approved by the FDA mainly for the treatment of cancer. It has been reported that both cisplatin and carboplatin (Figure 1.1) have similar effects against lung and ovarian tumors with the formation of identical adducts with

DNA. However, lower toxicity was noted for carboplatin and was attributed to the presence of bidentate ligands which slow down the hydrolysis of carboplatin into potential damaging species.[8] In addition to lower toxicity, carboplatin have been shown to work against cisplatin resistant malignant.

Cis-diamminedichlorido platinum (II)(cisplatin)

Dichloro(ethylenediamine) platinum (II) (Pten)

Cis- diammine(1,1-cyclobutanedicarboxylato)platinum (Carboplatin)

Figure 1.1. Platinum complexes used in this work.

Dichloro(ethylenediamine)platinum(II) (Pten) is a known derivative of platinum that has the amine group tethered by an ethylene group. The Pten complex has been shown to be biologically active against cancer cells.[9, 10] Clinical studies on a closely related analogue, such as ethylenediamino malonate platinum II revealed nephrotoxicity coupled with low potency lead to the discontinuation of it clinical studies.[1, 11, 12]

1.2 Curcumin

Curcumin is a polyphenol; found naturally in the perennial herb Curcuma Longa also known as Turmeric. The curcuminoids which are yellow in color have three major components, which include cyclocurcumin (77%), demethoxycurcumin(17%) and bisdemethoxycurcumin(3%).[11, 13] The curcuminoid complex is also known as yellow ginger and is mainly grown in Asia. Curcumin can exist in enol form or di-keto form, with enol form being prevalent in solution stemming an important feature on radiacal-scavanging ability of curcumin. Curcumin has traditionally been used in food additives/ food flavoring example, Provide curry spices with distinctive yellow color and flavor, used in coloring of cheese and butter. It has also

been used as a therapeutic for conditions like respiratory condition, diabetic wounds cough, running nose, abdominal pain among others with modern scientific research confirming its effects as an anti-inflammatory, antitumor, antimicrobial, antioxidant and antiarthritic. No studies have shown any toxicity associated with curcumin irrespective of the concentration.[14]

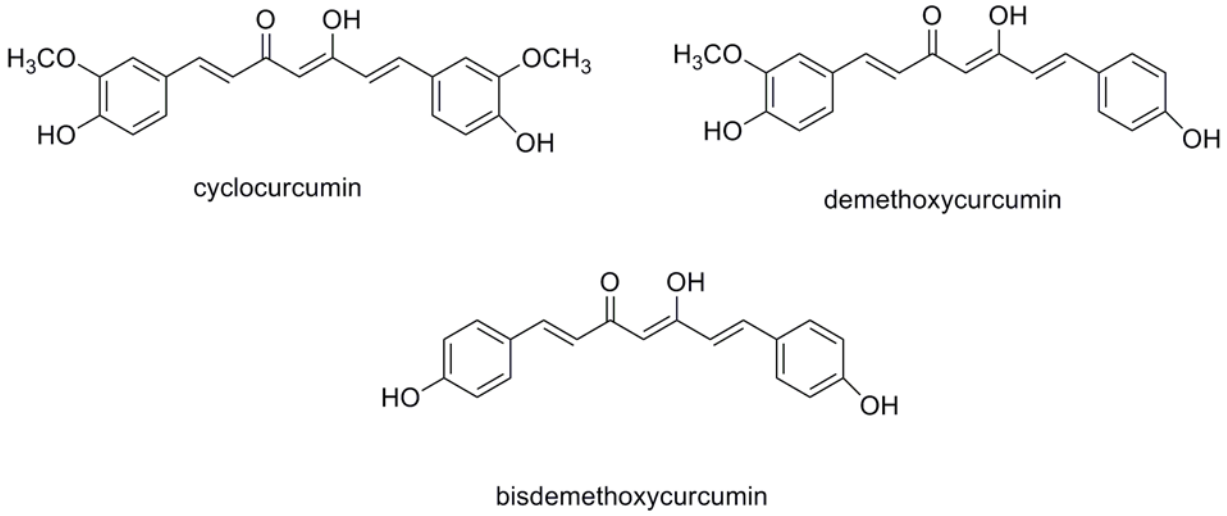

Figure 1.2 Structure of various forms of curcumin.

1.3 Polyamine Analogues

The polyamines are organic compounds having two or more primary amine groups. Examples include ethylenediamine and diethylenetriamine. Chelation of a polyamine to platinum has been shown to form small molecules that have anti-tumor activity.[15, 16] Polyamines play a key role in growth factor for normal and tumor cells. If cellular polyamine synthesis is inhibited, cell growth is stopped or severely retarded. In tumor cells the concentration of polyamines is elevated significantly than the surrounding normal tissues. Polyamines analogues have been proposed as alternative ways which polyamine metabolism in tumor cells can be blocked.[17, 18] Structure-activity studies of polyamine analogues reveal that slight structure alteration causes remarkable changes in their biological activity. *N*-alkylated polyamines have been found to alter the

neoplastic activity in various human tumor lines. Once the polyamine analogues have been administered it is thought to deplete polyamines by various mechanisms which include, compete for uptake, inducing catabolic enzymes and inhibit biosynthesis.[19, 20]

1.4 Targeted Chemotherapeutic Agents

There are various methods of targeting chemotherapeutics which include small molecules, hormones, antibody and peptides.[21-23] One common modern approach that is being used to increase the efficacy of chemotherapeutics is peptide targeting. The main aim of this area is to develop drug vectors capable of targeting tumor cells by specific recognition mechanism for selective destruction of malignant tissues. Tumor cell contain peptide receptors that are expressed in higher concentration than normal cell, example; intergrin αvβ3, αvβ5 and aminopeptidase N (APN/CD13) markers have been demonstrated to home in solid tumors with the aid of phage display libraries.[24] Two peptide sequences Asn-Gly-Arg (NGR) and Arg-Gly-Asp (RGD) were identified as potential cytotoxic warheads that could deliver selectively to tumor cells.

Another example of targeting sequence is LHRH peptide which has receptor expressed primarily on the cancerous cells. LHRH is a hormonal decapeptide produced by the hypothalamus, which plays a pivotal role in the regulation of the reproduction and pituitary gland. Receptors for LHRH were found primarily on human breast cancer, human ovarian and human prostate cancer. With the receptors not being expressed in normal cells, this also serves as a great warhead that can be used to deliver antineoplastic agent to the specific tumor target. A conjugate of LHRH- DOX was found to be more potent than DOX with reduced toxicity on normal cells.[25, 26]

The specificity of this cisplatin can be enhanced by efficient delivery of the drug and it's analogues to the nucleus of the cancer cells. In this study we present novel targeted peptide conjugates of platinum(II) and curcumin conjugates to investigate their toxicity effect on tumor

cells. Recent results on synthesis, characterization, purification, toxicity, selective localization and cell uptake studies of targeted peptide conjugates will be discussed in following chapters.

1.5 References

1. Jamieson, E., R; Lippard, S., J, Structure, Recognition, and Processing of Cisplatin-DNA Adducts. *Chemical Reviews (Washington, DC, United States)* **1999,** 99, 2467-2498.

2. Lippert, B., Multiplicity of metal ion binding patterns to nucleobases. *Coordination Chemistry Reviews* **2000,** 200-202, 487-516.

3. Fuertes, M. A.; Alonso, C.; Perez, J. M., Biochemical Modulation of Cisplatin Mechanisms of Action: Enhancement of Antitumor Activity and Circumvention of Drug Resistance. *Chemical Reviews (Washington, DC, United States)* **2003,** 103, (3), 645-662.

4. Soldatovic, T.; Bugarcic, Z., Study of the reactions between platinum(II) complexes and L-methionine in the presence and absence of 5'-GMP. *Journal of Inorganic Biochemistry* **2005,** 99, 1472–1479.

5. Reedijk, J., Why Does Cisplatin Reach Guanine-N7 with Competing S-Donor Ligands Available in the Cell? *Chemical Reviews (Washington, D. C.)* **1999,** 99, (9), 2499-2510.

6. Natile, G.; Marzilli, G. L., Non-covalent interactions in adducts of platinum drugs with nucleobases in nucleotides and DNA as revealed by using chiral substrates. *Coordination Chemistry Reviews* **2006,** 250, 1315-1331.

7. Eastman, A., Reevaluation of Interaction of cis-Dichloro(ethylenediamine)platinum(11) with DNA^{+}. *Biochemistry* **1986,** 25, 3912-3915.

8. Hamelers, I. H. L.; van Loenen, E.; Staffhorst, R. W. H. M.; de Kruijff, B.; de Kroon, A. I. P. M., Carboplatin nanocapsules: a highly cytotoxic, phospholipid-based formulation of carboplatin *Molecular Cancer Therapeutics* **2006,** 5, (8), 2007-2012.

9. Wirth, W.; Blotevogel-Baltronat, J.; Kleinkes, U.; Sheldrick, W. S., Interaction of (amine)M(II) complexes (amine=/dien, en; M=/Pd, Pt) with purine nucleoside 2'-, 3'- and 5'-monophosphates*/the role of the phosphate site for specific metal fragment-/nucleotide recognition by macrochelation. *Inorganica Chimica Acta* **2002,** 339.

10. Kevin, B. J.; J.Christoper, B.; Djuran I, M.; Mazid A, M.; Rau, T.; Sadler J, P., Outer-sphere macrochelation in [Pd(en)5'-GMP-N7)2].9H20 and [Pt(en)(5'-GMP-N7)2]..9H2O: X-ray crystallography and NMR Spectroscopy in solution. *Inorganic Chemistry* **1995**, (34), 2826-2832.

11. Lebwohl, D.; Canett, R., Clinical development of platinum complexes in cancer therapy: an historical perspective and an update. *European Journal of Cancer* **1998,** 34, (10), 1522-1534.

12. Sundquist, W. I.; Lippard, S. J.; Stollar, B. D., Monoclonal antibodies to DNA modified with cis- or trans-diamminedichloroplatinum(II). *Proceedings of the National Academy of Sciences of the United States of America* **1987,** 84, (23), 8225-9.

13. O'Connell, M. A.; Rushworth, S. A., Curcumin: potential for hepatic fibrosis therapy? *British Journal of Pharmacology* **2008,** 153, (3), 403-405.

14. Aggarwal, S.; Ichikawa, H.; Takada, Y.; Sandur, S. K.; Shishodia, S.; Aggarwal, B. B., Curcumin (Diferuloylmethane) Down-Regulates Expression of Cell Proliferation and Antiapoptotic and Metastatic Gene Products through Suppression of I{kappa}B{alpha} Kinase and Akt Activation. *Molecular Pharmacology* **2006,** 69, (1), 195-206.

15. Carlone, M.; Fanizzi, F. P.; Intini, F. P.; Margiotta, N.; Marzilli, L. G.; Natile, G., Influence of Carrier Ligand NH Hydrogen Bonding to the O6 and Phosphate Group of Guanine Nucleotides in Platinum Complexes with a Single Guanine Ligand. *Inorganic Chemistry* **2000,** 39, (4), 634-641.

16. Carlone, M.; Marzilli, L. G.; Natile, G., Platinum Complexes with NH Groups on the Carrier Ligand and with Only One Guanine or Hypoxanthine Derivative. Informative Models for Assessing Relative Nucleobase and Nucleotide Hydrogen-Bond Interactions with Amine Ligands in Solution. *Inorganic Chemistry* **2004,** 43, (2), 584-592.

17. Gilmour, S. K., Polyamines and nonmelanoma skin cancer. *Toxicology and Applied Pharmacology* **2007,** 224, (3), 249-256.

18. Wallace, H. M.; Niiranen, K., Polyamine analogues - an update. *Amino Acids* **2007,** 33, (2), 261-265.

19. Bergeron, R. J.; Huang, G.; McManis, S. J.; Yao, H.; Nguyen, J. N., Synthesis and Biological Evaluation of Aminopolyamines. *Journal of Medicinal Chemistry* **2005,** 48, 3099-3102.

20. Bernacki, R. J.; Bergeron, R. J.; Porter, C., Antitumor Activity of N,N'-Bis(ethyl)spermine Homologues against Human MALME-3 Melanoma Xenografts. *Cancer Research* **1992,** 52, 2424-2430.

21. van Zutphen, S.; Reedijk, J., Targeting platinum anti-tumour drugs: Overview of strategies employed to reduce systemic toxicity. *Coordination Chemistry Reviews* **2005,** 249, (24), 2845-2853.

22. Mukhopadhyay, S.; Barnes, C. M.; Haskel, A.; Short, S. M.; Barnes, K. R.; Lippard, S. J., Conjugated Platinum(IV)-Peptide Complexes for Targeting Angiogenic Tumor Vasculature. *Bioconjugate Chemistry* **2008,** 19, (1), 39-49.

23. Taquet, J.-p.; Frochot, C.; Manneville, V.; Barberi-Heyob, M., Phthalocyanines covalently bound to biomolecules for a targeted photodynamic therapy. *Current Medicinal Chemistry* **2007,** 14, (15), 1673-1687.

24. Zhang, Z.; Hatta, H.; Tanabe, K.; Nishimoto, S.-i., A New Class of 5-Fluoro-2'-deoxyuridine Prodrugs Conjugated with a Tumor-Homing Cyclic Peptide CNGRC by Ester Linkers: Synthesis, Reactivity, and Tumor-Cell-Selective Cytotoxicity. *Pharmaceutical Research* **2005,** 22, (3), 381-389.

25. Hansel, W.; Leuschner, C.; Enright, F., Conjugates of lytic peptides and LHRH or [beta]CG target and cause necrosis of prostate cancers and metastases. *Molecular and Cellular Endocrinology* **2007,** 269, (1-2), 26-33.

26. Nagy, A.; Schally, A. V., Targeting of cytotoxic luteinizing hormone-releasing hormone analogs to breast, ovarian, endometrial, and prostate cancers. *Biology of Reproduction* **2005,** 73, (5), 851-859.

CHAPTER 2. PEPTIDE TARGETING OF PLATINUM ANTI-CANCER DRUGS

2.1 Introduction

Platinum compounds are widely used in cancer chemotherapy.[1, 2] Cisplatin, like many anti-tumor drugs is an FDA-approved drug that is widely used for treatment of many types of cancers including lung, ovarian, head and neck cancer.[3, 4] Carboplatin, an analogue of cisplatin is used more because it has decreased non-specific toxicity and is active against cisplatin-resistant tumors.[2, 5-9] Both carboplatin and cisplatin have been shown to form similar adducts with DNA by the formation of covalent bonds with N7 purines. This results in interference with normal transcription and DNA replication mechanisms, leading to eventual cell death. While these drugs are effective, they have very serious side effects that include nephrotoxicity, myelotoxicity, neurotoxicity, vomiting and nausea.[10] Certain cancers can also develop resistance to drugs like cisplatin via efflux pumps as reported by Katano *et al.*[11, 12]

One method to make toxic drugs more effective is by altering their target-specific delivery. A number of peptide sequences are capable of mediating the delivery of therapeutic or imaging drugs.[13, 14] Recently, a doxorubicin (DOX)-peptide conjugate was shown to deliver DOX to cancerous cells more effectively than free DOX. Specifically, this has been reported for Asn-Gly-Arg (NGR) and Arg-Gly-Asp (RGD) peptides, which showed improved therapeutic effectiveness in a breast carcinoma mouse model.[15, 16] These DOX-peptide conjugates (DOX-RGD and DOX-NGR) also showed reduced toxicity to the liver and heart and caused specific vascular damage near the tumors. Therefore, DOX-peptide conjugate-treated animals had increased life expectancies relative to animals treated with DOX alone.[17] Similar studies using a conjugate of 5-fluoro-2'-deoxyuridine (5-FdUrd) and the NGR motif on the breast cancer cell line MDA-MB-231 and human fibrosarcoma HT-1080 revealed the selective accumulation of

conjugate in tumor cells that had CD 13 receptors. The 5-FdUrd-NGR motif also exhibited lower toxicity to normal cells compared to free 5-FdUrd.[18] In another study, luteinizing hormone releasing hormone (LHRH) has been used to target specific receptors that are found mainly in certain tumor cells.[19, 20] Studies on a conjugate of LHRH-DOX and LHRH-2-pyrrolino-DOX showed increased efficacy, as the drug maintained its highly targeted binding affinity while the analogues retained their cytotoxic effects on the tumor cells.[21-23]

Using phage display libraries, it has been discovered that several peptide sequences have the ability to target tumors.[24] For example, RGD-containing peptides have been shown to bind to integrins and also to reside preferentially in some tumor cell types.[25] In another study, the NGR motif was identified as a peptide that uniquely homed specifically to solid tumors in murine breast carcinoma models and that bound strictly to the endothelium of angiogenic blood vessels.[26] The NGR motif may be superior to the RGD-related motif for targeting, due to the type of cells that express the $\alpha_v\beta_3$ and $\alpha_v\beta_5$ integrins, which may lead to nonspecific toxicity.[25] Haubner *et al.* revealed that radiolabeled RGD peptide was found to concentrate rapidly in the liver, which can lead to liver toxicity in drugs that are based on RGD targeting, hence limiting the usefulness of these drugs.[25]

Angiogenesis occurs at extremely low levels in the adult organism; however, malignant tumors are an exception, with endothelial cells proliferating beyond the normal limits. In such tumors, new blood vessels are assembled, and this is required for tumor growth.[26, 27] Modulating the growth of blood vessels is one of the effective ways to control the growth and spread of tumors. Therefore, the search for targets that can regulate angiogenesis is important. Aminopeptidase N (APN), also referred to as CD13, is a cell-surface antigen that binds specifically to NGR peptides.[28, 29] CD13/APN is expressed exclusively on the endothelial cells of

angiogenic tissues and the vasculature of various carcinomas including kidney, colon, pancreas, prostate and lung[30-33]. It is not expressed in normal vasculature, which explains the tumor-specific destination of the NGR peptide.[3, 34]

Targeting the delivery to defined cancer cells can enhance the specificity of cisplatin and its analogues. By conjugating the water-soluble, cyclic peptide CNGRC to the conventional drugs cisplatin and Dichloro(ethylenediamine)platinum(II) ($PtenCl_2$), we propose to generate greater selectivity, increased specificity to cancer cells, and reduced toxicity to normal tissues. In this work, we describe the preparation of several malonyl CNGRC peptides and their platinum complexes and evaluate their specific targeting on tumor cells with CD13 receptors. Our final target compound is shown in Figure 2.1:

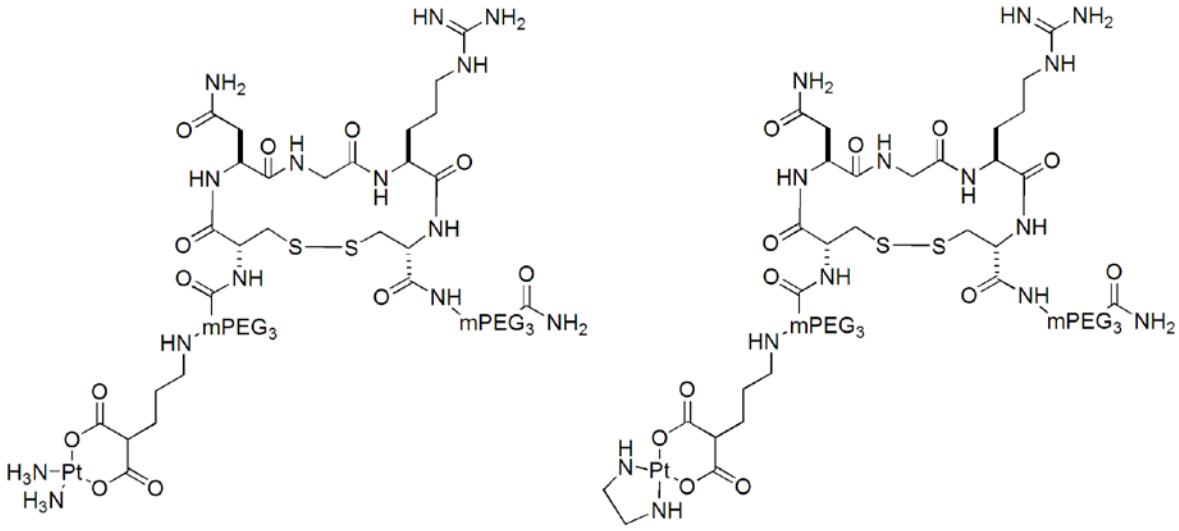

Figure 2.1. CNGRC-conjugate ligands that have been synthesized and examined in this chapter

2.2 Experimental Section

2.2.1 Starting Materials. All starting materials listed below were obtained from commercial sources and used without further purification: Di-tert-butyl malonate, dry solvents, $AgNO_3$, 3-bromopropylphthalimide, dichloro(ethylenediamine)platinum(II), cis-Diammineplatinum(II)

dichloride and glutaric anhydride were obtained from Aldrich (Milwaukee WI), Fmoc-11-amino-3,6,9-trioxaundecanoic acid (miniPEG) was obtained from Peptide International (Louisville, KY), and all amino acids and coupling reagents were obtained from Novabiochem (Gibbstown, NJ).

2.2.2 NMR Spectroscopy. ^{1}H NMR spectra were recorded on either 300 or 400 MHz spectrometers. Peak positions are referenced to TMS. All NMR data were processed with *XWINNMR* and *Mestre-C* software.

2.2.3 HPLC. HPLC was performed using a Water 600E multisolvent delivery system with a model 486 tunable detector controlled by Empower software and Water Deltaprep system, with detection at 220 nm. Different columns were used for analysis and purification of the peptides. Analytical and semi-preparative chromatography was performed on a Delta-Pak C_4 (5 µm;100 Aº) reverse phase column (8× 100 mm) at 1 mL/min (column 1). Preparative HPLC was performed on Waters Delta-Pak C_4 (15 µm;100 Aº) reverse phase column (25 × 100 mm) at 15 mL/min (column 2). Linear gradients of 0.1% aqueous TFA in H_2O (Eluent A) and 0.1% TFA in MeCN (Eluent B) in all HPLC were used.

2.2.4 Mass Spectrometry. Compounds were analyzed using MALDI-TOF on a Bruker Proflex III instrument with Xmass software, or using ESI on an Agilent Technologies instrument, processed with Analyst QS1.1.

2.2.5 Inductive Coupled Plasma-Optical Emission Spectroscopy. Platinum uptake was analyzed using a Varian, Vista MPX CCD simultaneous spectrometer. PlasmaCal Pt (1000 µg/ml) from SCP Science was used for calibration by diluting it to standard solutions of known concentration.

2.2.6 Synthesis

2.2.6.1 Peptide Synthesis. All peptides were synthesized using standard Fmoc solid phase chemistry. PAL-PEG-PS (Peptide Amide Linker resin: 0.2 mmol, 0.24 mmol/g loading) was placed in a normal resin column and washed with DMF in continuous flow mode using a Pioneer Peptide Synthesizer. The sidechain-protected aminoacid derivatives used in the sequence were resin, Fmoc-Cys(Acm)-OH, Fmoc-Arg(Pbf)-OH, Fmoc-Gly-OH, Fmoc-Asn(Trt)-OH, and Fmoc-Cys(Acm)-OH (Figure 2.2). Fmoc-mini-peg-3^{TM} solubilizing agent and the derivatized malonate linker di-tert-butyl 2-(3-glutaricaminopropyl)malonate were used, depending on the peptide sequence. All coupling utilized four equivalents each of amino acids, malonate, and PyAOP,[35] dissolved in 0.5 M DIEA in DMF (0.25 M final concentration) for 1 hour at room temperature. DMF was used for washing between reaction times, and a minimal preactivation time was used in the coupling. The Fmoc group was removed using 20% piperidine in DMF for 5 min. A further washing step yielded the desired peptide.

2.2.6.2 Synthesis of CNGRC-Mal (1). In an attempt to synthesize CNGRC-Mal, we synthesized cyclic CNGRC using the method described by Anizon *et al.* using NovaSyn TGT alcohol resin (0.20 mmol, 0.20 mmol/g loading).[17] Conjugation of CNGRC with di-tert-butyl 2-(3-aminopropyl)malonate was unsuccessful (Scheme 2.1).

2.2.6.3 Synthesis of Mal-Glut-CNGRC (2). Using standard Fmoc chemistry, we synthesized Mal-Glut-CNGRC using the procedure described in the peptide synthesis section, using PAL-PEG-PS resin without the Fmoc-mini-peg-3^{TM} solubilizing group. Coupling the peptide with di-tert-butyl 2-(3-glutaricaminopropyl)malonate gave crude Mal-Glut-CNGRC peptide, which was purified by reverse phase HPLC on column 1, using a linear gradient from 5% to 70% B eluent in 60 min, t_R 11 min. The product gave the expected $(M+H)^+$ Peak at 807.2893, as calculated for $C_{29}H_{48}N_{11}O_{12}S_2$.807.2925 (see Appendix B)**.** Using the procedure described for the preparation of

cyclic mPeg-CNGRC-Pt, the peptide was reacted with cis-$[Pt(NH_3)_2(H_2O)_2]^{2+}(NO_3)_2$ to give an insoluble yellow solid (Scheme 2.2). This was not suitable for further characterization.

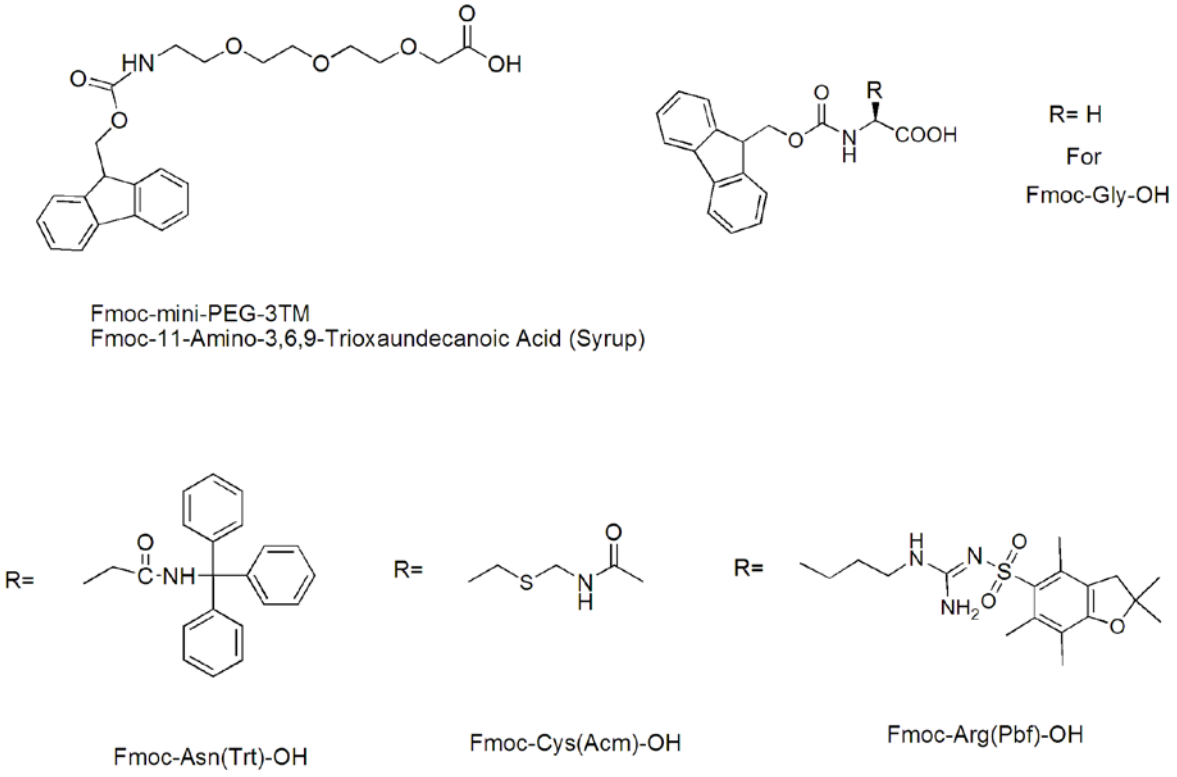

Figure 2.2 Structures of the amino acids used in the synthesis.

2.2.6.4 Synthesis of Di-tert-butyl 2-(3-Phthalimidopropyl)malonate (3). Di-tert-butyl 2-(3-phthalimidopropyl)malonate was synthesized by a known method (Scheme 2.3) with slight modifications.[36] NaH (0.38 g, 16 mmol) was suspended in dry THF (100 mL), and dry di-tert-butyl malonate (4.4 mL, 20 mmol) was added to the reaction mixture (with stirring) until gas evolution ceased. A solution of 2.68 g of 3-bromopropylphthalimide (10 mmol) was added dropwise to the reaction mixture, followed by stirring overnight. The THF was removed by evaporation, and the product was redissolved in CH_2Cl_2 and washed with 5% aqueous acetic acid. The organic fractions were combined, dried over $MgSO_4$ and concentrated. The final product was isolated using silica column chromatography (95% Hexane, 5% ethyl acetate). Di-

tert-butyl 2-(3-phthalimidopropyl)malonate was crystallized using a mixture of CH_2Cl_2 and hexane to give colorless plates (see Appendix B). The yield was 80% (3.22 g). Spectroscopic data obtained for this compound were in agreement with literature values.[36]

2.2.6.5 Synthesis of Di-tert-butyl 2-(3-aminopropyl)malonate (4). Compound **4** was prepared as described by Aronov *et al.*[36] Di-tert-butyl 2-(3-phthalimidopropyl)malonate was deprotected using hydrazine to give di-tert-butyl 2-(3-aminopropyl)malonate. The ^{1}H NMR spectrum of compound **4** (Scheme 2.3) in $CDCl_3$ matched the reported values.

2.2.6.6 Synthesis of Di-tert-butyl 2-(3-glutaricaminopropyl)malonate (5) Compound **5** was synthesized as previously described in the literature[36]. Glutaric anhydride was used for alkylation in this reaction, yielding di-tert-butyl 2-(3-glutaricaminopropyl)malonate (see Appendix B). The yield was 92%.^{1}H NMR ($CDCl_3$) (ppm): 3.27 (q, 2H), 3.14 (t, 1H), 2.41 (t, 2H), 2.28 (t, 2H), 1.98 (m, 2H), 1.81(m, 2H), 1.56 (m, 2H), 1.45(s, 18H).

2.2.6.7 Synthesis of Cyclic mPeg-CNGRC-mal (6). After synthesizing the linear mPeg-CNGRC-mal peptide and confirming its purity, the resin was suspended in DMF (60 mL), and the reaction mixture cooled to 0 ^{o}C in an ice bath before the addition of I_2 (10 equiv). The mixture was stirred at 0 ^{o}C for 2 h, filtered and washed with DMF (10 × 10 mL) and CH_2Cl_2 (10 × 10 mL). Using a cocktail of TFA:phenol:water:TIPS (88:5:5:2) (15 mL), the peptide was cleaved from the resin, precipitated and dried under vacuum to give crude peptide **6**. The crude peptide was purified using reverse phase HPLC on column 1 with a linear gradient from 5% to 70% B eluent in 60 min, t_R 28 min. This yielded cyclic mPeg-CNGRC-mal (**6**) at 35% yield. TOF-MS (ESI) gave a signal at 1184.4764 ($M + H^+$) calculated for $C_{45}H_{77}N_{13}O_{20}S_2$ is 1184.4849 (see Appendix B).

2.2.6.8 Synthesis of Cyclic mPeg-CNGRC-Pt (7). Cyclic mPeg-CNGRC-mal was dissolved in water, and the pH of the solution was adjusted to 7, by titration with 1M NaOH (Scheme 2.4). A solution of cis-$[Pt(NH_3)_2(H_2O)_2]^{2+}(NO_3)_2$ was made by stirring cis-$PtCl_2(NH_3)_2$ and $AgNO_3$ vigorously overnight in water in the dark. A precipitate was formed (AgCl) and then filtered to yield cis-$[Pt(NH_3)_2(H_2O)_2]^{2+}(NO_3)_2$ [37,38] A 2-fold excess of cis-$[Pt(NH_3)_2(H_2O)_2]^{2+}(NO_3)_2$ was reacted with compound **6** to form the crude cyclic mPeg-CNGRC-Pt conjugate (**7)**, which was then purified by gel filtration on Sephadex-G10 column to yield the final product at 15% yield. TOF-MS (ESI) gave a signal at 1412.4913 ($M + H^+$) calculated for $C_{45}H_{81}N_{15}O_{20}PtS_2$ is 1412.4955 (see Appendix B).

2.2.6.9 Synthesis of Cyclic mPeg-CNGRC-Pten (8). Cyclic mPeg-CNGRC-mal was dissolved in water, and the pH of the solution was adjusted to 7, by titration with 1M NaOH. Cis-$[Pt(en)(H_2O)_2]^{2+}(NO_3)_2$ was synthesized by stirring $Pt(en)Cl_2$ and $AgNO_3$ vigorously overnight, in water in the dark. A precipitate was formed (AgCl) and then filtered to yield cis-$[Pt(en)(H_2O)_2]^{2+}(NO_3)_2$.[39-41] A 2-fold excess of cis-$[Pt(en)(H_2O)_2]^{2+}(NO_3)_2$ was reacted with compound **6** to yield crude cyclic mPeg-CNGRC-Pten conjugate, which was then purified by gel filtration on Sephadex-G10 column to yield cyclic mPeg-CNGRC-Pten **(8)** at 10-12% yield**.** TOF-MS (ESI) gave a signal at 719.7571 $(M + H)^{2+}$ calculated for $C_{47}H_{83}N_{15}O_{20}PtS_2$ is 719.7571 (see Appendix B).

2.2.6.10 Synthesis of Cyclic mPeg-CNGRC (9). The peptide was assembled as described in the peptide synthesis section, without the malonate linker di-tert-butyl 2-(3-glutaricaminopropyl)malonate. The crude peptide was purified by reverse phase HPLC on column 1, with a linear gradient from 5% to 70% B eluent in 60 min, t_R 12 min, yielding cyclic

mPeg-CNGRC (**9**) at a 38% yield. ESI-MS (TOF) gave a signal at 927.4032 ($M + H^+$) calculated for $C_{34}H_{62}N_{12}O_{14}S_2$ is 927.4023 (see Appendix B).

2.2.7 Cell Culture Studies

2.2.7.1 Cell Culture. The prostate cancer cells LNCap (CRL-1740) and PC-3 (CRL-1435) were obtained from the American Type Culture Collection (Manassas, VA). Penicillin, streptomycin, RPMI 1640, and fetal bovine serum (FBS) were obtained from Invitrogen (Grand Island, NY). Both cell lines were cultured in RPMI 1640 supplemented with 10% FBS, 100 units/mL penicillin and 100 μg/mL streptomycin.

2.2.7.2 Fluorescence Microscopy. PC-3 and LNcap cells were seeded on 6-well plates (500,000 cells/well) and incubated for 24 h in RPMI 1640 media. The cells were treated with 200 μM of carboplatin, a mixture of carboplatin and free peptide, and Pt-peptide conjugates **7** and **8** for 48 h. After incubation, the cells were washed once with RPMI and then stained with JC-1 dye for 30 min. The stained cells were analyzed using a Leica DM RXA fluorescent microscope with Xenon lamp illumination, using a 40 x dip objective with an N.A. of 0.80. The filter cube for the green channel had the following characteristics: a 480/40 excitation filter, a 527/30 emission filter and a 505nm dichroic mirror. The filter cube used for the red channel had the following characteristics: a 537/45 excitation filter, an LP 590 emission filter, and a 580 nm dichroic mirror.

2.2.7.3 Cytotoxicity Assay. The cytotoxicity of the free carboplatin and two platinum conjugates (cyclic mPeg-CNGRC-Pt (**7**) and cyclic mPeg-CNGRC-Pten (**8**)) was assayed using the MTT (3-(4, 5-dimethylthiazol-2-yl)-2, 5-diphenyltetrazolium bromide) assay as described.[42] Briefly, 2,000 cells/well were incubated in 96-well plates in triplicate, using different concentrations of platinum complexes in a cell growth medium. Three wells were used as controls, receiving an

equivalent volume of medium alone. In the first experiment, the cells were treated with different concentrations (0 μM, 50 μM, 150 μM, 200 μM and 300 μM) of carboplatin, peptide **6**, and Pt-peptide conjugates **7** and **8** for 4 h. After this period, the regular cell growth medium was replaced, and the cells were incubated for a further 48 h. In another set of experiments, the cells were treated with the same set of compounds at different concentrations for 48 h. After 48 h, in both sets, a solution of MTT (5 mg/ml in PBS) was added to each well, and the cells were incubated for 2 h at 37^{o}C. The cells were then lysed using a lysis buffer (20% SDS and 50% DMSO). The lysed cells were incubated for 3 h at 37^{o}C, before the absorbance of the cell suspension was measured at 590 nm using an MRX Revelation 96-well multiscanner (Dynex Technologies, Chantilly, VA).

2.2.7.4 Drug Uptake Measurements. One million PC-3 and LNcap cells were plated in a 6-well plate one day prior to the treatment so that they had time to adhere to the plate. On the next day, the cells were treated with fresh medium containing 200 μM carboplatin, and Pt-peptide conjugates **7** and **8** for 24 h. After incubation, the cells were washed with PBS once, and the cells were collected in a tube for further analysis. Samples were dissolved in 0.25 ml nitric acid (trace metal grade) and heated for 2 h at 60 ^{o}C for digestion. Upon cooling, approximately 5 mL of deionized water was added to dilute the samples to the minimum volume required for the ICP spectrometer.

2.2.7.5 Cell Competition Assay

Using various concentrations of mPeg-CNGRC (**9**)**,** a cell competition assay for carboplatin and conjugates **7** was carried out using the MTT assay. A quantity of 2,000 cells/well was incubated in a 96-well plate in triplicate using various concentrations of the free peptide mPeg-CNGRC (**9**) (1 mM, 2 mM, 4 mM,, 8 mM and 10 mM) for 45 minutes. This was followed by the addition of

200 μM of carboplatin or conjugate **7** for 48 h. The plate was analyzed as described in the cell cytotoxicity assay.

2.3 Results and Discussion

Using PAL-PEG-PS resin, a pegylated CNGRC was synthesized in order to evaluate the effectiveness of the drug delivery of the platinum analogues. We chose this system (pegylated peptide) to increase the solubility and to provide additional spacing of the platinum ligand from the targeting peptide ligand. Figure 2.3 shows the two designs that we tested for the formation of Pt-peptide complexes, with design **B** being the more successful of the two.

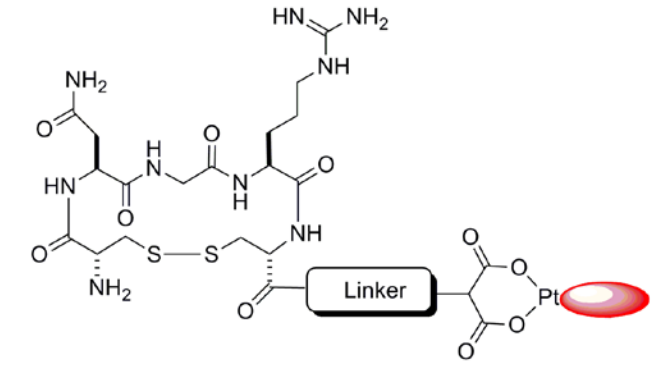

Design A

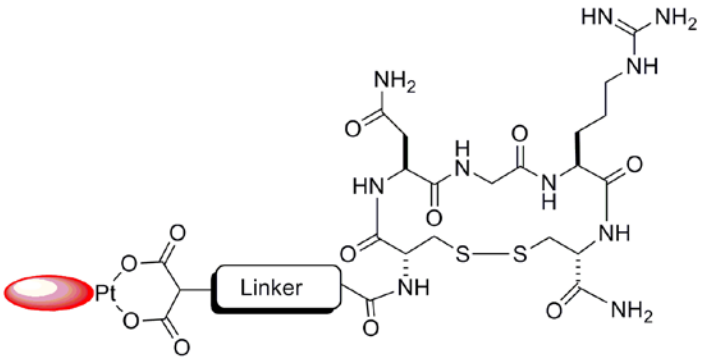

Design B

Figure 2.3. CNGRC model conjugate with platinum pro-drug

Our initial attempt was to couple the cyclic CNGRC peptide with di-tert-butyl 2-(3-aminopropyl)malonate using solution phase chemistry by conjugating the free carboxylic end of the cysteine with the free amine end of di-tert-butyl 2-(3-aminopropyl)malonate (Scheme 2.1). The Cyclic CNGRC peptide was prepared as described by Anizon *et al.*[17] where the trityl alcohol resin was converted to the trityl chloride derivative with acetyl chloride. This was followed by loading of the Fmoc-Cys(Acm)-OH onto resin, resulting in a 0.14 mmol/g (70%) loading yield. The resin was treated with Fmoc-Arg(Pbf)-OH, Fmoc-Gly-OH, Fmoc-Asn(Trt)-OH, and Fmoc-Cys(Acm)-OH to give crude CNGRC in high yield. The HPLC chromatogram and the mass spectrum revealed the expected $(M+H)^+$ peak at 550.76, which was in agreement with the reported values. Di-tert-butyl 2-(3-aminopropyl)malonate was prepared as described in the experimental section using a slight modification of the Aronov method.[36] The malonate was alkylated using a strong base to give product in 80% yield. A similar synthesis was achieved by the Aronov group using KOt-Bu as a base; however, using a stronger base (NaH) in the reaction improved the yields from 60% to 80%. A twofold excess of di-tert-butyl malonate was used to ensure monoalkylation and the ease of separation between the malonate and di-tert-butyl 2-(3-phthalimidopropyl)malonate. The excess of di-tert-butyl malonate that was used was easily removed by column chromatography.[36] Attempts to couple the cyclic peptide CNGRC and di-tert-butyl 2-(3-aminopropyl)malonate using various coupling reagents were unsuccessful (Scheme 2.1). We do not understand why the reaction failed, as similar reactions between CNGRC and DOX with similar functional groups have been successful.[17] Analysis of the crude product revealed high amounts of the starting materials, including CNGRC, di-tert-butyl 2-(3-aminopropyl)malonate, and coupling reagents.

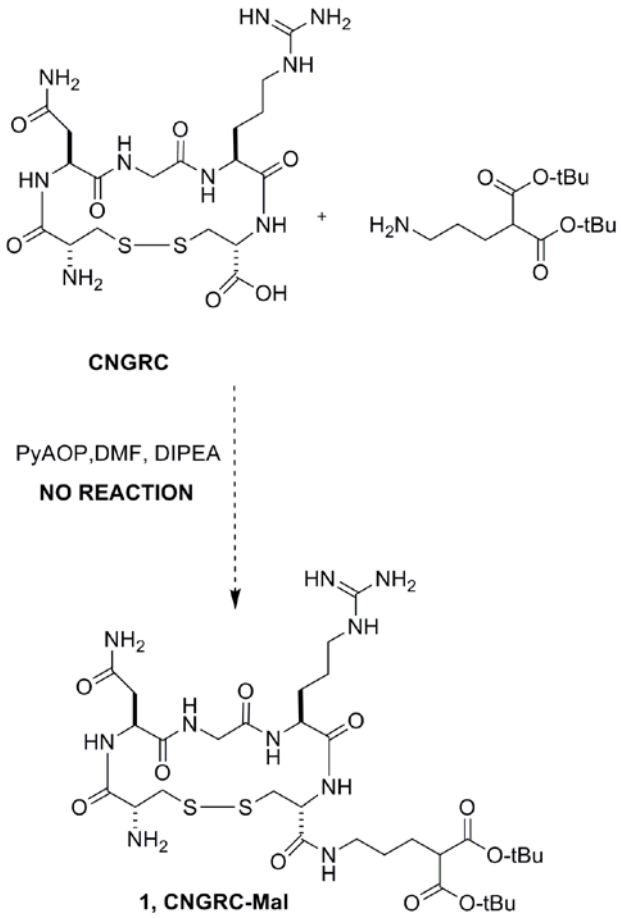

Scheme 2.1. Coupling of CNGRC with di-tert-butyl 2-(3-aminopropyl)malonate.

In order to overcome the above problem, we used PAL-PEG-PS resin. This enabled us to conjugate the linker on the N terminus of peptide resin, thereby avoiding solution phase chemistry in the conjugation of the linker to the peptide CNGRC, as shown in Scheme 2.2. To achieve this synthesis, malonate linker with a carboxylic acid end (**5**) was synthesized using glutaric anhydride and di-tert-butyl 2-(3-aminopropyl)malonate (**4**), as shown in Scheme 2.3. Using general Fmoc chemistry, the peptide was assembled using the same amino acids described above. This was then conjugated to di-tert-butyl 2-(3-glutaricaminopropyl)malonate and cyclized on the solid support to yield (Mal-Glut-CNGRC) as a single product. It eluted in 11 min on HPLC, demonstrating that it could be easily purified. Mass spectral analysis confirmed the

identity of the cyclic Mal-Glut-CNGRC, as it had a $(M+H)^+$ peak at 807.2893. Platination of the purified Mal-Glut-CNGRC using cis-$[Pt(NH_3)_2(H_2O)_2]^{2+}(NO_3)_2$ gave an insoluble yellow compound in most solvents, including water, DMSO, DMF, MeOH, acetone, MeCN, CH_3Cl, and CH_2Cl_2.

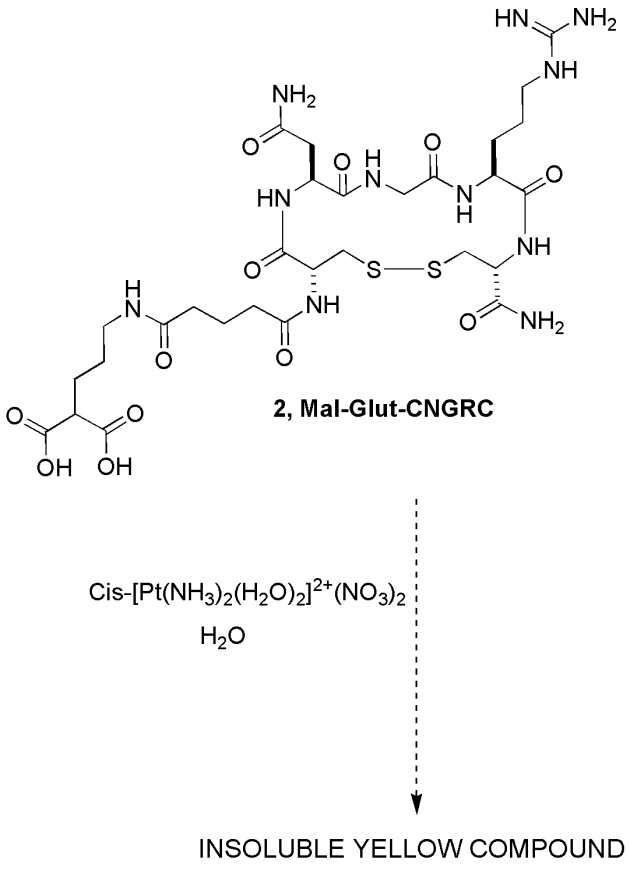

Scheme 2.2. Platination reaction using Mal-Glut-CNGRC

Our third and final approach was to pegylate the CNGRC sequence by adding miniPEG to each end of the sequence to improve the solubility of the compound and to provide additional spacing of the Pt-ligand from the targeting peptide ligand. Various studies have shown that pegylation does not affect targeting and may have other positive effects, such as an increase in stability that reduces the chance of the drug being effluxed and that it reduces or eliminates immunogenicity.[36] The linear peptide was cyclized on a solid support and cleaved to give target

compound **6** (Scheme 2.4), which was purified by HPLC and confirmed by mass spectra to have the expected $(M+H)^+$ peak at 1184.4764.

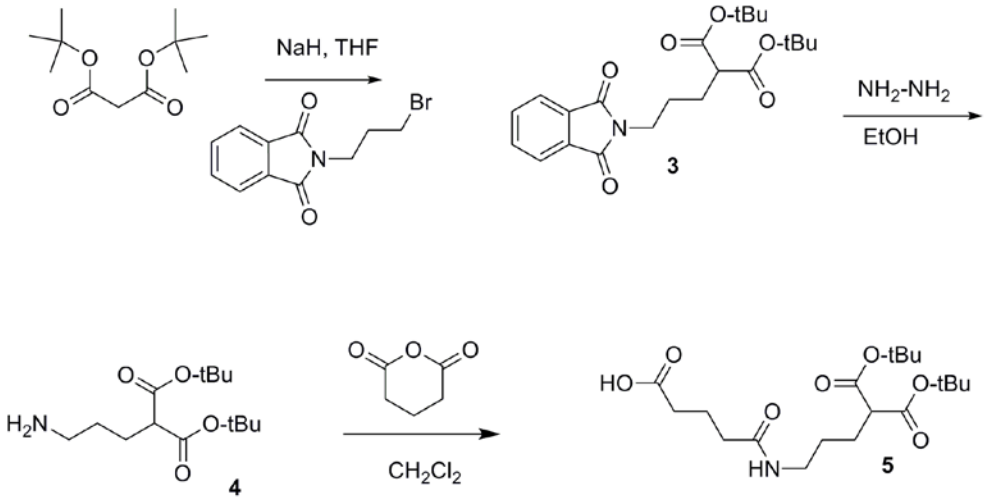

Scheme 2.3. Synthesis of Di-tert-butyl 2-(3-glutaricaminopropyl)malonate

2.3.1 Platinum Complexes

Platination with a twofold excess of activated cis-$[Pt(NH_3)_2(H_2O)_2]^{2+}(NO_3)_2$ and cis-$[Pt(en)(H_2O)_2]^{2+}(NO_3)_2$ using a standard procedure gave Pt-Peptide conjugates **7** and **8**, as shown in Scheme 2.4. The platinum complexes could not be purified by HPLC using either an acid or a neutral solvent system because the platinum complexes dissociated. The products were therefore purified by gel filtration to remove the excess platinum. Fractions containing the Pt-peptide complex in water were identified by ESI-MS and then combined and lyophilized to give pure platinum complexes for cyclic mPeg-CNGRC-Pt (**7**) and cyclic mPeg-CNGRC-Pten (**8**) at a 10-15% yield. Mass spectra revealed the expected $(M+H)^+$ peak at 1412.4913 for conjugate **7** and the $(M + 2H)^{2+}$ peak at 719.7571 for conjugate **8**. The two carboxylic acid groups at the end of the peptide enabled the formation of platinum chelate, binding in a bidentate fashion. During the study, we noticed that platinum complex **7** was not very stable in PBS at -20°C and formed precipitates after a day of storage. Any experiment using complex **7** had to be prepared freshly

and used immediately. Platinum complex **8** was stable at -20°C, and the stock solutions prepared could be used in later experiments. Both platinum conjugates were stable as lyophilized samples at -20°C and fresh samples were made by reconstituting the dry samples to the desired concentration. The stability of the complexes was confirmed by mass spectrometry. Scheme 2.4 shows the formation of the final platinum complexes synthesized.

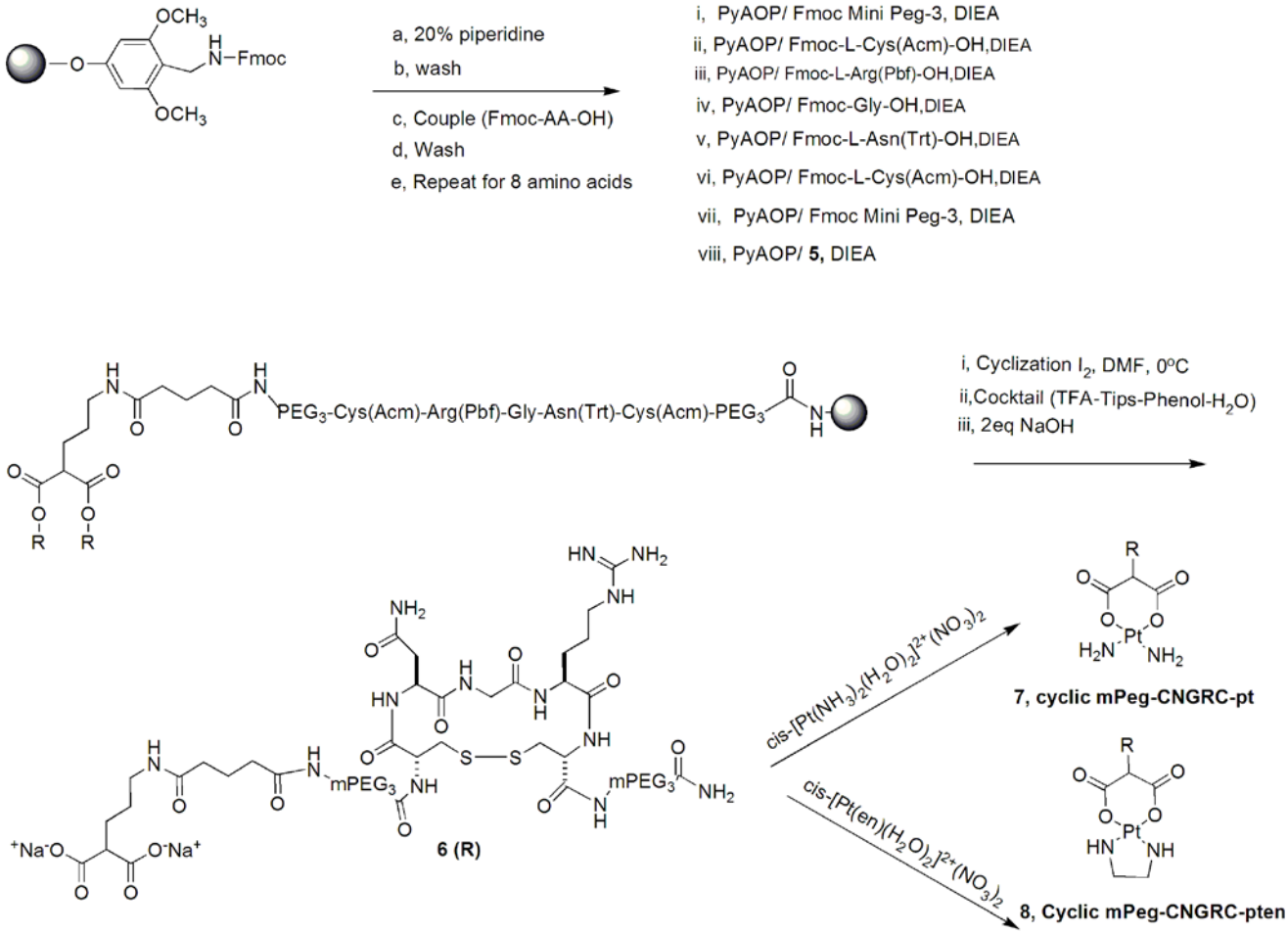

Scheme 2.4. Synthesis of cyclic mPeg-CNGRC-Pt **(7)** and cyclic mPeg-CNGRC-Pten **(8),** where Fmoc mini peg-3 is 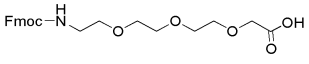 .

2.3.2 *In vitro* Studies on Pt-conjugates: Toxicity and Uptake

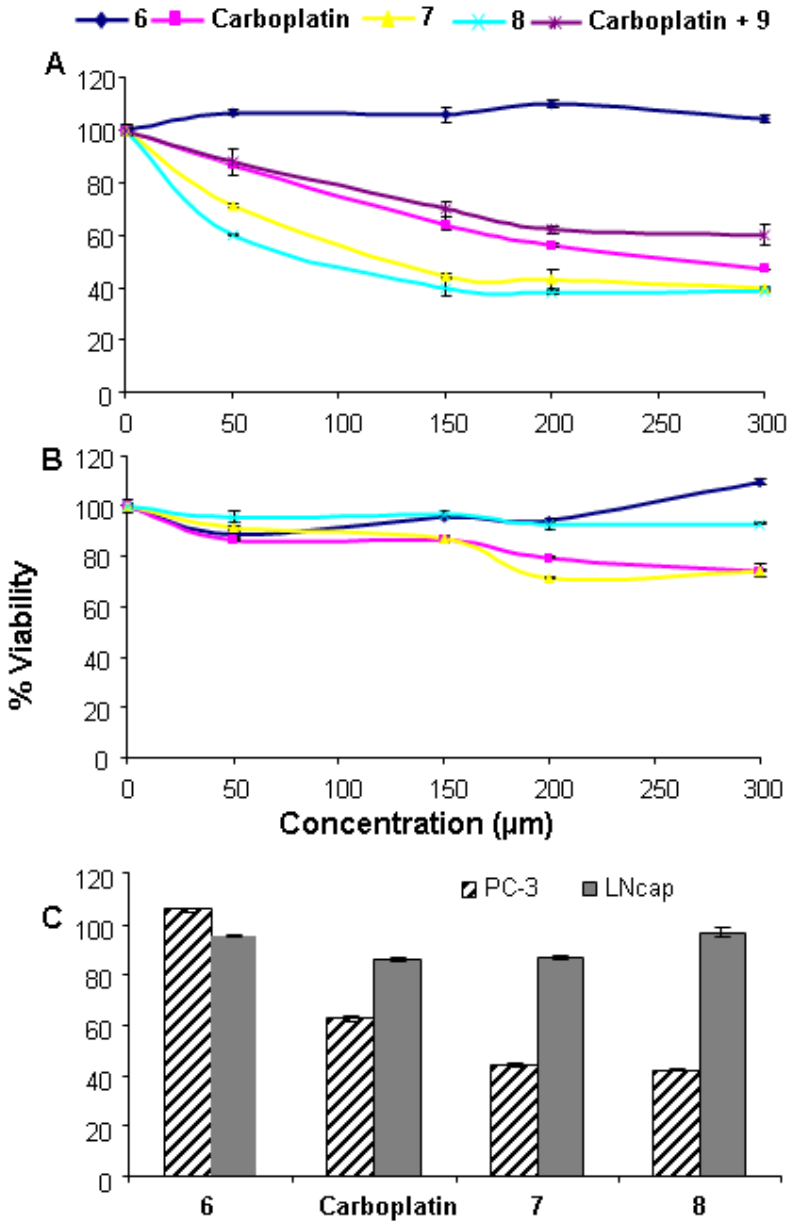

Figure 2.4. The effect of carboplatin **(**free peptide), cyclic mPeg-CNGRC-mal (**6**)**,** the mixture of carboplatin and mPeg-CNGRC **(9),** and the Pt-peptide conjugates; cyclic mPeg-CNGRC-Pt (**7**) and cyclic mPeg-CNGRC-Pten (**8**) on the proliferation of prostate cancer PC-3 (CD13 positive) cells and LNcap (CD13 negative) cells. (A) PC-3 cells and (B) LNcap cells were exposed to the compounds listed and incubated for 48 h at different concentrations. (C) A comparison of % viability of the PC-3 and LNcap cells at 150 µM ligand concentration. The data represents three independent experiments, $P < 0.04$ vs. carboplatin and is statistically significant ($P < 0.05$). The statistical significance was determined using the t-test.

It has been shown that the NGR motif binds specifically to the CD13 receptors that are expressed on some tumor cells. We examined the effect of the free peptide in a control experiment to determine the toxicity of the peptide. MTT-reduction levels were normalized to the positive control. As shown in Figure 2.4A, the free peptide (**6)** was not toxic to the PC-3 cells and caused a slight increase in the MTT assay, suggesting that the PC-3 receptors were activated by the NGR ligand. As expected, the targeted Pt-peptide conjugates **7** and **8** were more toxic to the PC-3 cells at all concentrations tested compared to the untargeted carboplatin (even at concentrations as low as 50 μM). Pt-conjugate **8** shows the highest effect on the suppression of cell proliferation, followed by Pt-conjugate **7** and carboplatin. Carboplatin was the least toxic to PC-3 cells of this series of platinum compounds, indicating that the platinum complexes bearing the CNGRC sequence are more effective at suppressing tumor cell proliferation. The % inhibition caused by the mixture of mPeg-CNGRC (**9**) and carboplatin was similar to that caused by carboplatin alone, suggesting that there was no effect of the peptide on the effectiveness of carboplatin. Treatment of LNcap cells with this series of platinum complexes did not have much effect on the proliferation of the cells, suggesting little platinum uptake due to lack of CD13 receptors (Figure 2.4B). No conclusions could be drawn from the cell toxicity data, as the LNcap cells were barely sensitive to carboplatin. A very high dose of carbopaltin 200 μM showed 10% cell killing, therefore, the result cannot be interpreted. Comparison between the two cell lines, PC-3 and LNcap, (Figure 2.4C), revealed a clear difference between the targeted and untargeted platinum complexes, when used at 150 μM. Less than 50% of the PC-3 cells were viable when exposed to the targeted Pt-peptide conjugates, compared to greater than 60% for the untargeted carboplatin drug. The targeted and untargeted platinum complexes had no significant difference

in their effect on the % viability of the LNcap cells. The free peptide **6** did not show any activation of the LNcap cell line in comparison to the PC-3 cell line.

The carboplatin, free peptide **6**, Pt-peptide conjugate **7** and Pt-peptide conjugate **8** were also tested at various concentrations (50 µM, 150 µM, 200 µM and 300 µM) by continuous exposure for 4 h followed by incubation for 48 h at 37°C in cell growth media (see appendix B) for both cell lines. Overall, similar trends on % viability were observed, with a lower toxicity that shows that the uptake of the drug starts after as little as 4 h after incubation with the compounds.

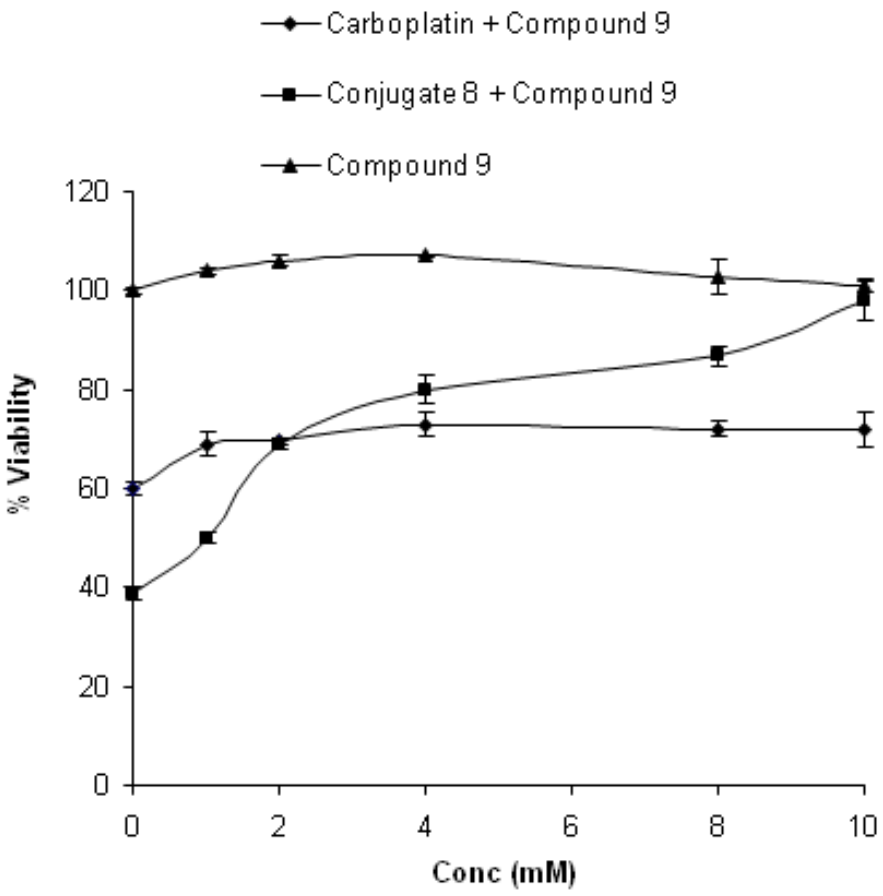

Figure 2.5. Competition assay on PC-3 cancer cells using carboplatin and conjugate **8** with free peptide **9**

Figure 2.5 demonstrates that the free peptide had no cytotoxic effect on the PC-3 cells. A slight increase in the % viability suggests the activation and nourishment of the PC-3 cells. Carboplatin

and conjugate **8** were incubated with various concentration of mPeg-CNGRC (**9**) as described in the methods**.** Incubation of carboplatin with various concentration of free peptide **9** had the same effect on the % viability irrespective of the amount of free peptide (**9**) used. Incubation of conjugate **8** with various concentrations of free peptide (**9**) showed that the free peptide was competing with conjugate **8** in targeting the CD 13 receptors. With an initial 5-fold excess of free peptide (**9**), conjugate **8** was more cytotoxic than free carboplatin, but with a 10-fold excess, the free peptide (**9**) was able to compete away the effect of conjugate **8** in comparison to carboplatin. A further 50-fold increase in the free peptide concentration resulted in the elimination of the cytotoxic effect from conjugate **8**. The results also demonstrate that the CNGRC motif contributes to the accumulation of platinum in the tumor cells, causing a significant difference in the suppression of the proliferation of PC-3 tumor cells.

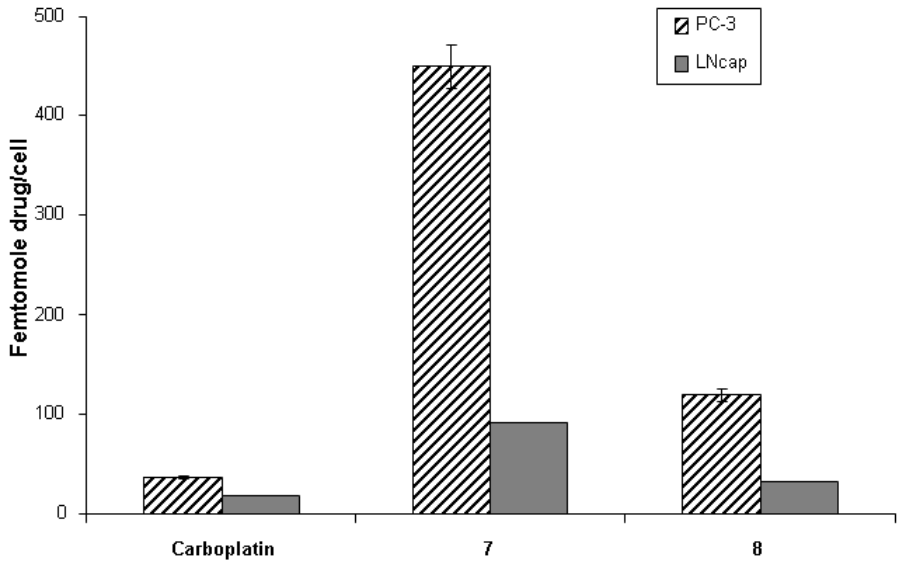

Figure 2.6. A study on the uptake of PC-3 (CD13 positive) and LNcap (CD13 negative) cancer cells. One million cells were incubated with carboplatin, and Pt-peptide conjugates **7** and **8** for 24 h at 200 μM. The results were analyzed as explained in the method section.

For cell death to occur, it is believed that platinum coordinates with N7 of the purines forming a 1,2-intrastand adduct, causing the destacking and bending of DNA that leads to eventual cell

death. To confirm the cell toxicity results obtained above, the uptake of platinum by LNcap and PC-3 cells was determined by exposing the cells to 200 μM carboplatin, Pt-peptide conjugate **7** and Pt-peptide conjugate **8** for 24 h. The greatest uptake occurred with platinum complex **7** followed by complex **8**, and the least uptake occurred with carboplatin, in PC-3 cells. Uptake in LNcap cells followed a similar trend, but at much lower levels compared to PC-3. The uptake of untargeted carboplatin was determined to evaluate the difference with the targeted complexes. From the data in Figure 2.6, platinum uptake by the PC-3 cells was 12-fold greater when using conjugate **7** and 3-fold greater when using conjugate **8**, compared to untargeted carboplatin. The uptake of platinum by the LNcap cells was 5-fold and 2-fold greater when Pt-peptide conjugates **7** and **8** were used, respectively, than when carboplatin was used. Figure 2.6 also reveals that the carboplatin uptake by PC-3 was double that of the LNcap cells, and similarly, the uptake of Pt-peptide conjugates **7** and **8** was 5 and 4-fold greater when using PC-3 cells as compared to the LNcap cells, respectively. These results clearly suggest that the PC-3 cells seem to be more susceptible to platinum uptake due to the presence of the CD13 receptors.

Another notable observation was the effect of targeted platinum complexes at the lowest concentration tested (50 μM) on PC-3 cells. A concentration of 200 μM showed the most substantial effect on cell proliferation (Figure 2.4). These results suggest that higher uptake of Pt leads to greater suppression of the proliferation of PC-3 cells. Our results are in agreement with other groups, who have shown that the CNGRC motif contributes to the increased intracellular concentration of drugs that are attached to this motif, due to targeting to CD13 positive cells. A 5-FdUrd conjugate bearing the homing peptide CNGRC was found to penetrate into the CD13 positive cells, HT-1080, but not to the CD13 negative cells, MDA-MB-231. This enhanced the selective accumulation of 5-FdUrd, resulting in more effective immunotherapy.[18]

High uptake seems related to the toxicity of Pt-peptide conjugate **7** and **8,** supporting the hypothesis that high uptake of platinum drugs results in high cytotoxicity. Our major concern during this experiment was to ensure that the cisplatin/carboplatin moiety detaches from the carrier at the right place at the right time. With this in mind, we chose carboplatin as our control drug in the experiment because we expected that our targeted compound would release the drug in a manner similar to carboplatin. When other targeting ligands have been used, cisplatin uptake and targeted platinum uptake in some cell lines show comparable values and trends to our results, where targeted drugs had a higher uptake than untargeted platinum drugs.[43-46] To our surprise, even though the uptake of Pt complex **8** was lower than that of Pt complex **7**, complex **8** was more toxic than complex **7**. This suggests that either the activation mechanism or the delivery pathway of complexes **7** and **8** might be different. Clinical trials of ethylene diamine platinum complexes were suspended, as previous animal studies have shown high nephrotoxicity relative to cisplatin.[47, 48] Our findings similarly show that even with low uptake of complex **8** (an analogue of the ethylene diamine platinum complexes), substantial toxicity was observed. This shows that care should be taken when interpreting whether high platinum uptake has a direct relationship with cell death, and that more studies need to be done on this area.

2.3.3 Fluorescence Microscopy

The cell toxicity was evaluated using fluorescence microscopy (Figure 2.7) and the JC-1 membrane potential kit, which measures the mitochondrial membrane potential. Images **A** and **D** show healthy cells grown in media, allowing the JC-1 dye to aggregate resulting in red fluorescence. The results shown in Figure B confirmed that targeted Pt-peptides and conjugates **7** (Image **B**) and **8** (see Appendix B) cause a decrease in the membrane potential, thereby causing death by apoptosis in the PC-3 cell line.

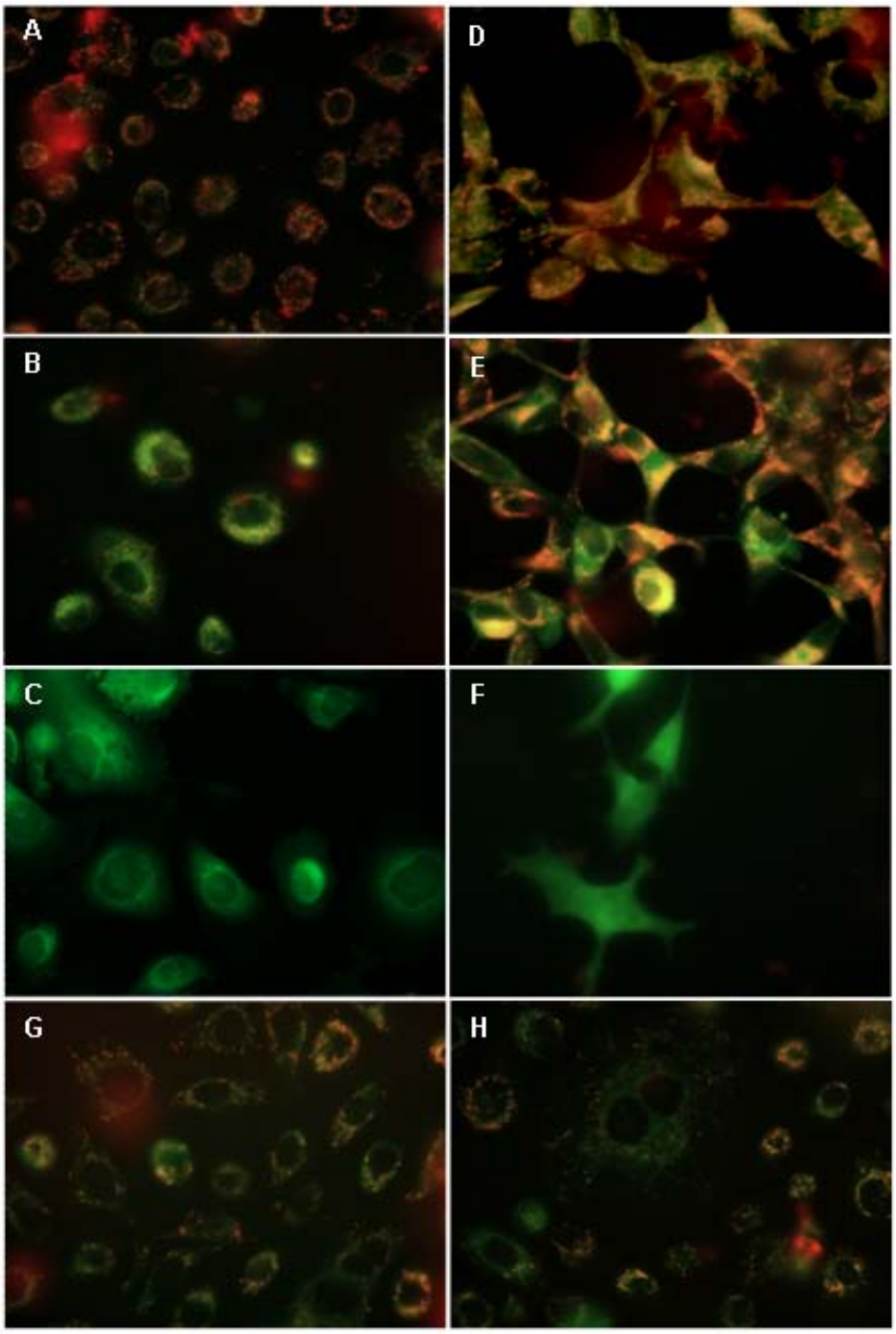

Figure 2.7. Fluorescence microscopy of cells that have been treated with various compounds, incubated for 48 h at 37°C and then imaged by JC-1 staining after a further 30 min of incubation. Images **A** and **D;** PC-3 and LNcap cells, respectively, treated with RPMI media only. Images **B** and **E;** PC-3 and LNcap cells, respectively, treated with 200 μM of Pt-peptide conjugate **8** in RPMI media. Images **C** and **F;** PC-3 and LNcap cells, respectively, treated with 50% DMSO. Images **G** and **H;** PC-3 cells incubated with a mixture of carboplatin/free peptide **9** (1:50) and carboplatin only, respectively.

Image **E** however, reveals that complexes **7** and **8** had either a minimal or no effect on LNcap cells, which do not have CD13 receptors. This is evident from the intense, red fluorescence in both untreated LNcap cells (**D**) and LNcap cells that had been treated with Pt-peptide conjugate **8** (**E**). As the toxicity is less towards the CD13-negative cell line (LNcap), this study suggests a lower toxicity for normal cells, which have no receptors. Apoptotic and dying cells have a low membrane potential resulting in a green fluorescence which is evident in images **C** and **F**. Images **G** and **H** show PC-3 cells treated with mixture of carboplatin/free peptide **9** (1:50) and carboplatin alone, respectively. The images show more viable cells when compared to PC-3 cells treated with targeted conjugate **8.**[49]

2.4 Conclusion

Our work focused on synthesizing novel targeted Pt-peptide conjugates using the NGR motif and a malonaly linker. The advantage of the targeted platinum analogues that we synthesized and studied in this work is that they increase the selectivity and specificity for cancer cells and are less toxic to normal tissues. This study reveals two new low molecular weight Pt-peptide conjugates that effectively deliver cisplatin and $PtenCl_2$ to tumor cells, thereby reducing the side effects on normal cells and increasing the toxicity towards tumor cells. Pegylation of the peptide CNGRC allowed us to study the carrier at physiological conditions; however, the solubility problem did not allow us to compare the difference in cytotoxicity of the non-pegylated conjugate relative to one without the miniPEG. The presence of the bidentate dicarboxylate ligand in carboplatin has been shown to slow the degradation of carboplatin into potentially damaging derivatives, thereby reducing nonspecific toxicity and increasing the potency relative to cisplatin.[50, 51] With the aid of the miniPEG group and the bidentate ligand, we show that Pt-

peptide complexes **7** and **8**, which are analogues of carboplatin, were able to target tumor cells that had CD13 receptors.

2.6 References

1. Lippert, B.; Editor, *Cisplatin: Chemistry and Biochemistry of a Leading Anticancer Drug*. 1999; p 563 pp.

2. Reedijk, J., Improved understanding in platinum antitumor chemistry. *Chemical Communications (Cambridge)* **1996**, (7), 801-6.

3. Shipp, M.; Look, T., Hematopoietic Differentiation Antigens That Are Membrane-Associated Enzymes: Cutting Is the Key! *Blood* **1993,** 82, 1052-1070.

4. Jamieson, E.; Lippard, S., Structure, Recognition, and Processing of Cisplatin-DNA Adducts. *Chemical Reviews (Washington, DC, United States)* **1999,** 99, 2467-2498.

5. Hamelers, I. H. L.; Van Loenen, E.; Staffhorst, R. W. H. M.; De Kruijff, B.; De Kroon, A. I. P. M., Carboplatin nanocapsules: a highly cytotoxic, phospholipid-based formulation of carboplatin. *Molecular Cancer Therapeutics* **2006,** 5, (8), 2007-2012.

6. Sood, P.; Thurmond, K. B., II; Jacob, J. E.; Waller, L. K.; Silva, G. O.; Stewart, D. R.; Nowotnik, D. P., Synthesis and Characterization of AP5346, a Novel Polymer-Linked Diaminocyclohexyl Platinum Chemotherapeutic Agent. *Bioconjugate Chemistry* **2006,** 17, (5), 1270-1279.

7. Bertini, I.; Gray, H. B.; Lippard, S. J.; Valentine, J. S., *Bioinorganic Chemistry*. 1994; p 611 pp.

8. Kaim, W.; Schwederski, B., *Bioinorganic Chemistry: Inorganic Elements in the Chemistry of Life. An Introduction and Guide*. 1994; p 401 pp.

9. Kelland, L. R.; Murrer, B. A.; Abel, G.; Giandomenico, C. M.; Mistry, P.; Harrap, K. R., Ammine/amine platinum(IV) dicarboxylates: a novel class of platinum complex exhibiting selective cytotoxicity to intrinsically cisplatin-resistant human ovarian carcinoma cell lines. *Cancer Research* **1992,** 52, (4), 822-8.

10. Cubeddu, L. X.; Hoffmann, I. S.; Fuenmayor, N. T.; Finn, A. L., Efficacy of ondansetron (GR 38032F) and the role of serotonin in cisplatin-induced nausea and vomiting. *The New England Journal of Medicine* **1990,** 322, (12), 810-6.

11. Ghezzi, A.; Aceto, M.; Cassino, C.; Gabano, E.; Osella, D., Uptake of antitumor platinum(II) complexes by cancer cells, assayed by inductively coupled plasma mass spectrometry (ICP-MS). *Journal of Inorganic Biochemistry* **2004,** 98, (1), 73-78.

12. Katano, K.; Kondo, A.; Safaei, R.; Holzer, A.; Samimi, G.; Mishima, M.; Kuo, Y.-M.; Rochdi, M.; Howell, S. B., Acquisition of resistance to cisplatin is accompanied by changes in the cellular pharmacology of copper. *Cancer Research* **2002,** 62, (22), 6559-6565.

13. van Zutphen, S.; Reedijk, J., Targeting platinum anti-tumour drugs: Overview of strategies employed to reduce systemic toxicity. *Coordination Chemistry Reviews* **2005,** 249, (24), 2845-2853.

14. Galanski, M.; Keppler, B. K., Searching for the magic bullet: anticancer platinum drugs which can be accumulated or activated in the tumor tissue. *Anti-Cancer Agents in Medicinal Chemistry* **2007,** 7, (1), 55-73.

15. Pasqualini, R.; Koivunen, E.; Kain, R.; Lahdenranta, J.; Sakamoto, M.; Stryhn, A.; Ashmun, R.; Shapiro, L.; Arap, W.; Ruoslahti, E., Aminopeptidase N Is a Receptor for Tumor-homing Peptides and a Target for Inhibiting Angiogenesis. *Cancer Research* **2000,** 60, 722-727.

16. Arap, W.; Pasqualini, R.; Ruoslahti, E., Cancer treatment by targeted drug delivery to tumor vasculature in a mouse. *Science (Washington, D. C., 1883-)* **1998,** 279, 377-380.

17. Anizon, F.; Boyle, T.; Fisher, J.; Kocienski, P., Synthesis and characterisation of a Doxorubicin-CNGRC Peptide conjugate that target tumor Vasculature. *Synthesis* **2002,** 18, 2733-2736.

18. Zhang, Z.; Hatta, H.; Tanabe, K.; Nishimoto, S.-i., A New Class of 5-Fluoro-2□-deoxyuridine Prodrugs Conjugated with aTumor-Homing Cyclic Peptide CNGRC by Ester Linkers: Synthesis,Reactivity, and Tumor-Cell–Selective Cytotoxicity. *Pharmaceutical Research* **2005,** 22, 381-389.

19. Hansel, W.; Enright, F.; Leuschner, C., Destruction of breast cancers and their metastases by lytic peptide conjugates in vitro and in vivo. *Molecular and Cellular Endocrinology* **2007,** 260-262, 183-189.

20. Leuschner, C.; Kumar, C. S. S. R.; Hansel, W.; Hormes, J., Targeting breast cancer cells and their metastases through luteinizing hormone releasing hormone (LHRH) receptors using magnetic nanoparticles. *Journal of Biomedical Nanotechnology* **2005,** 1, (2), 229-233.

21. Nagy, A.; Schally, A. V., Cytotoxic analogs of luteinizing hormone-releasing hormone (LHRH): a new approach to targeted chemotherapy. *Drugs of the Future* **2002,** 27, (4), 359-370.

22. Schally, A. V.; Nagy, A., Cancer chemotherapy based on targeting of cytotoxic peptide conjugates to their receptors on tumors. *European Journal of Endocrinology* **1999,** 141, (1), 1-14.

23. Schally, A. V.; Nagy, A., New approaches to treatment of various cancers based on cytotoxic analogs of LHRH, somatostatin and bombesin. *Life Sciences* **2003,** 72, (21), 2305-2320.

24. Pasqualini, R.; Koivunen, E.; Ruoslahti, E., A Peptide Isolated from Phage Display Libraries Is a Structural and Functional Mimic of an RGD-binding Site on Integrins. *Journal of Cell Biology* **1995,** 130, 1189-1196.

25. Haubner, R.; Wester, H.-J.; Burkhart, F.; Senekowitsch-Schmidtke, R.; Weber, W.; Goodman, S.; Kessler, H.; Schwaiger, M., Glycosylated RGD-Containing Peptides: Tracer for Tumor Targeting and Angiogenesis Imaging with Improved Biokinetics. *Journal of Nuclear Medicine* **2001,** 42, 326-336.

26. Bhagwat, S.; Lahdenranta, J.; Giordano, R.; Arap, W.; Pasqualini, R.; Shapiro, L., CD13/APN is activated by angiogenic signals and is essential for capillary tube formation. *Blood* **2001,** 97, (3), 652-659.

27. Hanahan, D.; Folkman, J., Patterns and Emerging Mechanisms Review of the Angiogenic Switch during Tumorigenesis. *Cell (Cambridge, Massachusetts)* **1996,** 86, 353–364.

28. Bhagwat, S.; Petrovic, N.; Okamoto, Y.; Shapiro, L., The angiogenic regulator CD13/APN is a transcriptional target of Ras signaling pathways in endothelial morphogenesis. *Blood* **2003,** 101, 1818-1826.

29. Birkenkamp-Demtroder, K.; Christensen, L. L.; Olesen, S. H.; Frederiksen, C. M.; Laiho, P.; Aaltonen, L. A.; Laurberg, S.; Sorensen, F. B.; Hagemann, R.; Orntoft, T. F., Gene expression in colorectal cancer. *Cancer Research* **2002,** 62, (15), 4352-4363.

30. Curnis, F.; Arrigoni, G.; Sacchi, A.; Fischetti, L.; Arap, W.; Pasqualini, R.; Corti, A., Differential Binding of Drugs Containing the NGR Motif to CD13 Isoforms in Tumor Vessels, Epithelia, and Myeloid Cells. *Cancer Research* **2002,** 62, 867-874.

31. Ikeda, N.; Nakajima, Y.; Tokuhara, T.; Hattori, N.; Sho, M.; Kanehiro, H.; Miyake, M., Clinical Significance of Aminopeptidase N/CD13 Expression in Human Pancreatic Carcinoma. *Cancer Research* **2003,** 9, 1503-1508.

32. Shepherd, F.; Sridhar, S., Angiogenesis inhibitors under study for the treatment of lung cancer. *Lung Cancer* **2003,** 41, 63-72.

33. Giguere, C., M.; Bauman, N., M.; Smith, R., J. H., New treatment options for lymphangioma in infants and children. *The Annals of Otology, Rhinology, and Laryngology* **2002,** 111, (12 Pt 1), 1066-75.

34. Hashida, H.; Takabayashi, A.; Kanai, M.; Adachi, M.; Kondo, K.; Kohno, N.; Yamaoka, Y.; Miyake, M., Aminopeptidase N is involved in cell motility and angiogenesis: its clinical significance in human colon cancer. *Gastroenterology* **2002,** 122, (2), 376-386.

35. Albericio, F.; Cases, M.; Alsina, J.; Triolo, S. A.; Carpino, L. A.; Kates, S. A., On the use of PyAOP, a phosphonium salt derived from HOAt, in solid-phase peptide synthesis. *Tetrahedron Letters* **1997,** 38, (27), 4853-4856.

36. Aronov, O.; Horowitz, A.; Gabizon, A.; Gibson, D., Folate-Targeted PEG as a Potential Carrier for Carboplatin Analogs. Synthesis and in Vitro Studies. *Bioconjugate Chemistry* **2003,** 14, 563-574.

37. Berners-Price, S. J.; Frenkiel, T. A.; Frey, U.; Ranford, J. D.; Sadler, P. J., Hydrolysis products of cisplatin: pKa determinations via [1H, 15N] NMR spectroscopy. *Journal of the Chemical Society, Chemical Communications* **1992**, (10), 789-91.

38. Appleton, T. G.; Hall, J. R.; Ralph, S. F.; Thompson, C. S. M., NMR study of acid-base equilibria and other reactions of ammineplatinum complexes with aqua and hydroxo ligands. *Inorganic chemistry* **1989,** 28, (10), 1989-93.

39. Appleton, T. G.; Berry, R. D.; Davis, C. A.; Hall, J. R.; Kimlin, H. A., Reactions of platinum(II) aqua complexes. 1. Multinuclear (platinum-195, nitrogen-15, and phosphorus-31) NMR study of reactions between the cis-diammineaquaplatinum(II) cation and the oxygen-donor ligands hydroxide, perchlorate, nitrate, sulfate, phosphate, and acetate. *Inorganic Chemistry* **1984,** 23, (22), 3514-21.

40. Palocsay, F. A.; Rund, J. V., Reaction between 1,10-phenanthroline and platinum(II) compounds. I. Reaction in aqueous solution. *Inorganic Chemistry* **1969,** 8, (3), 524-8.

41. Basolo, F.; Bailar, J. C., Jr.; Tarr, B. R., The stereochemistry of complex inorganic compounds. X. The stereoisomers of dichlorobis(ethylenediamine)platinum(IV) chloride. *Journal of the American Chemical Society* **1950,** 72, 2433-8.

42. Aggarwal, S.; Takada, Y.; Singh, S.; Myers, J. N.; Aggarwal, B. B., Inhibition of growth and survival of human head and neck squamous cell carcinoma cells by curcumin via modulation of nuclear factor-kB signaling. *International Journal of Cancer* **2004,** 111, (5), 679-692.

43. Milanesio, M.; Monti, E.; Gariboldi, M. B.; Gabano, E.; Ravera, M.; Osella, D., Trend in cytotoxic activity of a series of cis-[APtCl2] (A=ethylenediamine methylated at different positions) complexes. *Inorganica Chimica Acta* **2008,** 361, (9-10), 2803-2814.

44. Gabano, E.; Colangelo, D.; Ghezzi, A. R.; Osella, D., The influence of temperature on antiproliferative effects, cellular uptake and DNA platination of the clinically employed Pt(II)-drugs. *Journal of Inorganic Biochemistry* **2008,** 102, (4), 629-635.

45. Bonetti, A.; Apostoli, P.; Zaninelli, M.; Pavanel, F.; Colombatti, M.; Cetto, G. L.; Franceschi, T.; Sperotto, L.; Leone, R., Inductively Coupled Plasma Mass Spectroscopy Quantitation of Platinum-DNA Adducts in Peripheral Blood Leukocytes of Patients Receiving Cisplatin- or Carboplatin-based Chemotherapy'. *Clinical Cancer Research* **1996,** 2, 1829-1835.

46. Harris, A.; Yang, X.; Hegmans, A.; Povirk, L.; Ryan, J.; Kelland, L.; Farrell, N., Synthesis, Characterization, and Cytotoxicity of a Novel Highly Charged Trinuclear Platinum Compound. Enhancement of Cellular Uptake with Charge. *Inorganic Chemistry* **2005,** 44, 9598-9600.

47. Elferink, F.; van der Vijgh, W. J.; ten Bokkel Huinink, W. W.; Vermorken, J. B.; Klein, I.; Winograd, B.; Knobf, M. K.; Simonetti, G.; Gall, H. E.; McVie, J. G., Pharmacokinetics of ethylenediaminemalonatoplatinum(II) (JM-40) during phase I trial. *British Journal of Cancer* **1987,** 56, (4), 479-83.

48. Hydes, P. C.; Russell, M. J. H., Advances in platinum cancer chemotherapy. Advances in the design of cisplatin analogs. *Cancer and Metastasis Reviews* **1988,** 7, (1), 67-89.

49. Chaoui, D.; Faussat, A.-M.; Majdak, P.; Tang, R.; Perrot, J.-Y.; Pasco, S.; Klein, C.; Marie, J.-P.; Legrand, O., JC-1, a sensitive probe for a simultaneous detection of P-glycoprotein activity and apoptosis in leukemic cells. *Cytometry, Part B: Clinical Cytometry* **2006,** 70B, (3), 189-196.

50. Pasini, A.; Zunino, F., New cisplatin analogs: on the way to better carcinostatics. *Angewandte Chemie* **1987,** 99, (7), 632-41.

51. Reedijk, J.; Fichtinger-Schepman, A. M. J.; Van Oosterom, A. T.; Van de Putte, P., Platinum amine coordination compounds as anti-tumor drugs. Molecular aspects of the mechanism of action. *Structure and Bonding (Berlin)* **1987,** 67, (Coord. Compd.: Synth. Med. Appl.), 53-89.

CHAPTER 3. PEPTIDE TARGETING OF PLATINUM ANTICANCER DRUG AND CURCUMIN USING LHRH MOTIF

3.1 Introduction

Besides cancers of the lung and bronchus, breast and prostate cancers are the most common causes of cancer deaths among women and men, respectively. With most conventional drugs and methods of cancer therapy having various side effects, targeted chemotherapy has become an increasingly popular and efficient way to reduce side effects by improving the systemic administration of toxic drugs.[1, 2] Various studies have found that receptors for certain peptides and hormones are found in higher concentrations in tumor cells than in normal cells. Luteinizing hormone-releasing hormone (LHRH), also known as GNRH1, has receptors on several malignant tissues, including breast, oral, and renal cancers, brain tumors, melanomas, and liver and prostate cancers.[3] Targeting of cancer therapeutics with hormones and hormone analogs has become a well-established method to generate lower toxicity and more efficient therapies. Our overall goal is to target tumor cells using a conjugate of LHRH, which has receptors in various tumor cells, with the anti drugs cisplatin and curcumin. Figure 3.1 shows the final structures of our target compounds.

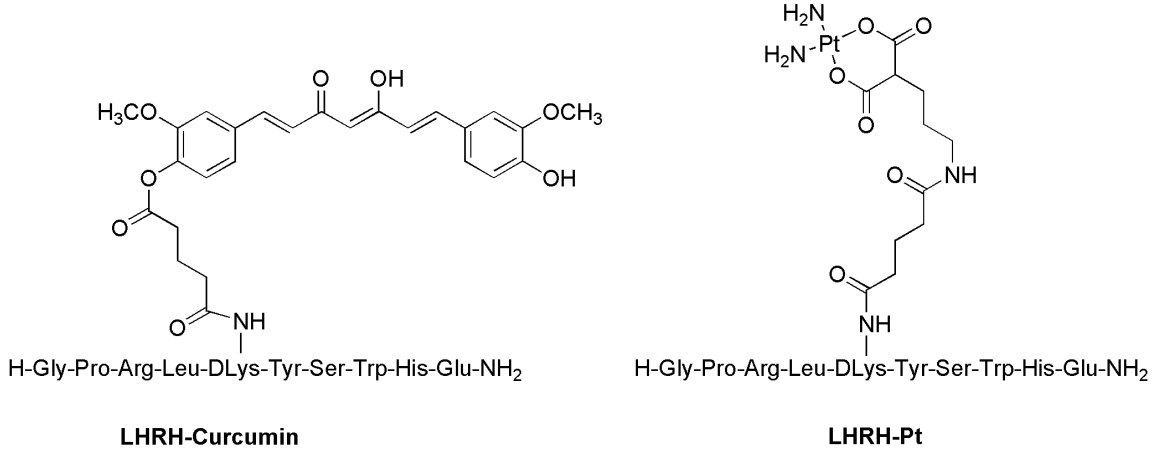

Figure 3.1. LHRH conjugates synthesized for this study.

Besides many hormonally targeted therapeutic agents developed for the treatment of various tumor cells, Schally et al. have extensively investigated LHRH, and found that the D-lys moiety offered the most convenient attachment of cytotoxic compounds without changing the intrinsic high-binding affinity of the peptide to receptors.[4-6] Previous studies had shown that substitution at position 6 of LHRH with a D-amino acid can allow further modification with large molecules, resulting in potent analogs with very high binding affinities.[3] Studies of conjugates of doxorubicin (DOX) and LHRH allowed the delivery of the cytotoxic DOX directly to the tumor cells, thereby increasing the concentration of the drug and sparing normal cells unnecessary exposure.[7, 8]

Curcumin, a polyphenol known to have antitumor effects, exists in three major curcuminoids components, which include cyclocurcumin (77%), demethoxycurcumin (17%) and bisdemethoxycurcumin (3%). Curcumin can exist in enol form or diketo form, with the enol form being prevalent in solution stemming an important feature on the radical-scavenging ability of curcumin. Apart from curcumin's traditional use in foods, mostly in Asia, it has also been used therapeutically for several ailments, including treatments for respiratory problems, diabetic wounds, cough, running nose, and abdominal pain; modern scientific research has confirmed its anti-inflammatory, antitumor, antimicrobial, antioxidant, and antiarthritic effects.[9-12] No studies have shown any toxicity associated with curcumin, irrespective of the concentration.[13-15]

Several platinum complexes discussed in the previous chapters are used in cancer chemotherapy; among them are cisplatin and its analogs. Besides the important use of cisplatin, various side effects make it usage limiting, the most common ones being nausea, nephrotoxity, vomiting, and neurotoxicity. Further, cancer patients are known to form a resistance to cisplatin, which is also a major issue. Targeting of cisplatin and its analogs helps to improve not only its

efficacy but also the therapeutic ratio of platinum agents. Interactions of platinum complexes, including cisplatin, carboplatin, and dichloro(ethylenediamine)platinum(II), among others, with DNA helps to arrest the replication and transcription process by being cytotoxic.[16,17]

We have designed two conjugates. One, a conjugate of curcumin and LHRH (LHRH-curcumin) addresses the hypothesis of whether or not free, diffusible curcumin is required for optimal anticancer activity. The second conjugate, a conjugate of cisplatin and LHRH, addresses a similar hypothesis and seeks to ameliorate the systemic side effects that cisplatin and currently approved tumor drugs have on normal cells. Targeting of cisplatin analogs using CNGRC, discussed in Chapter 2, has shown that targeted platinum complexes helps to increase specific damage to tumor cells. LHRH was coupled with di-tert-butyl 2-(3-glutaric aminopropyl)malonate, whose synthesis was reported in Chapter 2. LHRH-malonate allows the free bidentate carboxylic sites to react with activated cisplatin to form a targeted platinum complex (LHRH-Pt). With this in mind, we hypothesize that using LHRH, which has receptors in the tumor cell, is the most efficient way to deliver any chemotherapeutic agents to the tumor, hence improving the therapeutic ratio.

3.2 Experiment Section

3.2.1 Starting Materials. All starting materials listed below were obtained from commercial sources and used without further purification: di-tert-butyl malonate, glutaric anhydride (Aldrich), 3-bromopropyl phthalimide (Fluka). All amino acids and coupling reagents were obtained from EMD Biosciences.

3.2.2 NMR Spectroscopy. ^{1}H NMR spectra were recorded for solution in $CDCl_3$ on Bruker 400 MHz spectrometers. Peak positions are relative to TMS. All NMR data were processed with XWIN-NMR and MestRe-C software.

3.2.3 Peptide Purification and Characterization. All peptides were purified and characterized using protocols previously described in Chapter 2 unless otherwise stated. HPLC was performed using a Water 600E multisolvent delivery system with a model 486 tunable detector controlled by Empower software and Water Deltaprep system, with detection at 220 nm. Different columns were used for analysis and purification of the peptides. Analytical and semi-preparative chromatography was performed on a Delta-Pak C_4 (5 µm;100 Aº) reverse phase column (8× 100 mm) at 1 mL/min (column 1). Preparative HPLC was performed on Waters Delta-Pak C_4 (15 µm;100 Aº) reverse phase column (25 × 100 mm) at 15 mL/min (column 2). Linear gradients of 0.1% aqueous TFA in H_2O (Buffer A) and 0.1% TFA in MeCN (Buffer B) in all HPLC were used.

3.2.4 Procedure

3.2.4.1 Synthesis of Curcumin Glutarate Ester (1). Under dry conditions, a solution of curcumin (0.1 g, 0.271 mmol) in 1 mL of pyridine was allowed to stir at room temperature for 30 min. The solution was treated with glutaric anhydride (0.020 g, 0.180 mmol) and was left to stir overnight at 60 °C. The solution was concentrated by rotary evaporation, dissolved in CH_2Cl_2, and washed with 5% HCl. The organic fraction was dried over $MgSO_4$, and the solvent was removed by rotary evaporation. The solid product obtained was dried in a desiccator for eight hours to yield dry curcumin glutarate ester before proceeding to the next step (Scheme 3.2). Yield, 106 mg (90%). ^{1}H NMR (400 MHz, δ (ppm) in $CDCl_3$):7.61 (m, 2H), 7.16 (m, 5H), 6.94 (m, 1H), 6.53 (m, 2H). 5.83 (m, 2H), 3.95 (s, 3H), 3.87 (s, 3H), 2.70 (t, 2H), 2.56 (t, 2H), 2.11 (m, 2H). TOF-MS (ESI) 483.1657 ($M + H^+$), calculated for $C_{26}H_{26}O_9$ 483.16.

3.2.4.2 Synthesis of Di-tert-butyl 2-(3-glutaric aminopropyl)malonate (2). This was synthesized as described in chapter 2. The yield was 92%. ^{1}H NMR ($CDCl_3$) (ppm): 3.27 (q,

2H), 3.14 (t, 1H), 2.41 (t, 2H), 2.28 (t, 2H), 1.98 (m, 2H), 1.81(m, 2H), 1.56 (m, 2H), 1.45(s, 18H).

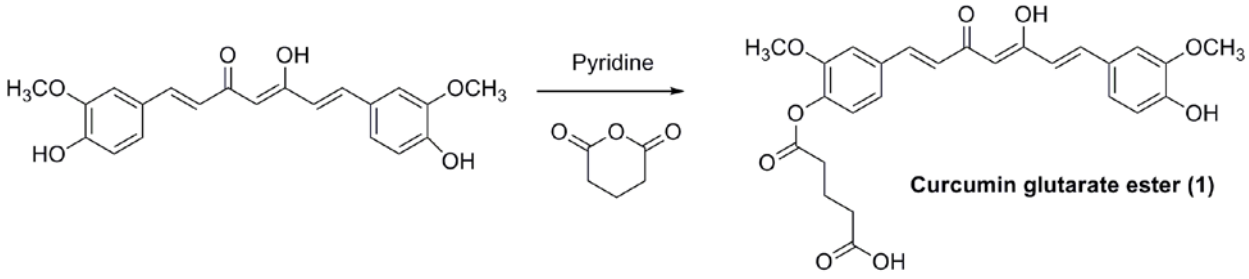

Scheme 3.1. Synthesis of curcumin glutarate ester.

3.2.4.3 Synthesis of LHRH-curcumin (3). LHRH-curcumin peptide was synthesized using standard Fmoc solid-phase chemistry. H-Rink Amide ChemMatrix resin (Scheme 3.2) (0.52 mmol) was placed in a normal resin column and washed with DMF. The side chain protected amino acid derivatives used in the sequence were Fmoc-Glu(OtBu)-OH, Fmoc-His(Trt)-OH, Fmoc-Trp(Boc)-OH, Fmoc-Ser(tBu)-OH, Fmoc-Tyr(tBu)-OH, Fmoc-D-Lys(Alloc)-OH, Fmoc-Leu-OH, Fmoc-Arg(Pbf)-OH, Fmoc-Pro-OH, and Boc-Gly-OH. The alloc-protecting group was removed using Pd(0) followed by double coupling of curcumin glutarate ester. All coupling utilized four equivalents each of amino acids, malonate, and PyAOP (sometimes HOBT and TBTU), dissolved in 0.5 M DIEA in DMF at room temperature (with a final concentration of 0.25 M). Washing between reaction times was done using DMF, and coupling involved minimal preactivation time. Deprotection of the Fmoc group was achieved using 20% piperidine in DMF for 5 min.

Once the peptide synthesis was complete, a 15 ml cocktail of TFA:phenol:water:TIPS (88:5:5:2) was added to the resin, and the mixture was agitated for 2.5 hours at room temperature. The mixture was filtered and the resin washed with TFA (5 mL). The combined aqueous TFA solutions were extracted with Et_2O and then freeze dried. The crude peptide was

purified by gel filtration to give pure aliquots of LHRH-curcumin. Yield, 0.09 g (36%), ESI-MS 1739.84 ($M + Na^+$), calculated for $C_{85}H_{108}N_{18}O_{21}$ 1717.88.

3.2.4.4 Synthesis of LHRH-malonate. LHRH-malonate was synthesized using standard Fmoc solid-phase chemistry, as described above. Similar side chain protected amino acid derivatives to those used in LHRH-curcumin peptide synthesis were used in this sequence. After the alloc-protecting group was removed using Pd(0), di-tert-butyl 2-(3-glutaric aminopropyl)malonate was coupled to the resin, followed by cleavage using the same cocktail cleavage solution described above. The crude peptide was purified by HPLC, where t_R = 25 min; yield, 0.10 g (39%), TOF-MS (ESI) 1529.75 $(M+H)^+$, calculated for $C_{70}H_{101}N_{19}O_{20}$ 1529.67.

3.2.4.5 Synthesis of LHRH-Pt (4). LHRH-malonate was dissolved in water, and the pH of the solution rose to 7 by titration with 1 M solution of NaOH to give neutral LHRH-malonate. The LHRH-malonate was diluted further using acetonitrile, yielding a solvent ratio of 1:2 (water:acetonitrile).

We prepared cis-$[Pt(NH_3)_2(D_2O)_2]^{2+}(NO_3)_2$ as described in Chapter 2. An excess of cis-$[Pt(NH_3)_2(D_2O)_2]^{2+}(NO_3)_2$ (2 fold) was reacted with LHRH-malonate solution to give crude LHRH-Pt conjugate, which was purified by gel filtration on a Sephadex G10 column. ESI-MS Yield 10% ESI-MS $(M + H)^{2+}$ Peak at 867.86 calculated for $C_{70}H_{103}N_{21}O_{19}Pt$ 1737.77.

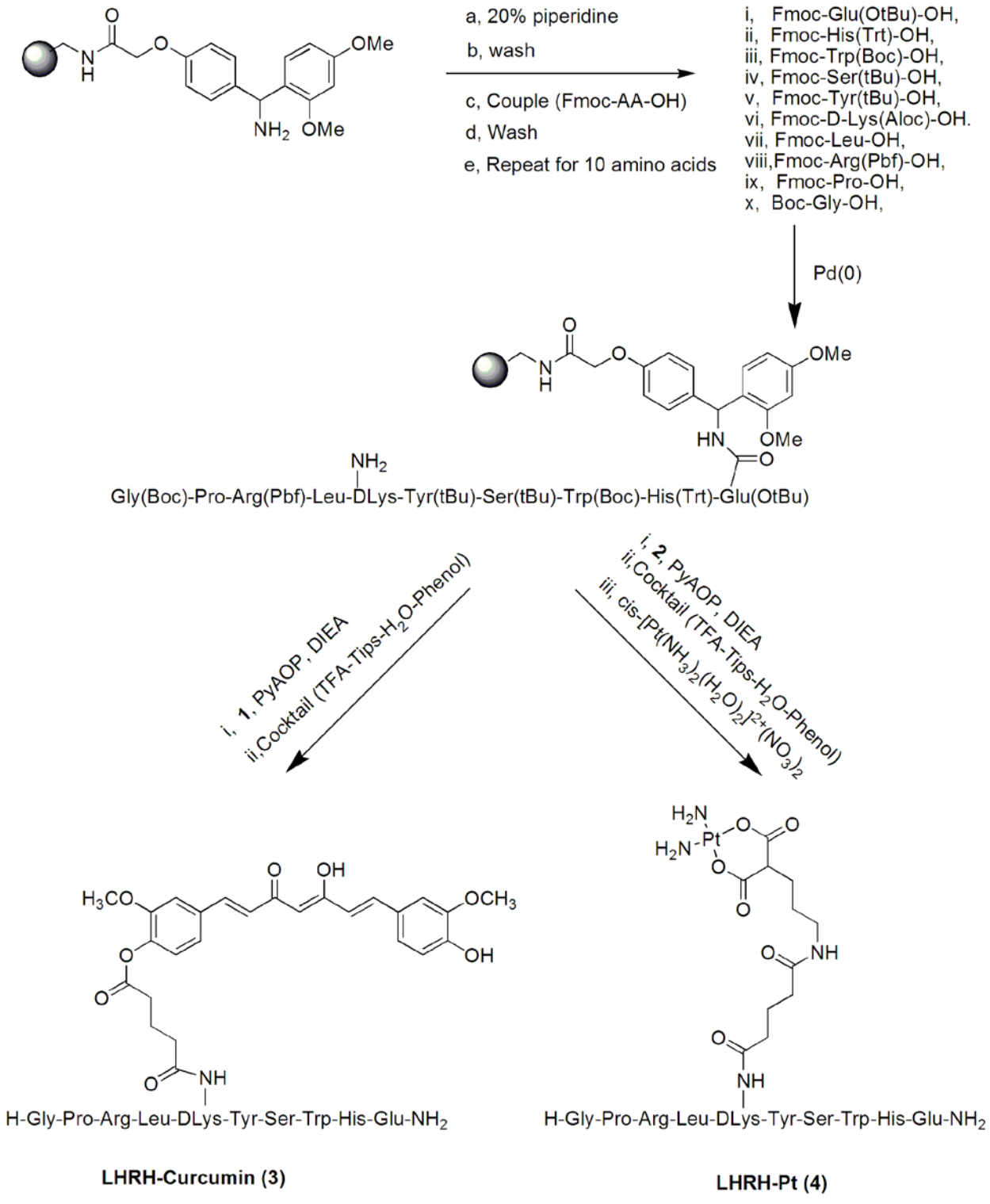

Scheme 3.2. Synthesis of LHRH-curcumin and LHRH-Pt.

3.3 Results and Discussion

The peptide LHRH was assembled using general Fmoc chemistry, using the amino acids described in the synthesis section. Once the peptide was assembled, a catalytic amount of Pd(0) was used to deprotect the primary amine at the D lysine in the presence of a nucleophile (morpholine), which mainly acts as a scavenger by capturing the carbocations generated.[18, 19] Sodium N,N-diethyldithiocarbamate in DMF was used in the washing step to help remove all of the palladium. A small amount of resin was cleaved and purified using HPLC and was analyzed by ESI to confirm the presence of all of the amino acids after removal of all protecting groups. Figure 3.2 shows the HPLC chromatogram of LHRH, which eluted in 8 min. The mass spectrum revealed the expected molecular weight with TOF-MS (ESI) $(M+H)^+$ at 1271.63 (Figure 3.3).

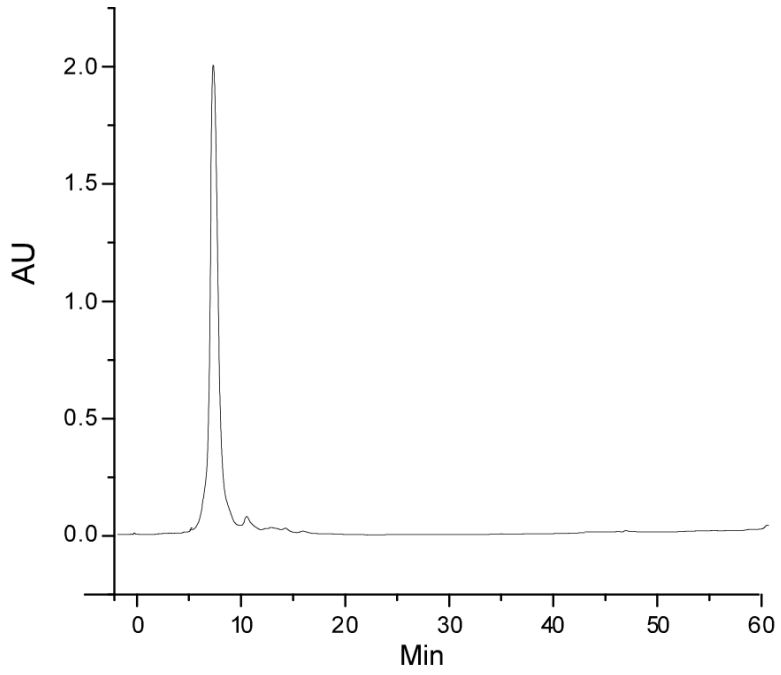

Figure 3.2. HPLC chromatogram of LHRH.

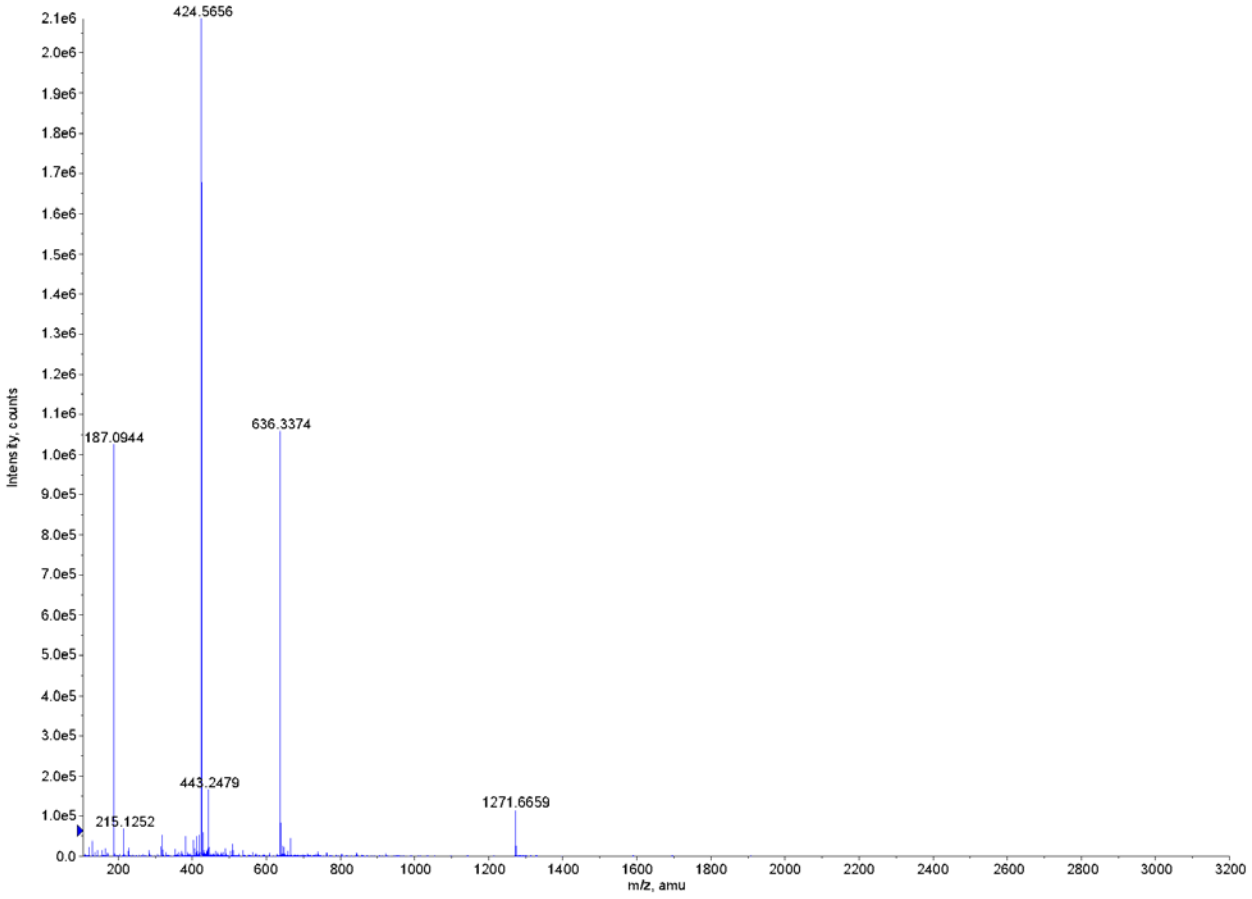

Figure 3.3. Mass spectra of LHRH free peptide.

Taking advantage of the well-established selective reactivity of the phenol group of curcumin, the reaction of glutaric anhydride with curcumin in the presence of a mild base such as pyridine gives the curcumin glutarate ester derivative. The ^{1}H NMR (Figure 3.4) and mass spectrum (Figure 3.5) revealed the formation and presence of the desired compound **1**.

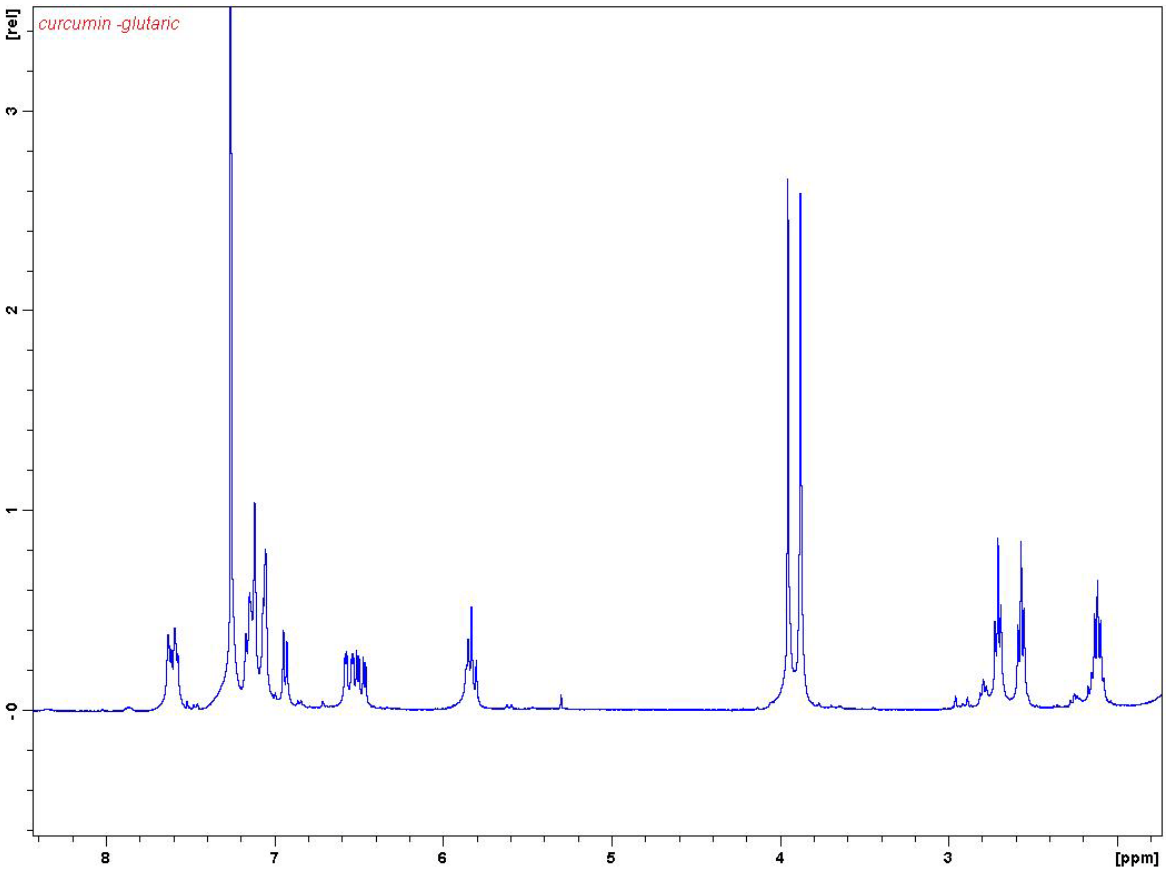

Figure 3.4. ^{1}H NMR of curcumin glutarate ester.

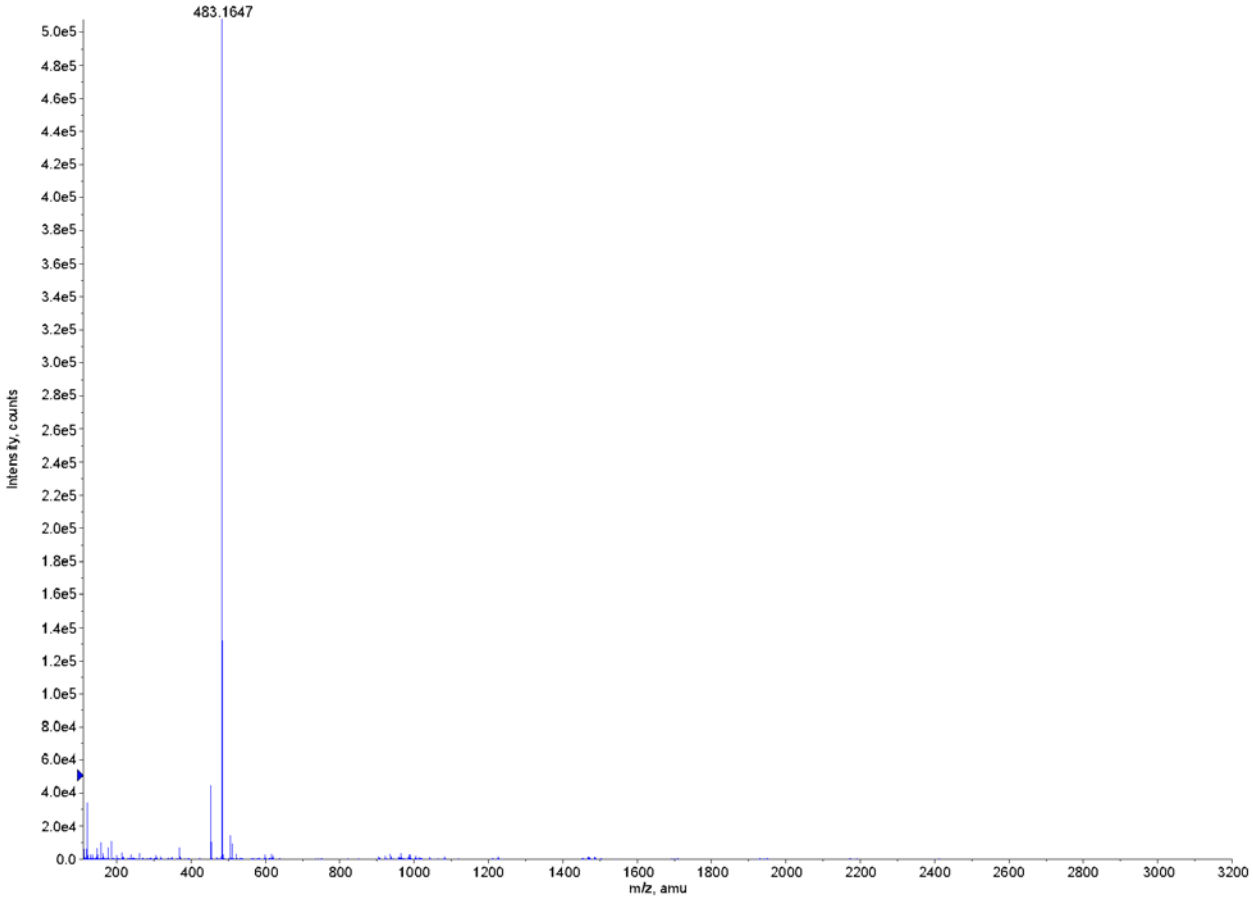

Figure 3.5. The mass spectrum of curcumin glutarate ester.

Coupling this derivative to [DLys^6]-LHRH was done in solid-phase synthesis of the peptide to give [DLys^6]-LHRH-curcumin. The curcumin should be readily released to the site of action, causing specific vascular damage to the tumor cells. *In vivo* and *in vitro* studies of the conjugate are still ongoing. Figure 3.6 shows the mass spectrum (ESI-MS), revealing the expected $(M+H)^+$ LHRH-curcumin peak at 1739.84 ($M + Na^+$), calculated for $C_{85}H_{108}N_{18}O_{21}$ 1717.88.

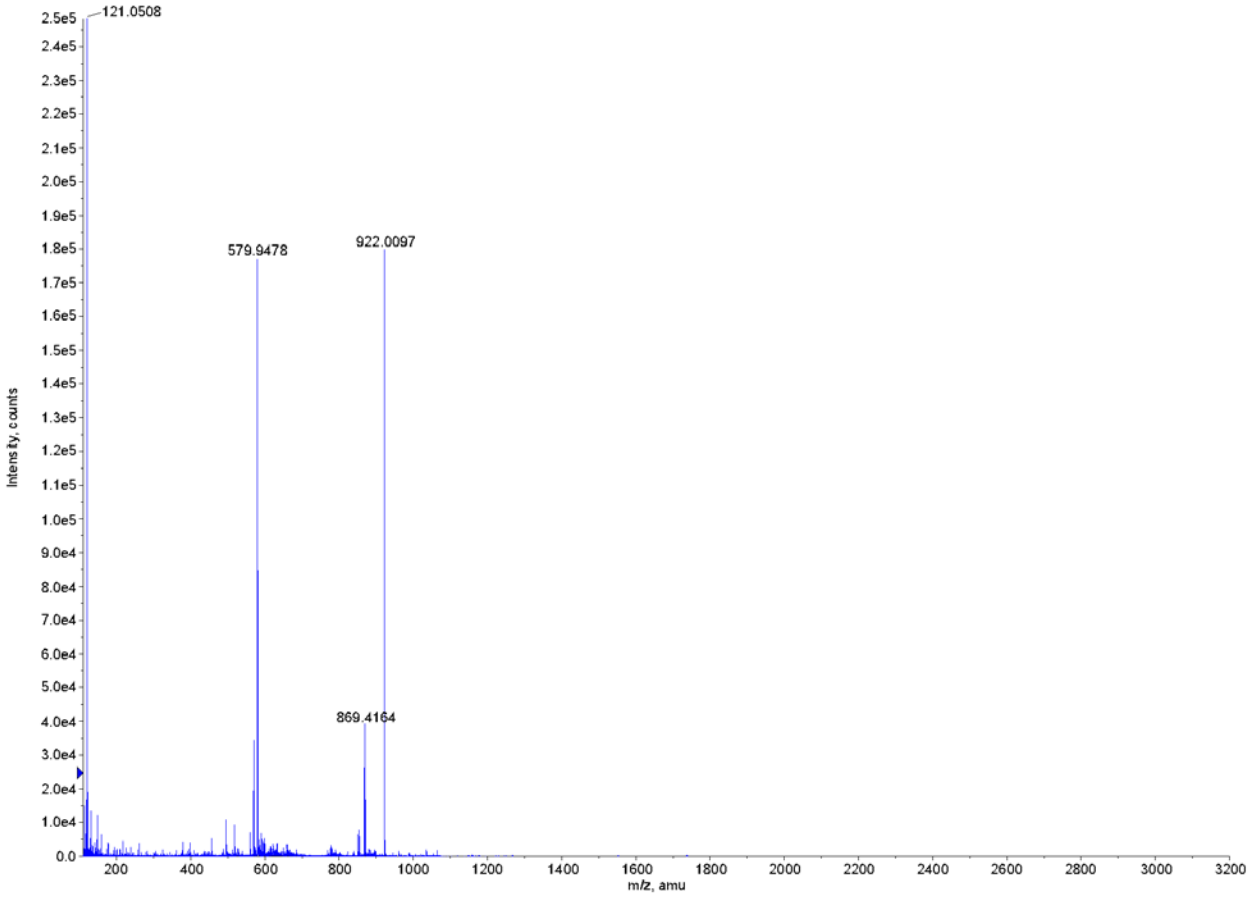

Figure 3.6. Mass spectra of LHRH-curcumin conjugate.

Coupling of di-tert-butyl 2-(3-glutaric aminopropyl)malonate on the free lysine of LHRH was achieved with the coupling agent PyAOP using solid-phase synthesis to give the LHRH-malonate. Purification of the peptide gave a single chromatogram of LHRH-malonate, which eluted in 25 min (Figure 3.7). Analysis by ESI revealed a strong peak at 1529.75 $(M+H)^+$, but the expected $(M+H)^+$ peak was 1511.65. Without cyclization to form pyroglutamic acid, we observed a molecular weight which matched the observed molecular weight at 1528.75.

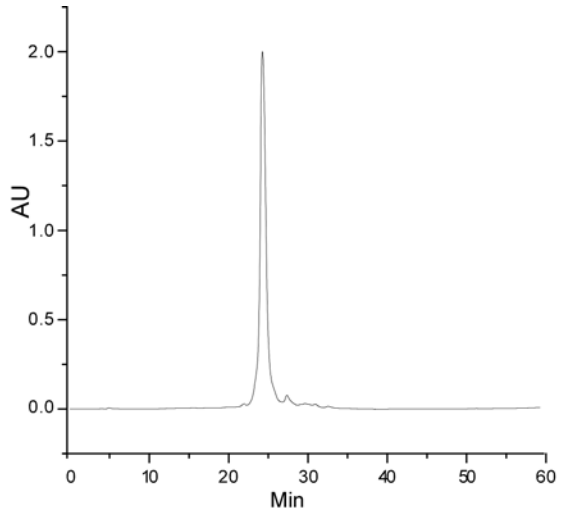

Figure 3.7. HPLC chromatogram of LHRH-malonate.

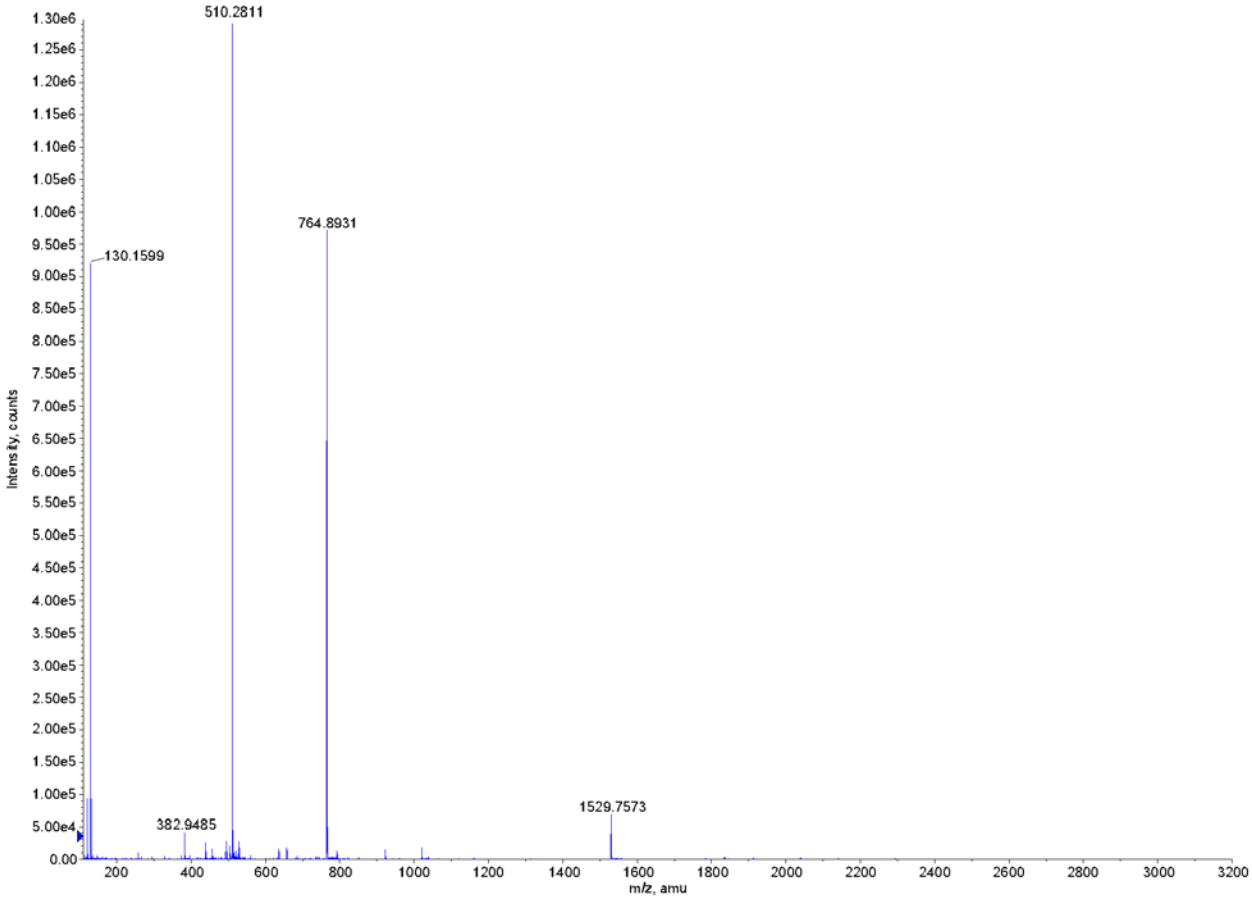

Figure 3.8. Mass spectrum of linear LHRH-malonate.

The dicarboxylic end of LHRH-malonate allows the chelation of the platinum ligand in a bidentate fashion on the peptide. A mixture of water:acetonitrile (50:50) was used in the platination step, allowing the solubility of LHRH-malonate at higher pH. On platination, separation was achieved by gel filtration on Sephadex G10 to give pure aliquots of LHRH-Pt conjugate; yield 10% $(M+2H)^{2+}$ peak at 867.86 calculated $C_{70}H_{103}N_{21}O_{19}Pt$ MW = 1737.77. *In vivo* and *in vitro* studies on the conjugate are still ongoing. Figure 3.9, below, shows the mass spectrum, revealing the expected LHRH-Pt

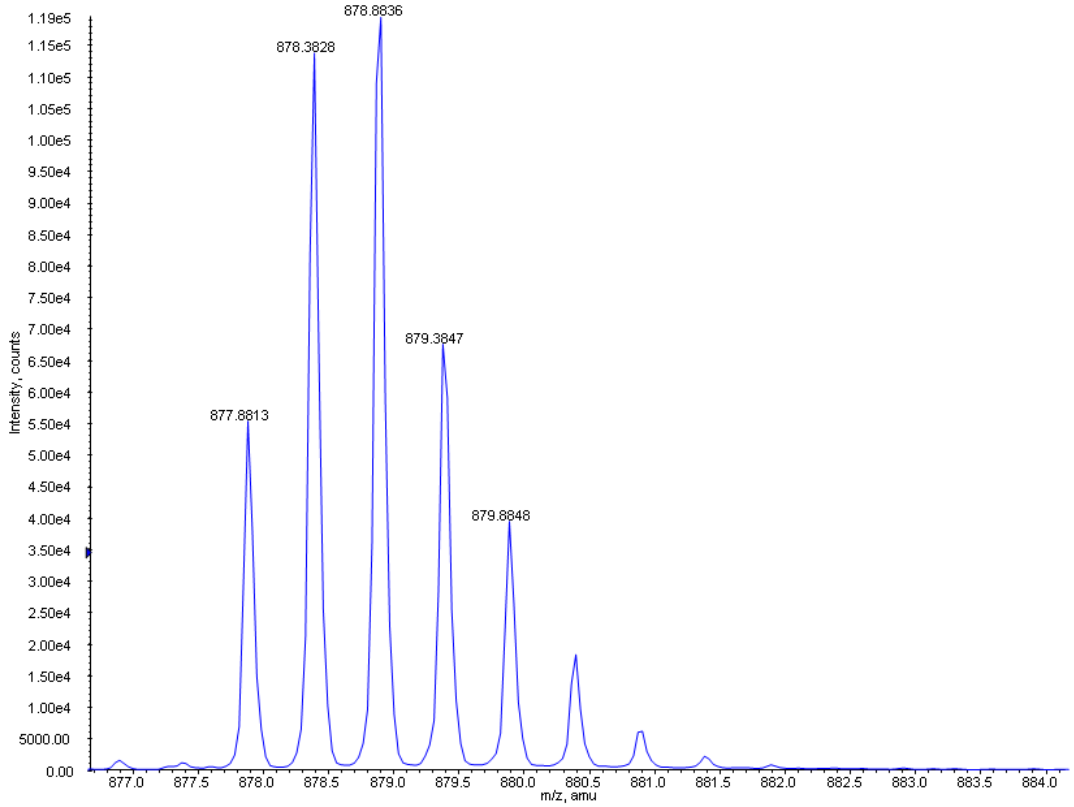

Figure 3.9. Mass spectrum of LHRH-Pt.

3.4 Conclusion

We accomplished the synthesis and characterization of LHRH-curcumin and LHRH-Pt, which are potential targeted antitumor agents. *In vitro* and *in vivo* studies are still ongoing.

3.5 References

1. van Zutphen, S.; Reedijk, J., Targeting platinum anti-tumour drugs: Overview of strategies employed to reduce systemic toxicity. *Coordination Chemistry Reviews* **2005,** 249, (24), 2845-2853.

2. Galanski, M.; Keppler, B. K., Searching for the magic bullet: anticancer platinum drugs which can be accumulated or activated in the tumor tissue. *Anti-Cancer Agents in Medicinal Chemistry* **2007,** 7, (1), 55-73.

3. Schally, A. V.; Nagy, A., New approaches to treatment of various cancers based on cytotoxic analogs of LHRH, somatostatin and bombesin. *Life Sciences* **2003,** 72, (21), 2305-2320.

4. Schally, A. V.; Nagy, A., Cancer chemotherapy based on targeting of cytotoxic peptide conjugates to their receptors on tumors. *European Journal of Endocrinology* **1999,** 141, (1), 1-14.

5. Nagy, A.; Schally, A. V., Cytotoxic analogs of luteinizing hormone-releasing hormone (LHRH): a new approach to targeted chemotherapy. *Drugs of the Future* **2002,** 27, (4), 359-370.

6. Nagy, A.; Schally, A. V., Targeting cytotoxic conjugates of somatostatin, luteinizing hormone-releasing hormone and bombesin to cancers expressing their receptors: a "smarter" chemotherapy. *Current Pharmaceutical Design* **2005,** 11, (9), 1167-1180.

7. Nagy, A.; Schally, A. V.; Armatis, P.; Szepeshazi, K.; Halmos, G.; Kovacs, M.; Zarandi, M.; Groot, K.; Miyazaki, M.; et al., Cytotoxic analogs of luteinizing hormone-releasing hormone containing doxorubicin or 2-pyrrolinodoxorubicin, a derivative 500-1000 times more potent. *Proceedings of the National Academy of Sciences of the United States of America* **1996,** 93, (14), 7269-7273.

8. Nakagawa-Goto, K.; Yamada, K.; Nakamura, S.; Chen, T.-H.; Chiang, P.-C.; Bastow, K. F.; Wang, S.-C.; Spohn, B.; Hung, M.-C.; Lee, F.-Y.; Lee, F.-C.; Lee, K.-H., Antitumor agents. Syntheses and evaluation of dietary antioxidant-taxoid conjugates as novel cytotoxic agents. *Bioorganic & Medicinal Chemistry Letters* **2007,** 17, (18), 5204-5209.

9. Rieks, A.; Kaehler, M.; Kirchner, U.; Wiggenhorn, K.; Kinzer, M. Preparation of curcumin esters for use in cosmetics, pharmaceuticals, and food additives. 2002-1024598810245988, 20021001., 2004.

10. Rieks, A.; Kaehler, M.; Kirchner, U.; Wiggenhorn, K.; Kinzer, M. Preparation of novel curcumin/tetrahydrocurcumin derivatives for use in cosmetics, pharmaceuticals and for nutrition. 2003-EP107722004031122, 20030926., 2004.

11. Liu, J.; Jiang, F., Design, synthesis, and primary evaluation on curcumin derivative as prodrugs of antitumor. *Zhongguo Yaoshi (Wuhan, China)* **2005,** 8, (7), 543-545.

12. Sethi, S. C.; Rao, B. C. S., Coloration of vanaspati. *Indian Journal of Technology* **1964,** 2, (16), 208.

13. Aggarwal, S.; Ichikawa, H.; Takada, Y.; Sandur, S. K.; Shishodia, S.; Aggarwal, B. B., Curcumin (diferuloylmethane) down-regulates expression of cell proliferation and antiapoptotic and metastatic gene products through suppression of IkBalpha kinase and akt activation. *Molecular Pharmacology* **2006,** 69, (1), 195-206.

14. Goel, A.; Kunnumakkara, A. B.; Aggarwal, B. B., Curcumin as "Curecumin": From kitchen to clinic. *Biochemical Pharmacology* **2008,** 75, (4), 787-809.

15. O'Connell, M. A.; Rushworth, S. A., Curcumin: potential for hepatic fibrosis therapy? *British Journal of Pharmacology* **2008,** 153, (3), 403-405.

16. Bruhn, S. L.; Toney, J. H.; Lippard, S. J., Biological processing of DNA modified by platinum compounds. *Progress in Inorganic Chemistry* **1990,** 38, 477-516.

17. Heiger-Bernays, W. J.; Essigmann, J. M.; Lippard, S. J., Effect of the antitumor drug cis-diamminedichloroplatinum(II) and related platinum complexes on eukaryotic DNA replication. *Biochemistry* **1990,** 29, (36), 8461-6.

18. Zorn, C.; Gnad, F.; Salmen, S.; Herpin, T.; Reiser, O., Deprotection of N-Alloc amines by Pd(0)/DABCO-an efficient method for in situ peptide coupling of labile amino acids. *Tetrahedron Letters* **2001,** 42, (40), 7049-7053.

19. Loffet, A.; Zhang, H. X., Allyl-based groups for side-chain protection of amino acids. *International Journal of Peptide and Protein Research* **1993,** 42, (4), 346-51.

CHAPTER 4. EXPLORING WATER SOLUBLE *N*-TRIDENTATE Pt(II) COMPLEXES USEFUL FOR SPECTROSCOPIC AND BIOLOGICAL LABELING

4.1 Introduction

The interaction of nucleotides with transition metals, particularly platinum has been widely reported in recent years; however, with many cellular organelles that can be targeted, the search for its biological target and mechanism continues.[1, 2] *Cis*-diamminedichloroplatinum(II), cisplatin, is one of the widely used anticancer drugs. When administered, it can interact with various cellular components which include glutathione, mitochondria, RNA and DNA, with DNA generally accepted as the primary target.[1, 3-6] The interaction of Pt complexes with mixed metallothionein and glutathione is believed to be the main cause of resistance and other shortcomings associated with Pt (II) species.[7-9] Interaction of cisplatin with DNA has been widely studied.[1, 10] Cisplatin reacts with DNA by the formation of covalent bonds with N7 purines. It's interaction with various biological targets and formation of various adducts on interaction with DNA makes its study too complicated.[11, 12]

There is need to develop model compounds that have suitable pharmaceutical properties, are simple and can be monitored spectroscopically to allow further studies on interaction with DNA. The diethylenetriamine (dien) complex, $[Pt(dien)Br]^+$ and [Pt(dien)Cl]Cl have been extensively used as monofunctional model compounds to study the binding of metal complexes, particularly platinum complexes, to DNA and proteins, giving some insight on complicated reactions formed by bidentate platinum complexes.[6,10, 13]

Structure-activity study of polyamine analogues reveals that slight structure alteration causes remarkable changes in their biological activity. *N*-alkylated polyamines have been found to alter the neoplastic activity in various human tumor lines.[11, 14] The combination of the

antitumor ligand (polyamine) and the transition metal, Pt(II), with a labeling agent can find application in many methods in biological research and medical diagnosis. By labeling, we can analyze the tagged biomolecule and its metabolites in addition to other information about location, size, amount, and properties of biological systems.[15, 16]

Our desire for a good spectroscopic probe for studies on the binding of [Pt(dien)X]X-type complexes to biomolecules has prompted us to select *N*′-[7-(acetamido)-4-(trifluoromethyl)coumarin]diethylenetriamine (atfcdien) and 2-(bis(2-aminoethyl)amino)acetic acid (acdien) tridentate ligands for Pt. (Scheme 4.1). These diethylenetriamine derivatives are simple with good spectroscopic properties and atfcdien has the 7-amino-4-(trifluoromethyl)coumarin (atfc) fluorophore which is fluorescent.

We report the synthesis, and ^{1}H NMR characterization of the *N*′-[7-(acetamido)-4-(trifluoromethyl)coumarin] diethylenetriamine (atfcdien) ligand (HBr salt), 2-(bis(2-aminoethyl)amino)acetic acid (acdien)(Scheme 4.1) and their platinum complexes (Scheme 4.2). Our synthetic approach gave good yields and a tractable product. We directly prepared and crystallized there water-soluble [Pt(atfcdien)Br][Pt(Me_2SO)Br_3] and [Pt(acdien)Br]Br complexes. ^{1}H NMR investigation of the interaction [Pt(acdien)Br]Br with guanosine 5′-monophosphate (5′-GMP) in D_2O solution confirmed binding and the presence of one set of ^{1}H NMR signals implying rapidly inter-converting rotamers. Interaction between [Pt(atfcdien)Br]Br complex and 5′-GMP gave a Pt(atfcdien)(5′-GMP) adduct which had two H1′ (5′-GMP moiety) and two different H5, H6 and H8(coumarin moiety) signals implying slow rate of rotation about the Pt-N7 bond.

4.2 Experimental Section

4.2.1 Starting Materials. Diethylenetriamine (dien), bromoacetyl bromide, benzyl 2-bromoacetate and 5′-GMP were obtained from Aldrich and atfc was obtained from Lancaster and used without further purification. *N*,*N*′′-bis(*tert*-butyloxycarbonyl)diethylenetriamine (Bocdien), 7-(bromoacetamido)-4-(trifluoromethyl)coumarin (atfcBr), and *cis*-$Pt(Me_2SO)_2Cl_2$ were prepared by known methods.[17-21]

4.2.2 Instrumental measurement

4.2.2.1 NMR Spectroscopy. ^1H NMR spectra were recorded for solution in DMSO-d_6, $CDCl_3$, and D_2O on Bruker 300 MHz, and 400 MHz spectrometers. Peak positions are relative to TMS. All NMR data were processed with *XWINNMR* and *Mestre-C* softwares. For all integrations each proton is represented as 1H.

4.2.2.2 Fluorescence Spectroscopy. DMSO solutions (5 μM) of 7-amino-4-(trifluoromethyl)coumarin (atfc), 7-(bromoacetamido)-4-(trifluoromethyl)coumarin (atfcBr), *N*′-[7-(acetamido)-4-(trifluoromethyl)coumarin]diethylenetriamine **(**atfcdien), and the $[Pt(atfcdien)Br]^+$ cation were prepared for fluorescence studies. The emission spectra were recorded at the excitation wavelength of 369 nm at 25 °C in 10 mm quartz cuvettes using a Spex Fluorolog-3 spectrofluorimeter equipped with a 450 W xenon lamp and photomultiplier tube detector.

4.2.2.3 X-ray Data Collection and Structure Determination. Intensity data were collected for the four compounds at T=110K, using graphite monochromated MoKα radiation (λ = 0.71073 Å) on a Nonius KappaCCD diffractometer fitted with an Oxford Cryostream cooler. Data reduction included absorption corrections by the multi-scan method. Crystal data and experimental details are given in Table **4.2** and **4.3**. Structures were solved by direct methods and

refined by full-matrix least squares, using *SHELXL97*.[22] C-H hydrogen atoms were treated as riding in idealized positions, with a torsional parameter refined for each methyl group. The N-H hydrogen atom of atfcBr (**2**) was refined, and all others were treated as for C-H. One water H atom for both compound (**8**) and (**9**) could not be located. All residual electron density peaks greater than 1 eÅ^{-3} were located near heavy-atom positions.

4.2.3 Synthesis

4.2.3.1 *N,N′′*-bis(tert-butyloxycarbonyl)diethylenetriamine (Bocdien, 1). The Bocdien (**1**) ligand was prepared in 50% yield by a known method.[19] Briefly, Dry toluene (150 mL), *tert*-butanol (40 mmol), KOH (1 mmol), and 1,1′-carbonyldiimidazole (40 mmol) were added to a 250 mL round-bottom flask fitted with a dry N inlet and magnetic stirrer and heated to 60 °C with stirring for 3 h. Dien (20 mmol) was added drop-wise. The solution was left to stir at 60 °C for a further 3h. The clear mixture was left to cool. The reaction was concentrated in vacuo, dissolved in CH_2Cl_2 (100 mL), and washed three times with water (3 X 50 mL). The solution was dried with anhydrous Na_2SO_4 and concentrated in vacuo to give colorless oil. ^{1}H NMR chemical shifts matched the reported values. Colorless needle-shaped crystals of **1**•HCl were obtained by dissolving Bocdien (**1**) in a equal volume of toluene and dichloromethane and the solution was allowed to stand at 25 °C for 5 days.

4.2.3.2 7-(Bromoacetamido)-4-(trifluoromethyl)coumarin (atfcBr, 2). AtfcBr (**2**) was prepared in 95% yield by a known method.[21] Briefly 7- amino-4-(trifluoromethyl)coumarin (0.42 g, 1.0 mmol) was added to an ice-cold solution of 0.2 mL (2.3 mmol) of bromoacetyl bromide in 1 mL of tetrahydrofuran. After 30 min at room temperature, 10 mL of ice water was added. The product was separated, washed with water, dried, and recrystallized from ethyl acetate. Yellow blade-shaped crystals were obtained by dissolving atfcBr (**2**) in ethyl acetate and minimal amount of hexane and the solution was allowed to stand at 25 °C for 3 days. The measured

melting point, 200.00 °C, agrees with the reported value. ^{1}H NMR (300 MHz, δ (ppm) in DMSO-d_6): 7.86 (s, 1H), 7.72 (d, 1H), 7.54 (d, 1H), 6.93 (s, 1H), 4.09 (s, 2H), 10.96 (NH).

4.2.3.3 *N′*-[7-(acetamido)-4-(trifluoromethyl)coumarin]diethylenetriamine (atfcdien, 4). A solution of Bocdien (**1**) (1.0 g, 3.3 mmol) in 10 mL of THF-H_2O (25:1) was treated with a solution of atfcBr (**2**) (0.835 g, 4.8 mmol) and K_2CO_3 (0.29 g, 2.1 mmol) in 5 mL of THF-H_2O (25:1) and allowed to stir at 25 °C for 12 hours. The solution was concentrated to 5 ml by rotary evaporation, loaded onto a silica gel column (2 × 19 cm, 100-200 mesh, Davisil, Grade 634, Type 60A) and eluted with ethylacetate-hexane (2:98) until all of atfcBr (**2**) was removed. The product was then eluted with 100% ethyl acetate. Removal of all solvent by rotary evaporation produced *N*,*N″*-bis(*tert*-butyloxycarbonyl)diethylenetriaminly-*N′*-[7-(acetamido)-4-(trifluoromethyl)coumarin] (Bocdienatfc) (**3**) as a yellow solid; yield, 1.21 g, (71%). ^{1}H NMR (400 MHz, δ (ppm) in DMSO-d_6): 7.90 (s, 1H), 7.73 (d, 1H), 7.67 (d, 1H), 6.91 (s, 1H), 3.02 (t, 4H), 2.58 (t, 4H), 3.83 (s, 2H), 1.32 (s, 18H), 10.12 (NH).

A solution of Bocdienatfc (**3**) (1.06 g, 1.85 mmol) in 10 mL of 30% HBr in acetic acid was heated at 90 °C for 12 h in a pressure-resistant tube. A light brown solid (atfcdien•3HBr) was obtained upon cooling the solution at 25 °C, the precipitate was collected by filtration, washed with ether, and dried under vacuum; yield, 0.79 g (70%). ^{1}H NMR (400 MHz, δ (ppm) in D_2O): 7.81 (s, 1H), 7.79 (d, 2H), 7.42 (d, 1H), 6.87 (s, 1H), 3.58 (s, 2H), 3.10 (t, 4H), 2.94 (t, 4H).). Anal. Calcd for $C_{16}H_{21}F_3N_4O_4$: •3HBr: C, 30.35; H, 3.82; N, 8.85. Found: C, 30.07; H, 3.70; N, 8.61.

4.2.3.4 *N,N″*-bis(*tert*-butyloxycarbonyl)diethylenetriaminly-*N′*-glycine (Bocdienac, 6). Using the same procedure described for the preparation of **3**, a solution of Bocdien **(1)** was treated with benzyl 2-bromoacetate to obtain *N,N″*-bis(*tert*-butyloxycarbonyl)diethylenetriaminly-*N′*-

[glycine-benzylester] (Bocdienbz) **5** (Scheme 4.1); yield, 5.46 g, (92%). ^{1}H NMR (400 MHz, δ (ppm) in D_2O): 7.36 (m, 5H), 5.15 (s, 2H), 3.43 (s, 2H), 3.15 (t, 4H), 2.74 (t, 4H), 1.45 (s, 18H).

Bocdienbz (**5)** (3.45 g, 7.65 mmol) was dissolved in 50 ml EtOH-cyclohexene (2:1). Pd/C (5%, 1.5 g) was added using additional 50 ml EtOH-cyclohexene (2:1). The mixture was stirred for 12 h under H_2 and then filtered through celite and washed with methanol. The solvent was removed by rotary evaporation to yield an off-white solid which was crystallized from MeOH/Ether. The solid obtained was washed with ether and air dried to give Bocdienac (**6**); yield, 2.62 g (95%) ^{1}H NMR (400 MHz, δ (ppm) in $CDCl_3$): 1.47 (s, 18H), 3.41 (t, 4H), 3.51 (t, 4H), 3.80 (s, 2H). Anal. Calcd for $C_{16}H_{31}N_4O_6$: C, 53.17; H, 8.65; N, 11.63. Found: C, 53.02; H, 8.63; N, 11.45.

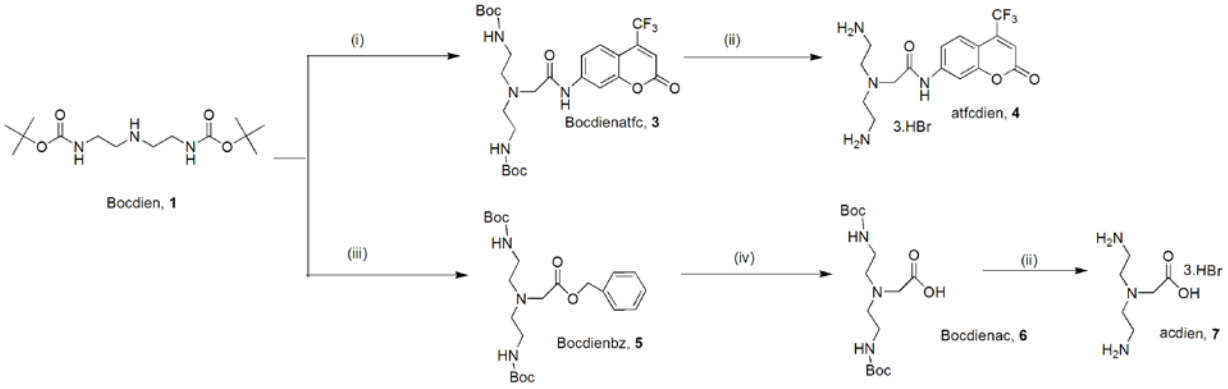

Scheme 4.1. Synthesis of atfcdien and acdien. Reagents and conditions: (i) **2**, THF, H_2O, K_2CO_3 25 °C, 12 h; (ii) 30% HBr in acetic acid; (iii) benzyl 2-bromoacetate, THF, H_2O, K_2CO_3; (iv) cyclohexene, MeOH, Pd/c, H_2.

4.2.3.5 2-(Bis(2-aminoethyl)amino)acetic acid (acdien•3HBr, 7). Bocdienac (**6)** (Scheme 4.1) was deprotected using the procedure for atfcdien•3HBr (**4**) to give 2-(bis(2-aminoethyl)amino)acetic acid (acdien•3HBr) **7;** yield, 0.67 g (90%). Briefly, a solution of Bocdienac (**6**) (0.66 g, 1.85 mmol) in 10 mL of 30% HBr in acetic acid was heated at 90 °C for 12 h in a pressure-resistant tube. A light yellow solid (acdien•3HBr) was obtained upon cooling the solution at 25 °C, the precipitate was collected by filtration, washed with ether, and dried

under vacuum. ^{1}H NMR (400 MHz, δ (ppm) in D_2O): 3.01 (t, 4H), 3.15 (t, 4H), 3.56 (s, 2H). Anal. Calcd for $C_6H_{18}N_3O_2$•3HBr•H_2O: C, 17.08; H, 4.78; N, 9.96. Found: C, 17.20; H, 4.82; N, 9.90.

4.2.3.6 [Pt(atfcdien)Br][Pt(Me$_2$SO)Br$_3$]. A solution of atfcdien•3HBr (**4)** (31.1 mg, 0.049 mmol) in 1 mL of H_2O was neutralized by the addition of aqueous KOH (8.2 mg in 0.5 mL), under stirring to give the free amine. *cis*-Pt$(Me_2SO)_2Cl_2$ (20.6 mg, 0.049 mmol) was suspended in 10 mL of acetone with stirring. The solution of the free amine was added drop wise to the *cis*-Pt$(Me_2SO)_2Cl_2$ suspension, and a bright yellow solution was obtained. The yellow solution was stirred overnight and then reduced to ~2 mL under vacuum. The yellow precipitate, [Pt(atfcdien)Br]Br formed was collected by filtration and the clear filtrate upon keeping at 5 °C for 2 weeks gave orange plate like crystals of [Pt(atfcdien)Br][Pt$(Me_2SO)Br_3$] (Scheme 4.2). ^{1}H NMR of the yellow powder [Pt(atfcdien)Br]Br and [Pt(atfcdien)Br][Pt$(Me_2SO)Br_3$] were similar; yield for [Pt(atfcdien)Br][Pt$(Me_2SO)Br_3$] (**8a**): 10 mg, (35%); yield for [Pt(atfcdien)Br]Br(**8b**): 10.6 mg, (30%) ^{1}H NMR (400 MHz, δ (ppm) in DMSO-d_6): 7.92 (s, 1H), 7.78 (d, 1H), 7.57 (d, 1H), 7.02 (s, 1H), 4.45 (s, 2H), 5.79 (NH), 5.48 (NH), 3.47-2.97(br m, 8H, CH_2). Anal. Calcd for $C_{18}H_{25}Br_4F_3N_4O_4Pt_2S$•$CH_3COCH_3$•$H_2O$: C, 20.40; H, 2.69; N, 4.53. Found: C, 20.45; H, 2.46; N, 4.83.

4.2.3.7 [Pt(acdien)Br]Br (9a). [Pt(acdien)Br]Br was synthesized and crystallized as a monohydrate using the experimental procedure described in the synthesis of [Pt(atfcdien)Br][Pt$(Me_2SO)Br_3$]; yield 18 mg, (75%). ^{1}H NMR (400 MHz, δ (ppm) in D_2O): 5.42 (br s, NH), 4.97 (br s, NH), 4.29 (d, 2H), 3.65-2.99 (br m, 8H, CH_2). Anal. Calcd for $C_6H_{15}Br_2N_3O_2Pt$•0.5CH_3OH: C, 14.67; H, 3.22; N, 7.90. Found: C, 14.51; H, 3.03; N, 7.99.

4.2.3.8 [Pt(acdien)Cl]Cl (9b). 4 M HCl in dioxane was used for the deprotection of Bocdienac as described in the experimental procedure for the synthesis of atfcdien•3HBr (**4**) to give an off white solid of atfcdien•3HCl. Briefly, a solution of Bocdienac (**6**) (1.00 g, 2.77 mmol) in 10 mL of 4 M HCl in dioxane was heated at 90 °C for 12 h in a pressure-resistant tube. A white solid was obtained upon cooling the solution at 25 °C, the precipitate was collected by filtration, washed with ether, and dried under vacuum to give acdien•3HCl; yield 0.37 mg, (50%). This was further treated with *cis*-$Pt(Me_2SO)_2Cl_2$ as described in the synthesis of Pt(atfcdien)Br][$Pt(Me_2SO)Br_3$] to give [Pt(atfcdien)Cl]Cl; yield 20 mg, (78%). ^{1}H NMR (400 MHz, δ (ppm) in D_2O): 5.42 (br s, NH), 4.97 (br s, NH), 4.26 (d, 2H), 3.73-3.15 (br m, 8H, CH_2). Anal. Calcd for $C_6H_{15}Cl_2N_3O_2Pt$: C, 16.87; H, 3.54; N, 9.84. Found: C, 17.00; H, 3.76; N, 9.63.

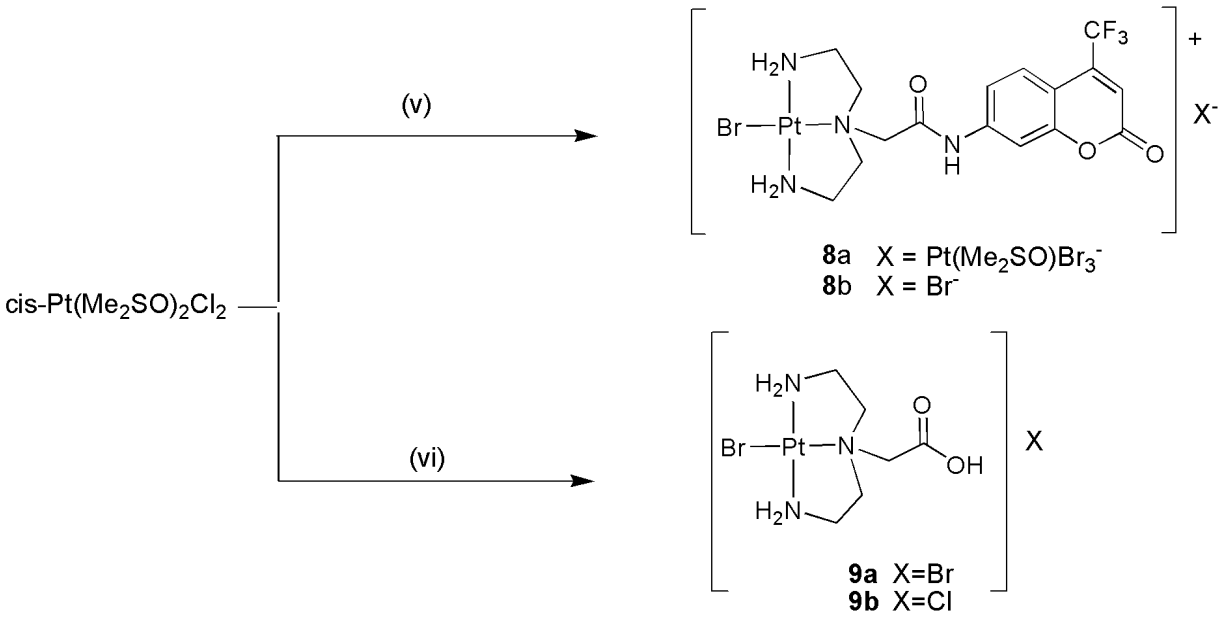

Scheme 4.2. Synthesis of $[Pt(atfcdien)Br]^+$ and $[Pt(acdien)Br]^+$**.** Reagents and conditions: (v) **4**, acetone, H_2O, KOH; (vi) **7**, acetone, H_2O, KOH.

4.2.3.9 Formation of Pt(acdien)(5′-GMP) and Pt(atfcdien)(5′-GMP). A solution of Pt(acdien)(5′-GMP) and Pt(atfcdien)(5′-GMP) was prepared by treatment of [Pt(acdien)Br]Br and [Pt(atfcdien)Br]Br (5 mM) respectively in D_2O (600 μL) with 5′-GMP in a stoichiometric

amount at pH = 4.2. The solution was maintained at 25 °C and monitored by ^{1}H NMR spectroscopy until no change in signal intensity was observed. DNO_3 and NaOD solutions (0.1 M in D_2O) were used to adjust the pH of D_2O solutions directly in the NMR tube when necessary.

4.3 Results and Discussion

4.3.1 Atfcdien and Acdien Synthesis. The general strategy of the synthesis of atfcdien and acdien is shown in Scheme 4.1. Synthesis of Bocdien and atfcBr provide us with universal starting materials for all the subsequent syntheses. AtfcBr was first reported by Bissell *et al.*[21] and was characterized by melting point only. In addition to the melting point, we were able to crystallize the product (Figure 4.1) and characterize by ^{1}H NMR spectroscopy.

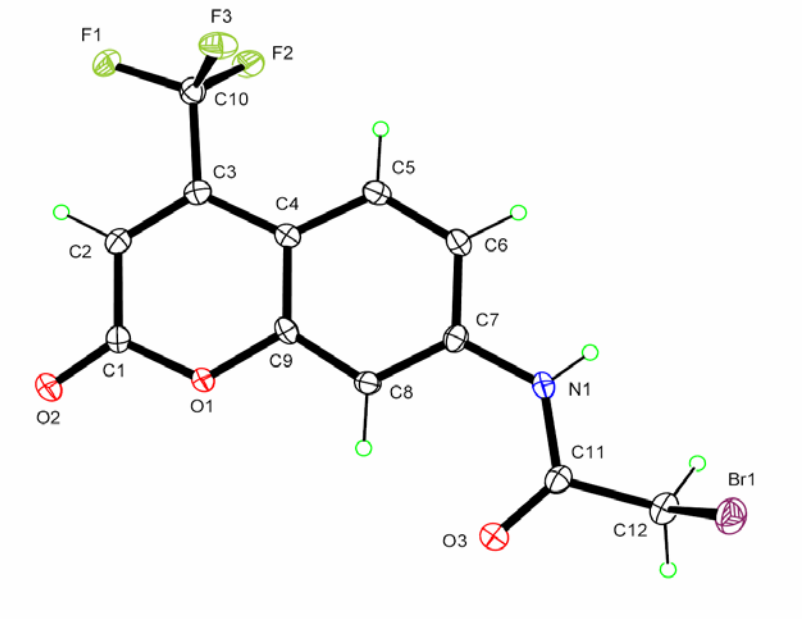

Figure 4.1 Ortep rendering of the structure of atfcBr (**2)** (50% probability ellipsoids).

The synthesis of Bocdien was reported by Rannard *et al.*[19] Selective protection of the primary amines allow as to put desirable function on the secondary amine. Beside high yields being reported by Rannard group (95%), we were only able to obtain 50% yield (Figure 4.2).

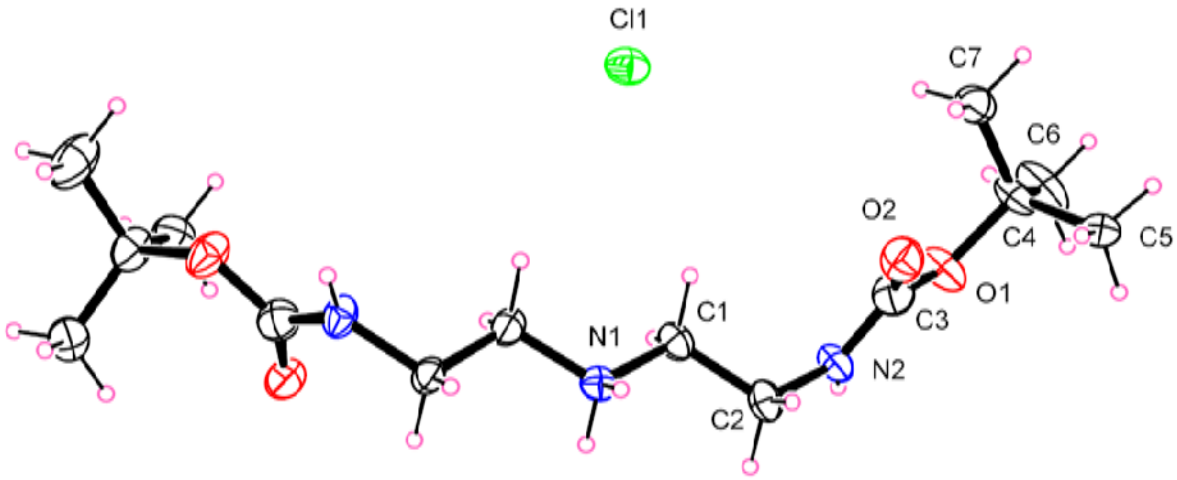

Figure 4.2. Ortep rendering of the structure of Bocdien (**1**) (50% probability ellipsoids).

AtfcBr was treated with Bocdien to give Bocdienatfc by alkylation of the secondary amine by using K_2CO_3 base. Similar procedure was used in the alkylation of the secondary amine using benzyl 2-bromoacetate. Due to the difficulty in separating modified and unmodified protected dien, an excess of the benzyl 2-bromoacetate and atfcBr was used in the alkylation reaction to increase the yield and simplify the purification process. Efficient deprotection of the Z-group in Bocdienbz ligand was achieved by applying Pd/C which resulted in Bocdienac (95%) yield. This was followed by another deprotection of tert-butyloxycarbonyl group (Boc) on the primary amine in Bocdienatfc and Bocdienac ligands. By using the 30% HBr in acetic acid mixture the Boc group was efficiently removed to give atfcdien•3HBr (70%) and acdien•3HBr (90%).[23-25] This specific procedure has been successfully applied in deprotection of the tosyl group from dien-type ligand by Carlone et al. (unpublished results). Removal of the Boc group can also be achieved by using 4 M HCl in dioxane mixture to give HCl salts of the free primary amines. The chemical shifts of the ligands **2**, **3**, **4**, and **8** are listed in Table **4.1** (See Figure 4.4 for numbering).

Table 4.1. ^{1}H NMR Chemical Shifts (ppm) in DMSO-d_6 for species containing atfc

	H3	H5	H6	H8	N'H	N''H	H12
Atfc	6.44	7.35	6.66	6.51		6.52	
atfcBr	6.93	7.54	7.72	7.86		10.96	4.09
Bocdienatfc	6.91	7.67	7.73	7.90	6.88	10.12	3.83
Atfcdien	6.94	7.61	7.68	7.98	7.68	10.50	3.53
[Pt(atfcdien)Br]Br	7.02	7.57	7.78	7.92	5.48	10.99	4.45
					5.79		
[Pt(atfcdien)Me_2SO]Br^+	7.04			7.95	6.24		
					6.40		
[Pt(atfcdien)Br][Pt(Me_2SO)Br_3]	7.02	7.57	7.78	7.92	5.48	10.99	4.45
					5.79		
[Pt(atfcdien)Me_2SO][Pt(Me_2SO)Br_3]	7.04			7.95	6.24		
					6.40		

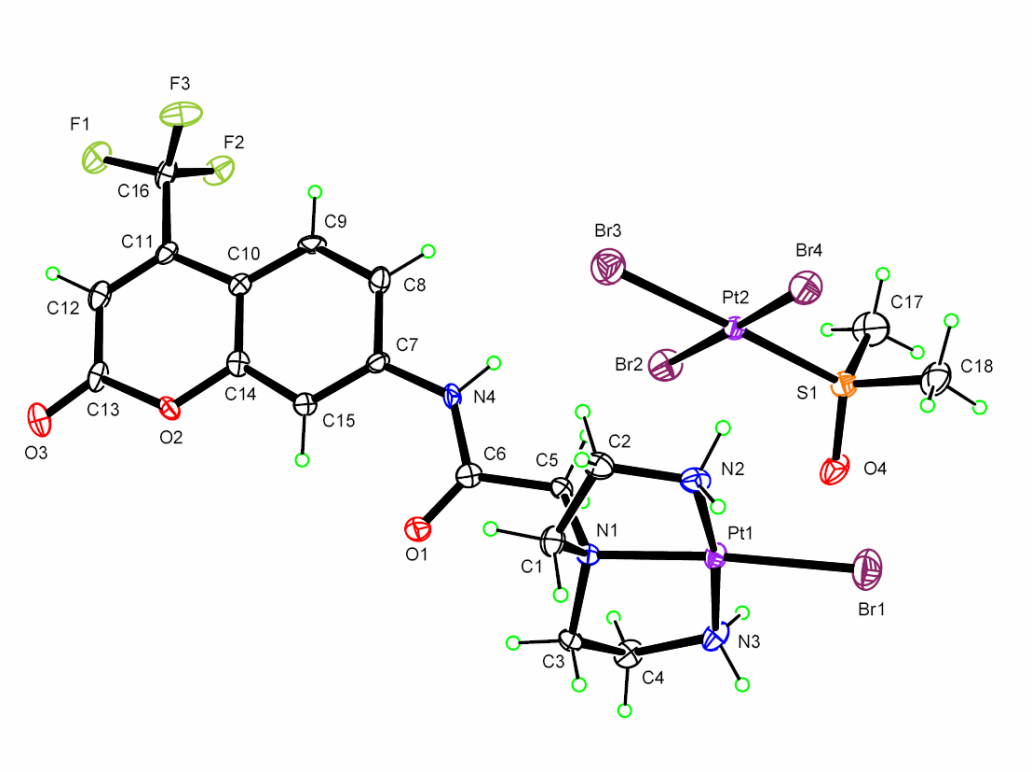

Figure 4.3. Ortep rendering of the structure of [Pt(atfcdien)Br][Pt(Me_2SO)Br_3] (**8a**) (50% probability ellipsoids).

4.3.2 [Pt(atfcdien)Br][Pt(Me$_2$SO)Br$_3$]. The reaction between atfcdien and *cis*-Pt(Me$_2$SO)$_2$Cl$_2$ gave orange crystals of [Pt(atfcdien)Br][Pt(Me$_2$SO)Br$_3$]•H$_2$O (Figure 4.3) after filtration of [Pt(atfcdien)Br]Br precipitate and the clear filtrate was kept at 5 °C for 2 weeks. Soon after **8a** was dissolved in DMSO-d$_6$ the ^{1}H NMR spectrum in DMSO-*d*$_6$ (Figure 4.4) showed the presence of two species, which were assigned to the [Pt(atfcdien)Br][Pt(Me$_2$SO)Br$_3$] (70%) and [Pt(atfcdien)Me$_2$SO][Pt(Me$_2$SO)Br$_3$] (30%). The minor downfield set was assigned to the solvolysis product Pt(atfcdien)**(**Me$_2$SO)]$^{2+}$. Presence of the solvated species [Pt(atfcdien)Me$_2$SO]$^{2+}$ was confirmed by addition of [Et$_4$N]Br to the solution where the signals of [Pt(atfcdien)**(**Me$_2$SO)]$^{2+}$ disappeared and [Pt(atfcdien)Br]$^+$ signals increased in size (not shown). The NMR data is summarized in Table 4.1. The ^{1}H NMR aromatic signals of [Pt(atfcdien)Br][Pt(Me$_2$SO)Br$_3$] in DMSO-d$_6$ compared to atfcdien•3HBr were also not significantly affected by the binding of Pt to atfcdien•3HBr ligand. Once the ligand binds to Pt through N′H (See Figure 4.4 for numbering), the amine signals appeared which we attributed to slower NH exchange for the coordinated ligand. Because of the size of the [Pt(atfcdien)Br]$^+$ cation, a large [Pt(Me$_2$SO)Br$_3$]$^-$ counterion favored the formation of crystals. Formation of a similar counterion ([Pt(Me$_2$SO)Cl$_3$]$^-$), was reported by Veldman et al.[26]

4.3.3 [Pt(atfcdien)Br]Br. As described above, the reaction between atfcdien and *cis*-Pt(Me$_2$SO)$_2$Cl$_2$ gave [Pt(atfcdien)Br]Br as a yellow powder. Similarly one major and one minor set of NH signals were observed on dissolving **8b** in DMSO-d$_6$. The two species were assigned to the [Pt(atfcdien)Br]Br (70%) and a downfield set of [Pt(atfcdien)**(**Me$_2$SO)]Br$^+$ (30%) and similarly confirmed by addition of [Et$_4$N]Br. No significant difference was observed between [Pt(atfcdien)Br]Br and **[**Pt(atfcdien)Br][Pt(Me$_2$SO)Br$_3$] for both aromatic signals and NH

signals. The ^{1}H NMR spectrum of yellow powder [Pt(atfcdien)Br]Br had similar chemical shifts as that of [Pt(atfcdien)Br][Pt(Me_2SO)Br_3].

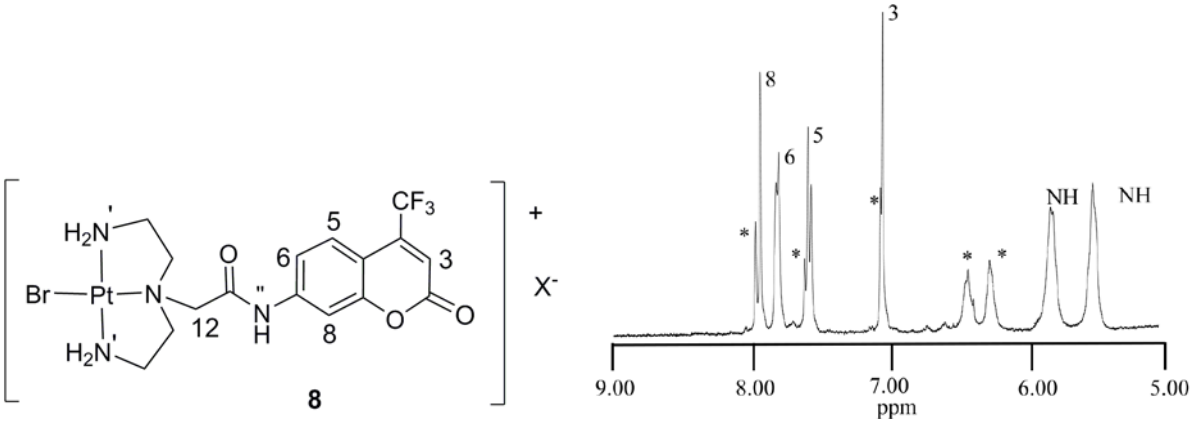

Figure 4.4. ^{1}H NMR spectrum in DMSO-d_6 (ppm) of $[Pt(atfcdien)Br]^{+}$ and $[Pt(atfcdien)(Me_2SO)]^{2+}$ for peaks labeled with *.

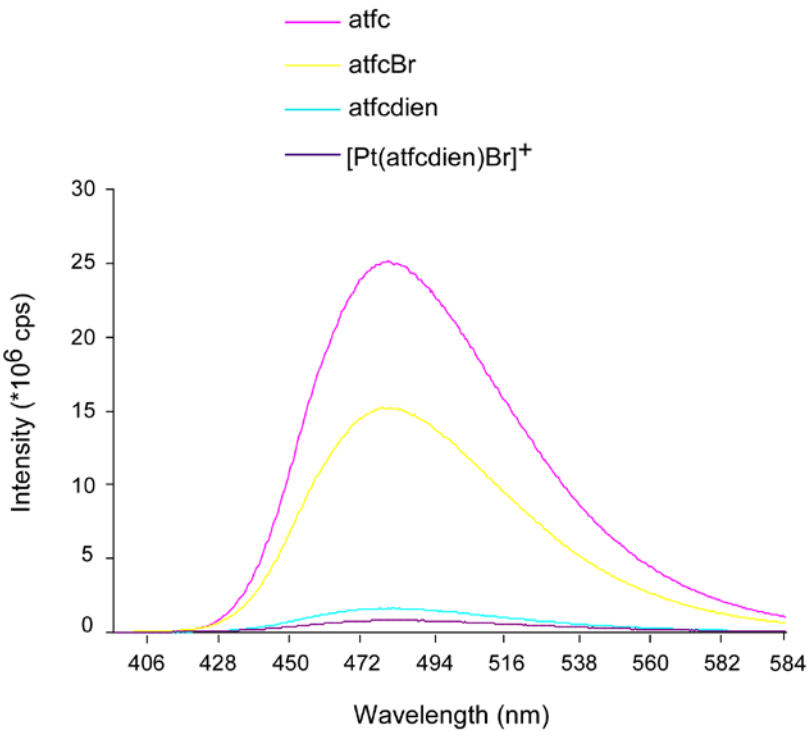

Figure 4.5. Fluorescence emission spectrum of atfc derivatives solutions (5 μM, DMSO).

Figure 4.5 shows the emission spectra of atfc, atfcBr, atfcdien and **[**Pt(atfcdien)Br][X]. The fluorescence intensity of coumarin was quenched by 90% after addition of Pt(II). AtfcBr ligand emission intensity was significantly quenched when compared to that of the original atfc ligand due to the formation of the acetyl bromide bond. Substitution at position 7 with a group that has an electron withdrawing effect is known to weaken the fluorescence intensity.[27] The presence of electron withdrawing groups like carbonyl group attached to the primary amine of atfc pumps electrons out of the atfc ring also contributing to the quenching effect. In addition to an electron withdrawing effect, the presence of bromide atom in the atfcBr contributes to about 30% decrease in fluorescence intensity. Addition of more bromide atoms on the ligands increases the quenching effect. This is illustrated by atfcdien which has 3HBr salts causing a dramatic decrease of fluorescence intensity to about 10%. The fluorescence intensity of [Pt(atfcdien)Br]X decreases further with the presence of the platinum metal. The presence Pt(II) and Br atoms changes the electronic properties of the fluorophore, enhancing the spin forbidden process therefore we attribute the significant decrease in fluorescence to the "heavy atom effect".[28-32]

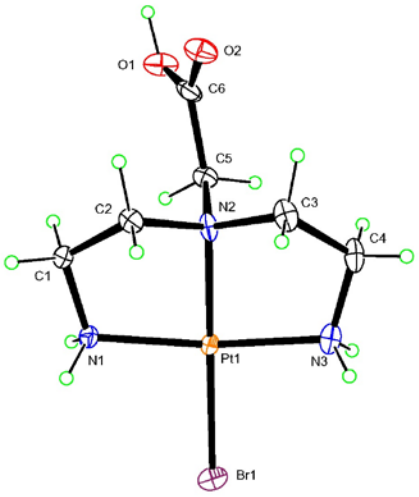

Figure 4.6. Ortep rendering of the structure of [Pt(acdien)Br][Br] (**9**) (50% probability ellipsoids).

4.3.4 [Pt(acdien)Br]Br. The reaction between acdien•3HBr and *cis*-Pt(Me_2SO)$_2Cl_2$ gave colorless crystals of [Pt(acdien)Br][Br] (Figure 4.6) and a non-crystalline yellow powder. The yellow precipitate was collected by filtration and recrystallized further using methanol to give pure [Pt(acdien)Br]Br confirmed by ^{1}H NMR (Figure 4.7) and elemental analysis. The acdien ligand is bound to Pt(II) in a tridentate fashion. Broad signals were observed for the dien region which integrated to 8H as expected and a singlet was observed for the hydrogen of the α carbon next to the carboxylic moiety. The two different signals observed for the NH were attributed to the magnetically in equivalent set of hydrogen.

Immediately upon dissolution of **9a** the ^{1}H NMR spectrum in DMSO-d_6 showed the presence of two sets of NH signals which were assigned to the [Pt(acdien)Br]Br (> 90%) and [Pt(acdien)(Me$_2$SO)]Br species (<10%). Dissolution of **9a** in D_2O showed the presence of one sets of NH signals which were assigned to the [Pt(acdien)Br]Br species. We attribute the presence of the NH signals in D_2O to be due to the acid nature of D_2O solvent used in the NMR analysis.

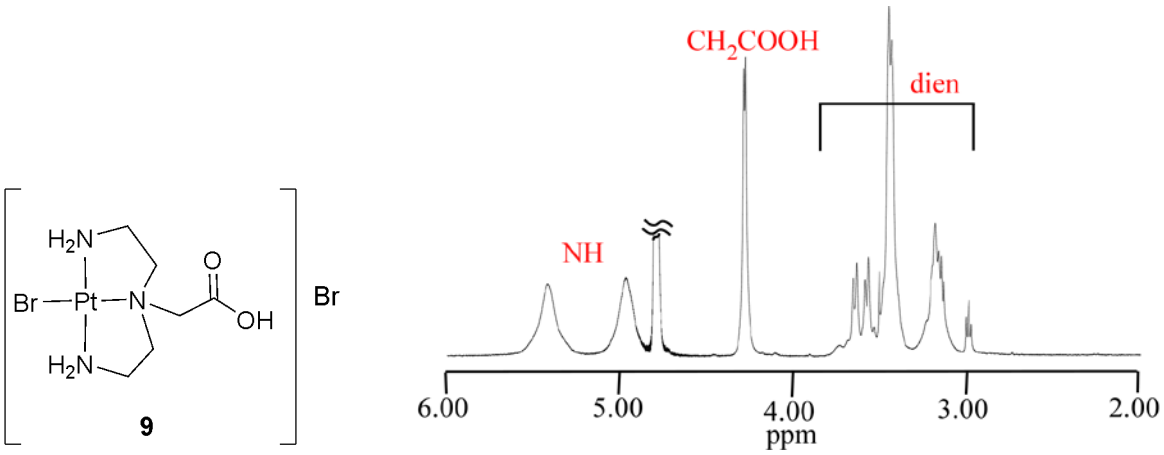

Figure 4.7. ^{1}H NMR spectrum in 400 MHz D_2O (ppm) for [Pt(acdien)Br]Br.

4.3.5 [Pt(acdien)Cl]Cl. Pt(acdien)Cl]Cl was prepared by treating *cis*-Pt(Me_2SO)$_2Cl_2$ with atfcdien•3HCl. Atfcdien•3HCl was made by deprotecting Bocdienac with 4 M HCl in dioxane. Similar deprotection method has been report by Han et al.[33] Dissolution of **9b** in D_2O or DMSO-d_6 showed the presence of one sets of NH signals which were assigned to the [Pt(acdien)Cl]Cl in both cases. Characterization results for both the Pt(acdien)Cl]Cl and [Pt(acdien)Br]Br were very closely related, however; Pt(acdien)Cl]Cl was very hygroscopic and it required careful handling. Similar hygroscopic compounds have been synthesized before including [Pt(dien)Cl]Cl.[34, 35]

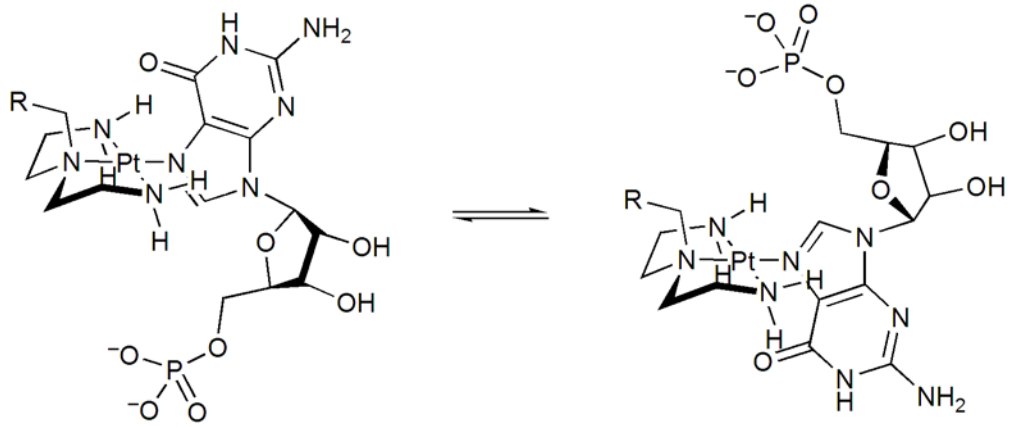

Figure 4.8. Two possible rotamers of Pt(acdien)(5′-GMP) and Pt(atfcdien)(5′-GMP) adducts where R is acOH or CH_2COatfc groups.

4.3.6 Pt(acdien)(5′-GMP).The ^{1}H NMR spectrum of Pt(acdien)(5′-GMP) adduct at equilibrium (pH= 4.2) had one H8 and one H1′ signals that each integrated to one proton. The ^{1}H NMR signals of the free 5′-GMP were upfield compared to the signals of Pt(acdien)(5′-GMP) adduct. The product H8 signal (Figure 4.9) at 8.56 ppm shifted downfield by ca. 0.4 ppm compared to that of the H8 signal of the free 5′-GMP (8.15 ppm) as a result of the binding of 5′-GMP to Pt through N7.[36, 37] The product H1′ signal at 5.78 ppm shifted downfield compared to that of the H1′ signal of the free 5′-GMP at 6.01 ppm. Christoforou *et al.* also observed similar results with Pt(DNSH-dien)(5′-GMP) where single signals for both H1′ and H8 were observed irrespective of the possession of unsymmetrical carrier ligand on the tridentate dien-type ligand (DNSH=5-

(dimethylamino)naphthalene-1-sulfonamide).[38] Other studies on Pt(N-Me_3dien)(5′-GMP) showed temperature dependence would allow the formation of more than one rotamer.[39]

Beside lack of steric hindrance at the terminals N-H of the dien, we suggest that the presence of -CH_2CO_2H moiety of the acdien is a significantly better hydrogen-bond donor than the -CH_2 (hindered amide) moiety of atfcdien, then the carboxylic acid could speed up the Pt-N bond rotation through hydrogen-bonding to the carboxylic acid in a quasi-stable intermediate halfway between the two possible double N-H hydrogen-bonded rotamers. The presence of one pair of signals for the protons suggests that the adduct formed has a rate of rotation about the Pt–N(7) bond that is too rapid (Figure 4.8) for the observation of a set of signals for each possible rotamer.[37, 40]

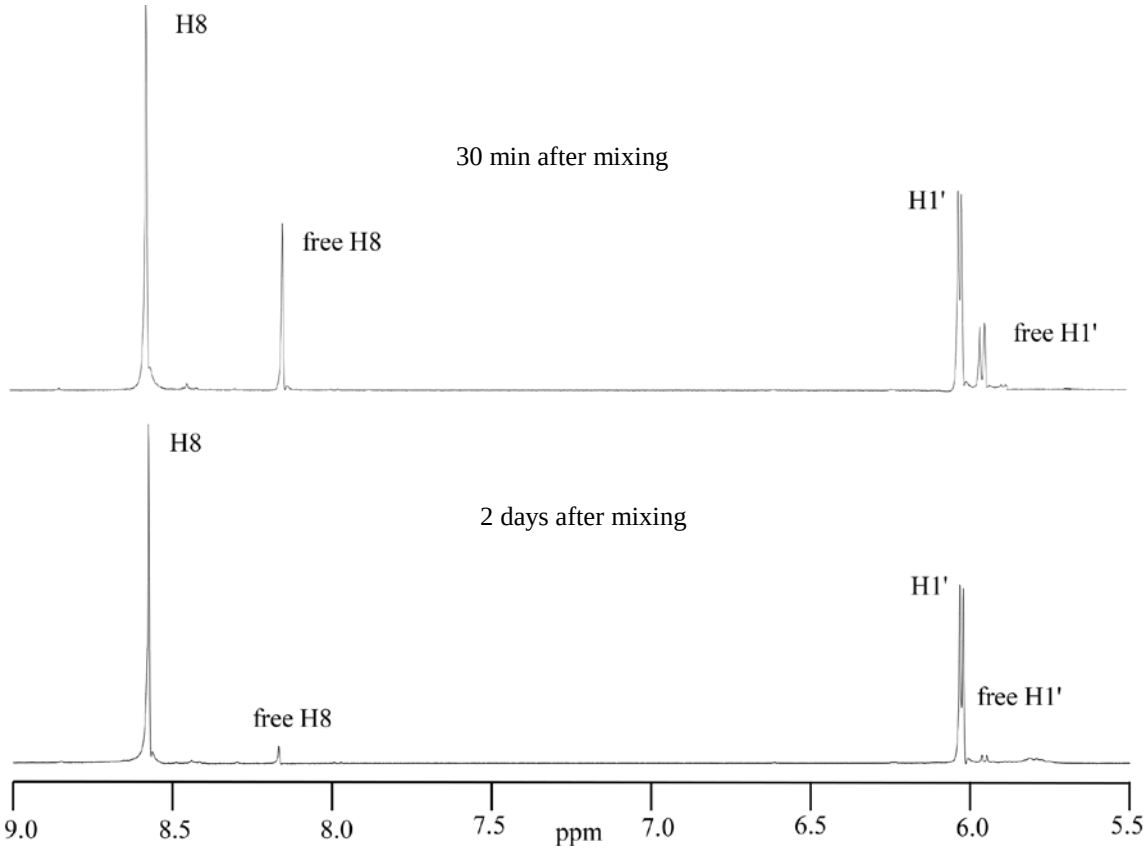

Figure 4.9. 1H NMR of Pt(acdien)(5′-GMP) (400 MHz) in D_2O at 25 °C.

4.3.7 Pt(atfcdien)(5′-GMP). The reaction between the [Pt(atfcdien)Br]Br complex and guanosine 5′-monophosphate (5′-GMP) gave a Pt(atfcdien)(5′-GMP) adduct which had one H8 and two H1′ signal that integrated to one proton each. In the aromatic region the signal at 8.64 ppm, assigned to the [Pt(atfcdien)(5′-GMP) H8, is shifted downfield by ca. 0.5 ppm with respect to the free 5′-GMP H8 signal (at 8.13 ppm), characteristic of N7 binding.[36, 37] A downfield shift was also observed for the H1′ sugar proton signals (Figure 4.12). The ^{1}H NMR spectrum of the Pt(atfcdien)(5′-GMP) at higher field (700 mHz) permitted observation of both the signal for H1′ and some atfc minor rotamer with more clarity (Figure 4.13). Similar results were observed for Me_3dienPt(5′-GMP) which has both terminal primary amines substituted with methyl group (Figure 4.10), where two H8 signals were observed indicating the formation of two rotamers due slow rotation about the Pt–N(7) bond attributed to steric hindrance from the presence of the methyl groups. [13,36, 41]

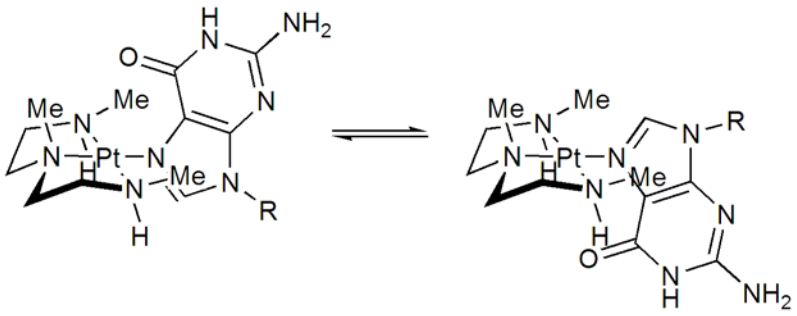

Figure 4.10. Two perpendicular rotamers of Me_3dienPt(5′-GMP).

In our case it seems unlikely that the free amine end would cause any steric hindrance. We see two different H1′ and two different signals for H5, H6 and H8 of the atfc (see table 4.4 for numbering) suggesting we have two rotamers. We suggest that the planar conformer indicated in Figure 4.11 is more stable due to hydrogen bonding than the perpendicular conformer in figure 4.8. The formation of this planar conformer might allow the rate of rotation about the Pt–N7

bond to be relatively slow enough to allow the observation of more signals due to rotamer, however; more study need to be done to confirm this hypothesis.

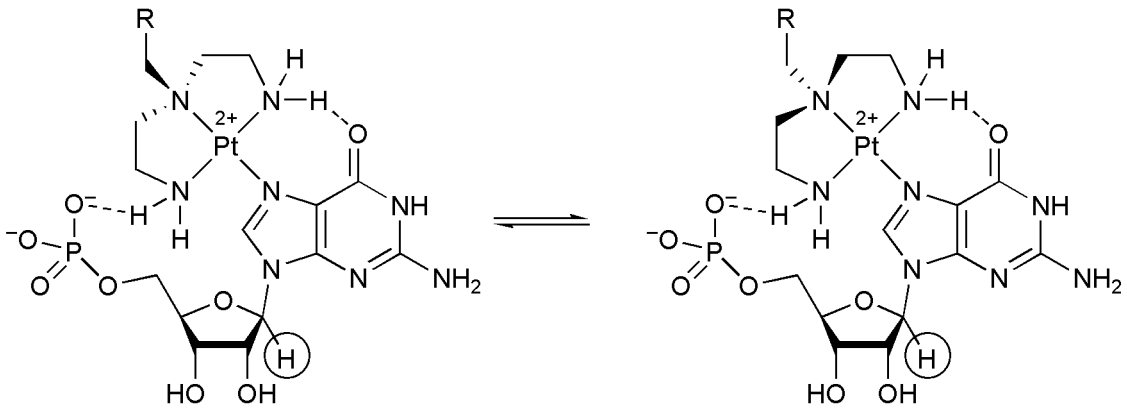

Figure 4.11. Two possible planar rotamers of Pt(atfcdien)(5′-GMP).

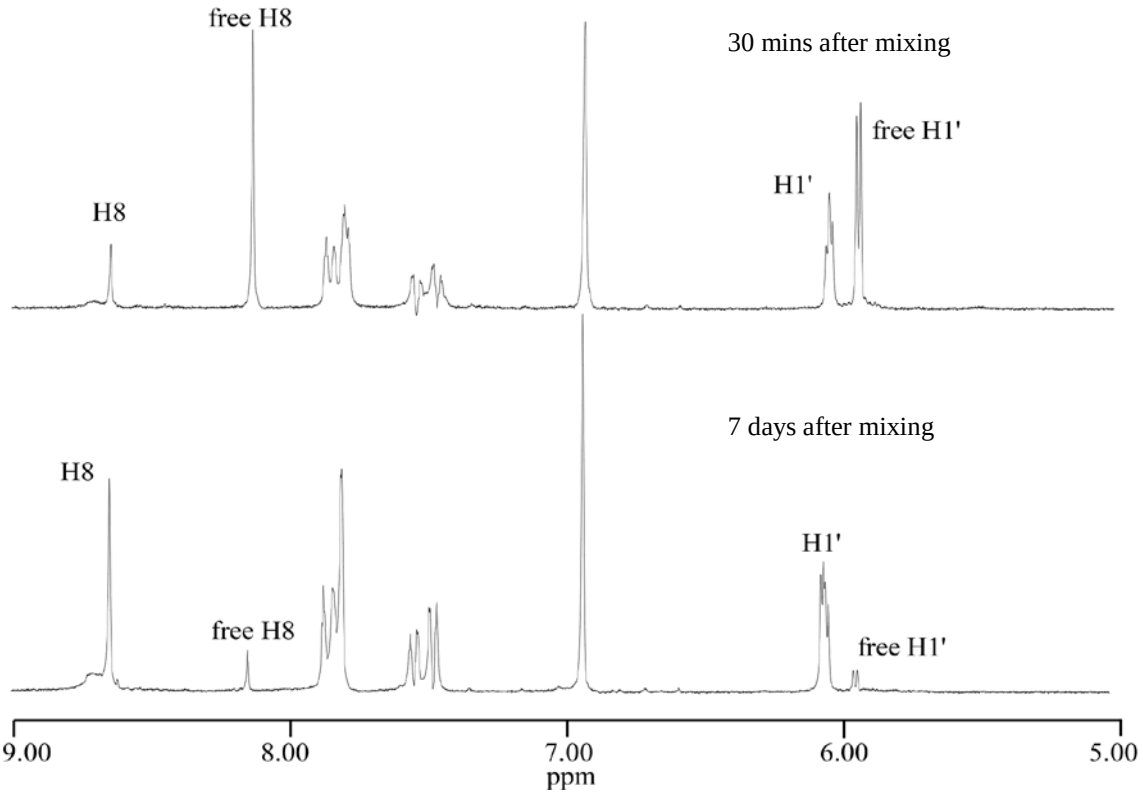

Figure 4.12. ^{1}H NMR spectrum (400 MHz) in D_2O of Pt(atfcdien)(5′-GMP) at 25° C.

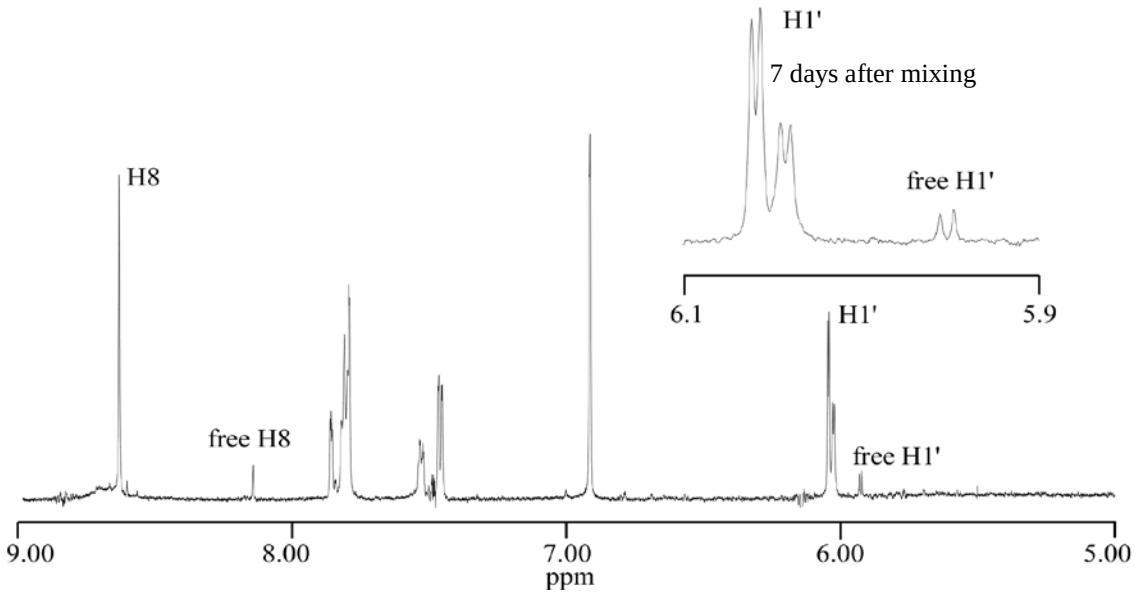

Figure 4.13. ^{1}H NMR spectrum (700 MHz) in D_2O of Pt(atfcdien)(5′-GMP) at 25 °C**.**

4.3.9 X-ray Crystallographic Structural Studies.

4.3.9.1 Bocdien (**1**). Both cation and chloride ion lie on crystallographic C_2 axes and are illustrated in Figure 4.2. The $N(CH_2)_2NH_2(CH_2)_2N$ chain is fully extended, with torsion angles 178.6(7)˚ about N1-C1 and 176.6(5)˚ about C1-C2. However, the Boc moieties are folded away from this line, with C1-C2-N2-C3 torsion angle 84.4(8)˚. The central ammonium forms hydrogen bonds to chloride (N…Cl 3.122(6) Å), and the Boc NH group forms N2-H…O2 intermolecular hydrogen bonds with distance 2.874(8) Å.

4.3.9.2 atfcBr (**2**). The 11-atom atfc ring system is coplanar to within a maximum deviation of 0.021(2) Å (for C2), and the $NHCOCH_2$ group also lies nearly in this plane. The C8-C7-N1-C11 torsion angle is -2.1(3)˚, and the C7-N1-C11-C12 torsion angle is 178.20(18)˚. The amide N -H group forms an intermolecular hydrogen bond with the atfc carbonyl oxygen atom, N1-H…O2 (at 3/2+x, 3/2-y, 1/2+z) distance 2.871(2) Å and angle about H 168(2)˚, as illustrated in Figure 4.1.

Table 4.2. Crystal data, data collection and refinement parameters.

Compound	Bocdien.HCl **1**	atfcBr **2**	[Pt(atfcdien)Br][Pt(Me_2SO)Br_3] **8**	[Pt(acdien)Br]Br **9**	Pt(tmbSO_2-*N*,*N*-Me_2dien)Cl **10**
CCDC deposit no.	663056	663057	663058	663059	
Formula	$[C_{14}H_{30}N_3O_4]$ Cl	$C_{12}H_7BrF_3NO_3$	$[C_{16}H_{19}BrF_3N_4O_3Pt][C_2H_6Br_3OPtS]\bullet H_2O$	$[C_6H_{15}BrN_3O_2Pt]Br\bullet H_2O$	$C_{15}H_{26}ClN_3O_2PtS$
Formula weight	339.86	350.1	1178.32	534.14	542.99
Space group	Pccn	$P2_1/n$	P-1	P-1	$P2_1/c$
Temp., K	110	110	110	110	90
a, Å	34.40(4)	4.4945(10)	8.1663(10)	6.7892(10)	15.075 (3)
b, Å	5.069(5)	24.582(4)	8.3103(10)	8.2078(15)	13.191 (3)
c, Å	10.888(10)	10.978(2)	22.631(3)	11.583(2)	9.6030 (15)
β, deg.	90	99.197(8)	87.098(6)	78.924(9)	105.167(13)
Cell volume, $Å^3$	1899(3)	1197.3(4)	1391.5(3)	624.80(18)	1843.1(6)
Formula units/unit cell	4	4	2	2	4
Dcalc, g cm^{-3}	1.189	1.942	2.812	2.839	1.957
Rint	0.091	0.02	0.035	0.030	0.057
Independent reflections	1193	2730	6152	4874	6660
R (obs)	0.092	0.026	0.042	0.033	0.044
R_w, F^2(all data)	0.245	0.053	0.118	0.077	0.093
GOF	1.11	1.04	1.04	1.06	1.03
Max resid. Peaks ($eÅ^{-3}$)	0.66, -0.30	0.38, -0.36	2.70, -3.84	1.98, -2.06	4.01, –2.09

$^a R = (\Sigma||Fo| - |Fc||)/\Sigma|Fo|$; $^b wR2 = [\Sigma[w(Fo^2 - Fc^2)^2]/\Sigma[w(Fo^2)^2]]^{1/2}$

4.3.9.3 [Pt(atfcdien)Br][Pt(Me_2SO)Br_3] (**8a**). This salt crystallizes as the monohydrate (H_2O not shown in Fig. 3). The anion has Pt-Br distances in the range of 2.4161(11) - 2.4371(11) Å and Pt-S distance of 2.219(2) Å. While we find no other salts of the $[Pt(Me_2SO)Br_3]^-$ anion in the

Cambridge database, it contains a number of salts of $[Pt(Me_2SO)Cl_3]^-$, most of which have Pt(II)-containing cations, e.g. $[Pt_2(terpy)_2Cl_2]$ $[Pt(Me_2SO)Cl_3]$.[42] In the cation, the three Pt-N distances are statistically indistinguishable, within the range of 2.031(7) - 2.044(7) Å, while the Pt-Br distance is 2.4058(11) Å. The coordination geometry of the cation is slightly pyramidally-distorted square planar, with Pt1 lying 0.1005(5) Å out of the N_3Br plane. Cations and anions alternate in stacks with Pt1…Pt2 distances 3.987(1) and 4.432(1) Å and a dihedral angle of 17.8(3)˚ between their anion coordination planes. The conformation of the atfc-amide side chain is similar to that seen in atfcBr (**1**), with the torsion angle about C7-N4 3.3(15)˚ and that about N4-C6 173.4(8)˚.

Cini and coworkers[42] discussed extensively the $[Pt(Me_2SO)Cl_3]^-$ torsional angles, which are different from those in **8a**. This deviation is attributed to difference between the Br group attached to the platinum counter ion complex compare to the chloride group attached to their complex. In the bromo compound, a methyl group is nearly eclipsed with the Br, with a torsional angle Br4 Pt2 S1 C18 -2.1(4) which is smaller than the reported torsional angle. In the chloro complex[42], the S=O is nearly eclipsed with Cl, having Cl-Pt-S-O torsional angle as 3.1(6)˚ However aside from the differences in Pt-Cl vs Pt-Br distance there is little structural difference between $[Pt(Me_2SO)Br_3]^-$ and $[Pt(Me_2SO)Cl_3]^-$.

4.3.9.4 [Pt(acdien)Br]Br (9). The Pt-Br distance is 2.4055(7)Å, and the Pt-N distances are equal within experimental error, falling within the range of 2.035(4) - 2.050(4)Å. The coordination plane is slightly nonplanar, with a slight folding along the central axis. Thus, N1 and N3 both lie 0.061(2)Å out of the N3PtBr best plane, while N2, Pt1, and Br1 lie 0.041(2), 0.0550(14), and 0.0266(15)Å out of plane, respectively, on the opposite side. So, the N1/N2/Pt/Br plane forms a dihedral angle of 5.79(5)˚ with the N3/N2/Pt/Br plane. The carboxyl group forms a hydrogen

bond to the bromide ion, with O…Br distance 3.133(4)Å and 173° angle about H. All NH_2 hydrogen atoms are involved in intermolecular hydrogen bonds to bromide, coordinated bromo, and carboxyl O2. Both platinum complexes [Pt(atfcdien)Br][Pt(Me_2SO)Br_3] and [Pt(atfcdien)Br]Br have comparable N-Pt-Br bond distances showing little influence of ligands attached to the tertiary N hence no trans influence.

Table 4.3. Selected Bond distances (A^o) and Angle (deg) for [Pt(atfcdien)Br][Pt(Me_2SO)Br_3] (**8**) and [Pt(acdien)Br]Br (**9**).

Bond Distances	**8**	**9**
Pt1- N1	2.031(7)	2.047(4)
Pt1- N2	2.044(7)	2.050(4)
Pt1- N3	2.039(8)	2.035(4)
Pt1- Br1	2.4058(11)	2.4055(7)
Pt2- S1	2.219(2)	
Pt2- Br2	2.4161(11)	
Pt2- Br3	2.4234(12)	
Pt2- Br4	2.4371(11)	
S1- O4	1.486(7)	
S1- C17	1.771(11)	
S1- C18	1.768(11)	
Bond Angles		
N1- Pt1- N3	170.1(3)	168.96(17)
N1- Pt1- N2	85.8(3)	85.21(16)
N2- Pt1- N3	85.7(3)	85.85(17)
N1- Pt1- Br1/Cl1	94.2(2)	95.21(12)
N2- Pt1- Br1/Cl1	174.7(2)	178.82(11)
N3- Pt1- Br1/Cl1	93.9(2)	93.60(14)
S1- Pt2 Br3	177.09(7)	
S1- Pt2- Br2	87.79(7)	
Br2 Pt2- Br3	89.30(4)	
S1- Pt2- Br4	94.33(7)	
Br2- Pt2- Br4	177.61(4)	
Br3- Pt2- Br4	88.58(4)	

4.4 Conclusion

Complexes **8a**, **8b, 9a** and **9b** are bound in a tridentate fashion, evidence being the two NH1 signals indicative of H atoms attached to the N that are chemically different in space but equal for both terminal NH1 giving the two signals. In DMSO-d_6, Br and Cl ligands are slowly displaced giving rise to minimal solvated species for each platinum complex. Similar behavior has been reported for [Pt(DNSH-tren)Cl]Cl by Christoforou et al.[38] Immediately on dissolution in DMSO-d_6, [Pt(DNSH-tren)Cl]Cl showed two sets of NH NMR signals. The upfield set was assigned to [Pt(DNSH-tren)Cl]Cl and the downfield was assigned to [Pt(DNSH-tren) Me_2SO-d_6]$^{2+}$. Our finding on minimal solvolysis of [Pt(atfcdien)Br]X agree with their findings confirming that the presence of the alkyl group in the central N decreases DMSO-d_6 solvolysis.

We accomplished the synthesis and solution characterization of [Pt(atfcdien)Br][Pt(Me_2SO)Br_3], Pt(atfcdien)Br]Br, [Pt(acdien)Br]Br and [Pt(acdien)Cl]Cl complexes by employing various synthetic steps. Complexes **8** and **9** offer various advantages for their use as biological probes. The presence of atfc groups on the carrier ligand introduces the fluorescence property to the ligand, which would allows us to monitor and study the ligand interaction with biological molecules by spectroscopic techniques, however; due to the decrease fluorescence intensity no much fluorescence information could be obtained from the model ligand. The carboxylate groups allow studying of the monofunctional Pt complex spectroscopically by giving a simple spectrum that can be followed and studied by NMR. Also the solubility of both Pt complexes in water allows aqueous solution studies under physiological conditions, both with nucleotides and other biological molecules. These new complexes have desirable features for assessing the potential of tridentate platinum complexes for investigating selective monocoordination of metal complexes to DNA and to peptides.

4.6 References

1. Jamieson, E., R; Lippard, S., J, Structure, Recognition, and Processing of Cisplatin-DNA Adducts. *Chemical Reviews* **1999,** 99, 2467-2498.

2. Natile, G.; Marzilli, G. L., Non-covalent interactions in adducts of platinum drugs with nucleobases in nucleotides and DNA as revealed by using chiral substrates. *Coordination Chemistry Reviews* **2006,** 250, 1315-1331.

3. Fuertes, M. A.; Alonso, C.; Perez, J. M., Biochemical Modulation of Cisplatin Mechanisms of Action: Enhancement of Antitumor Activity and Circumvention of Drug Resistance. *Chemical Reviews* **2003,** 103, 645-662.

4. Wong, E.; Giandomenico, C. M., Current Status of Platinum-Based Antitumor Drugs. *Chemical Reviews* **1999,** 99, 2451-2466.

5. Reedijk, J., Why Does Cisplatin Reach Guanine-N7 with Competing S-Donor Ligands Available in the Cell? *Chemical Reviews* **1999,** 99, 2499-2510.

6. Soldatovic, T.; Bugarcic, Z., Study of the reactions between platinum(II) complexes and L-methionine in the presence and absence of 5'-GMP. *Journal of Inorganic Biochemistry* **2005,** 99, 1472–1479.

7. Berners-Price, S. J.; Frey, U.; Ranford, J. D.; Sadler, P. J., Stereospecific hydrogen-bonding in mononucleotide adducts of platinum anticancer complexes in aqueous solution. *Journal of the American Chemical Society* **1993,** 115, 8649-8659.

8. Djuran, M. I.; Lempers, E. L. M.; Reedijk, J., Reactivity of chloro- and aqua(diethylenetriamine)platinum(II) ions with glutathione, S-methylglutathione, and guanosine 5'-monophosphate in relation to the antitumor activity and toxicity of platinum complexes. *Inorganic Chemistry* **1991,** 30, 2648-2652.

9. van Boom, S. S. G. E.; Chen, B. W.; Teuben, J. M.; Reedijk, J., Platinum-Thioether Bonds Can Be Reverted by Guanine-N7 Bonds in $Pt(dien)^{2+}$ Model Adducts. *Inorganic Chemistry* **1999,** 38, 1450-1455.

10. Lippert, B., Multiplicity of metal ion binding patterns to nucleobases. *Coordination Chemistry Reviews* **2000,** 200-202, 487-516.

11. Bergeron, R. J.; Huang, G.; McManis, S. J.; Yao, H.; Nguyen, J. N., Synthesis and Biological Evaluation of Aminopolyamines. *Journal of Medicinal Chemistry* **2005,** 48, 3099-3102.

12. Eastman, A., Reevaluation of Interaction of cis-Dichloro(ethylenediamine)platinum(11) with DNA^{+}. *Biochemistry* **1986,** 25, 3912-3915.

13. Wirth, W.; Blotevogel-Baltronat, J.; Kleinkes, U.; Sheldrick, W. S., Interaction of (amine)M(II) complexes (amine=/dien, en; M=/Pd, Pt) with purine nucleoside 2'-, 3'- and 5'-monophosphates*/the role of the phosphate site for specific metal fragment-/nucleotide recognition by macrochelation. *Inorganica Chimica Acta* **2002,** 339.

14. Bernacki, R. J.; Bergeron, R. J.; Porter, C., Antitumor Activity of N,N'-Bis(ethyl)spermine Homologues against Human MALME-3 Melanoma Xenografts. *Cancer Research* **1992,** 52, 2424-2430.

15. Swieten, F. P.; Leeuwenburgh, A. M.; Kesslerb, M. B.; Overkleeft, S. H., Bioorthogonal organic chemistry in living cells: novel strategies for labeling biomolecules. *Organic & Biomolecular Chemistry* **2005,** 3, 20-27.

16. Patonay, G.; Salon, J.; Sowell, J.; Strekowski, L., Noncovalent Labeling of Biomolecules with Red and Near-Infrared Dyes. *Molecules* **2004,** 9, 40-49.

17. Christoforou, A. M.; Fronczek, F. R.; Marzilli, P. A.; Marzilli, L. G., fac-Re(CO)3L Complexes Containing Tridentate Monoanionic Ligands (L-) with a Seldom-Studied Sulfonamido Group As One Terminal Ligating Group. *Inorganic Chemistry* **2007,** 46, 6942-6949.

18. Krapcho, P., A. ; Kuell, S. C., Mono-Protected Diamines. N-tert-Butoxycarbonyl-α-ω–Alkanediamines from α-ω-Alkanediamines. *Synthetic Communications* **1990,** 20, 2559-2564.

19. Rannard, S. P.; Davis, N. J., The Selective reaction of primary amines with carbonyl imidazole containing compounds: Selective amide and carbamate synthesis. *Organic letters* **2000,** 2, 2117-2120.

20. Price, J. H., Palladium(II) and Platinum(II) Alkyl Sulfoxide Complexes. Examples of Sulfur-Bonded, Mixed Sulfur- and Oxygen-Bonded, and Totally Oxygen-Bonded complexes. *Inorganic Chemistry* **1972,** 11, 1280-1284.

21. Bissell, R. B.; Larson, D. K.; Croudance, C. M., Some 7-substituted 4-(trifluoromethyl)coumarins. *Journal of Chemical and Engineering Data* **1981,** 26, 348-350.

22. Sheldrick, G., *University of Gottingen, Germany*. 1997.

23. Gu, K.; Bowman-James, J., Synthesis of Polyammonium Macrocycles with Pendant Chains:. *Tetrahedron Letters* **1995,** 36, (12), 1977-1980.

24. Brand, G.; Hosseini, M. W.; Ruppert, R., Synthesis of Selectively Substituted Lipocyclopolyamines. . *Helvetica Chimica Acta* **1992,** 75, 721-728.

25. Banerjee, S.; Babich, J.; Zubieta, J., Bifunctional chelates with aliphatic amine donors for labeling of biomolecules with the $\{Tc(CO)_3\}^{+}$ and $\{Re(CO)_3\}^{+}$ cores: the crystal and

molecular structure of [$Re(CO)_3\{(H_2NCH_2CH_2)_2 N(CH_2)_4CO_2Me\}$]Br. *Inorganic Chemistry Communications* **2004,** 7, 481–484.

26. Veldman, N.; Spek, A. L., 4. N', N'-dimethyl-3-oxopiperazinium(1+)trichloro(dimethyl sulphoxide-S)platinate (1-),($C_6H_{12}N_2O$)[$PtCl_3(C_2H_6OS)$]. *Acta Crystallographica, Section C: Crystal Structure Communications* **1994,** 50, 1572-1574.

27. Setsukinai, K.-i.; Urano, Y.; Kikuchi, K.; Higuchi, T.; Nagano, T., Fluorescence switching by O-dearylation of 7-aryloxycoumarins. Development of novel fluorescence probes to detect reactive oxygen species with high selectivity. *Perkin 2* **2000**, 2453-2457.

28. Basu, G.; Kubasik, M.; Anglos, D.; Secor, B.; Kuki, A., Long-range electronic interactions in peptides: the remote heavy atom effect. *Journal of the American Chemical Society* **1990,** 112, 9410-11.

29. Turro, N. J.; Kavarnos, G. J.; Cole, T., Jr.; Scribe, P.; Dalton, J. C., Molecular photochemistry. XXXIX. External heavy-atom-induced spin-orbital coupling. Spectroscopic study of naphthonorbornanes. *Journal of the American Chemical Society* **1971,** 93, 1032-4.

30. de Silva, A. P.; Gunaratne, H. Q. N.; Gunnlaugsson, T.; Huxley, A. J. M.; McCoy, C. P.; Rademacher, J. T.; Rice, T. E., Signaling recognition events with fluorescent sensors and switches. *Chemical Reviews* **1997,** 97, 1515-1566.

31. Sabatini, C. A.; Pereira, R. V.; Gehlen, M. H., Fluorescence Modulation of Acridine and Coumarin Dyes by Silver Nanoparticles. *Journal of Fluorescence* **2007,** 17, 377-382.

32. Lakowicz, J., R., *Principles of Fluorescence Spectroscopy.* 2nd ed.; New York, 1999.

33. Han, G.; Tamaki, M.; Hruby, V. J., Fast, efficient and selective deprotection of the tert-butoxycarbonyl (Boc) group using HCl/dioxane (4 M). *Journal of Peptide Research* **2001,** 58, 338-341.

34. Constable, E. C.; Editor, *Metals and Ligand Reactivity: An Introduction to the Organic Chemistry of Metal Complexes*. 1995.

35. Shapley, J. R., *Inorganic Syntheses*. 2004; Vol. 34.

36. Carlone, M.; Fanizzi, F. P.; Intini, F. P.; Margiotta, N.; Marzilli, L. G.; Natile, G., Influence of Carrier Ligand NH Hydrogen Bonding to the O6 and Phosphate Group of Guanine Nucleotides in Platinum Complexes with a Single Guanine Ligand. *Inorganic Chemistry* **2000,** 39, 634-641.

37. Guo, Z.; Sadler, P. J.; Zang, E., Recognition of platinum(II) amine complexes by nucleotides: role of phosphate and carbonyl groups in ([15N3]diethylenetriamine)-

(guanosine 5A-monophosphate)platinum(ii). *Chemical Communications (Cambridge, United Kingdom)* **1997,** 1, 27-28.

38. Christoforou, M. A.; Marzilli, A. P.; Marzilli, G. L., The Neglected Pt-N(sulfonamido) Bond in Pt Chemistry. New Fluorophore-Containing Pt(II) Complexes Useful for Assessing Pt(II) Interactions with Biomolecules. *Inorganic Chemistry* **2006,** 45, 6771-6781.

39. Carlone, M.; Marzilli, G. L.; Natile, G., Platinum Complexes with NH Groups on the Carrier Ligand and with Only One Guanine or Hypoxanthine Derivative. Informative Models for Assessing Relative Nucleobase and Nucleotide Hydrogen-Bond Interactions with Amine Ligands in Solution. *Inorganic Chemistry* **2004,** 43, 584-592.

40. Bloemink, J. M.; Edwin, L. L. M.; Reedijk, J., Kinetic preference of 5'GMP over 3'GMP in reactions with platinum amine compounds as studied by competition reactions. *Inorganica Chimica Acta* **1990,** 176, 317-320.

41. Carlone, M.; Marzilli, L. G.; Natile, G., Platinum complexes with only one purine ligand (guanine, deoxyguanine, or adenine) flanked by two cis-NH(CH_3) groups - informative models for assessing the interaction of purine C6 substituents with cis-amines. *European Journal of Inorganic Chemistry* **2005**, (7), 1264-1273.

42. Cini, R.; Donati, A.; Giannettoni, R., Synthesis and structural characterization of chloro(2,2';6',2''-terpyridine)platinum(II)trichloro(dimethylsulfoxide)platinate(II). Density functional analysis of model molecules. *Inorganica Chimica Acta* **2001,** 315, 73-80.

CHAPTER 5. CONCLUSIONS

This dissertation has focused on design, synthesis, and structural analysis of short targeting peptides conjugated to conversational drugs and synthesis of small platinum complexes. Two targeting sequences used were, LHRH and CNGRC both of which have receptors in the tumor cells. Development of new strategies to overcome the side effects associated with current cancer drugs is significant in drug development. Synthesis of targeted anticancer drugs and study of their biological properties is crucial for potential therapeutic agent development.

Chapter 2 of this dissertation describes the synthesis of targeted platinum complexes using CNGRC sequence. Based on the fact the CNGRC sequence have been successful used to target tumor cell, two platinum complexes were designed where minipeg group was placed on each side of the sequence to enhance on solubility. A malonoly linker was synthesized to improve on the spacing and provided a terminus for platination. The biological data of the final complex revealed that targeted platinum complexes were more effective at suppressing proliferation of prostate tumor cells that had CD13 receptors and had low toxicity to tumor cell that had no receptors compared to free carboplatin drug tested.

Chapter 3 describes the synthesis of targeted curcumin and platinum complexes using the LHRH sequence. Curcumin possesses hydroxide groups which can be readily alkylated under mild basic conditions. The assembly of the LHRH-curcumin peptide was by solid phase synthesis. Similarly the LHRH-malonate synthesis was achieved by solid phase synthesis followed by platination using solution phase synthesis to give LHRH-Pt. Biological studies on these structures are still ongoing.

Chapter 4 of this dissertation addresses the synthesis of small platinum complexes and their application as potential biological labeling probes. The presence of atfc groups on the carrier ligand introduces the fluorescence property in the ligand, which allows us to monitor and study the ligand interaction with DNA by spectroscopic techniques. The platinum complexes have desirable features for assessing the potential of tridentate platinum complexes for investigating selective monocoordination of metal complexes to DNA and to peptides.

APPENDIX A. ONGOING WORK AND FUTURE STUDIES

A.1 Synthesis of Targeted Phthalocyanines

Phthalocyanine and related compounds like porphyrins, have been the subject of intense interest due to their biological importance and their physical, chemical, and spectroscopic properties.[1] A phthalocyanine is a macrocyclic compound which absorbs light at high wavelength around 650-800 nm in comparison to porphyrin giving a bigger optical window necessary for photodynamic therapy (PDT) application. PDT involves combination of light and photosensitizer to affect biological outcome. The cytotoxic effect of PDT is caused by interaction of photosensitizer's excited states with endogenous oxygen in the target cell.[2, 3]

Although phthalocyanines are effective class of photosensitizers, they have been identified with major disadvantages that impact their effectiveness in PDT. An example is lack of cellular localization and cytotoxicity where the mechanism of their localization is still vague.[4]

Our overall goal is to target phthalocyanine PDT agents to tumor cells using CNGRC and LHRH sequence as described before in the earlier chapters

A.2 Results

Scheme A.1 show one of the proposed and attempted synthesis of CNGRC-Phythalocynine conjugate. The Pythalocynine on resin was synthesized by Sibel Edem. Addition of amino acids on the resin was achieved using solid phase chemistry and the linear CNGRC – phythalocynine conjugate was confirmed by mass spectra (Maldi) where M +H peak was 2290.37 calculated $C_{102}H_{138}N_{24}O_{29}S_2Zn$ 2291.88. Cyclization of the CNGRC –phythalocynine was not successful. Scheme A.2 shows ongoing synthesis of phthalocyanine with LHRH pentynoic acid. The LHRH-pentynoic was confirmed to have the expected M +H peak 1350.70 calculated for $C_{64}H_{90}N_{18}O_{15}$ 1350.68. The phthalocyanine in this scheme was synthesized by Mercy Mudyiwa.

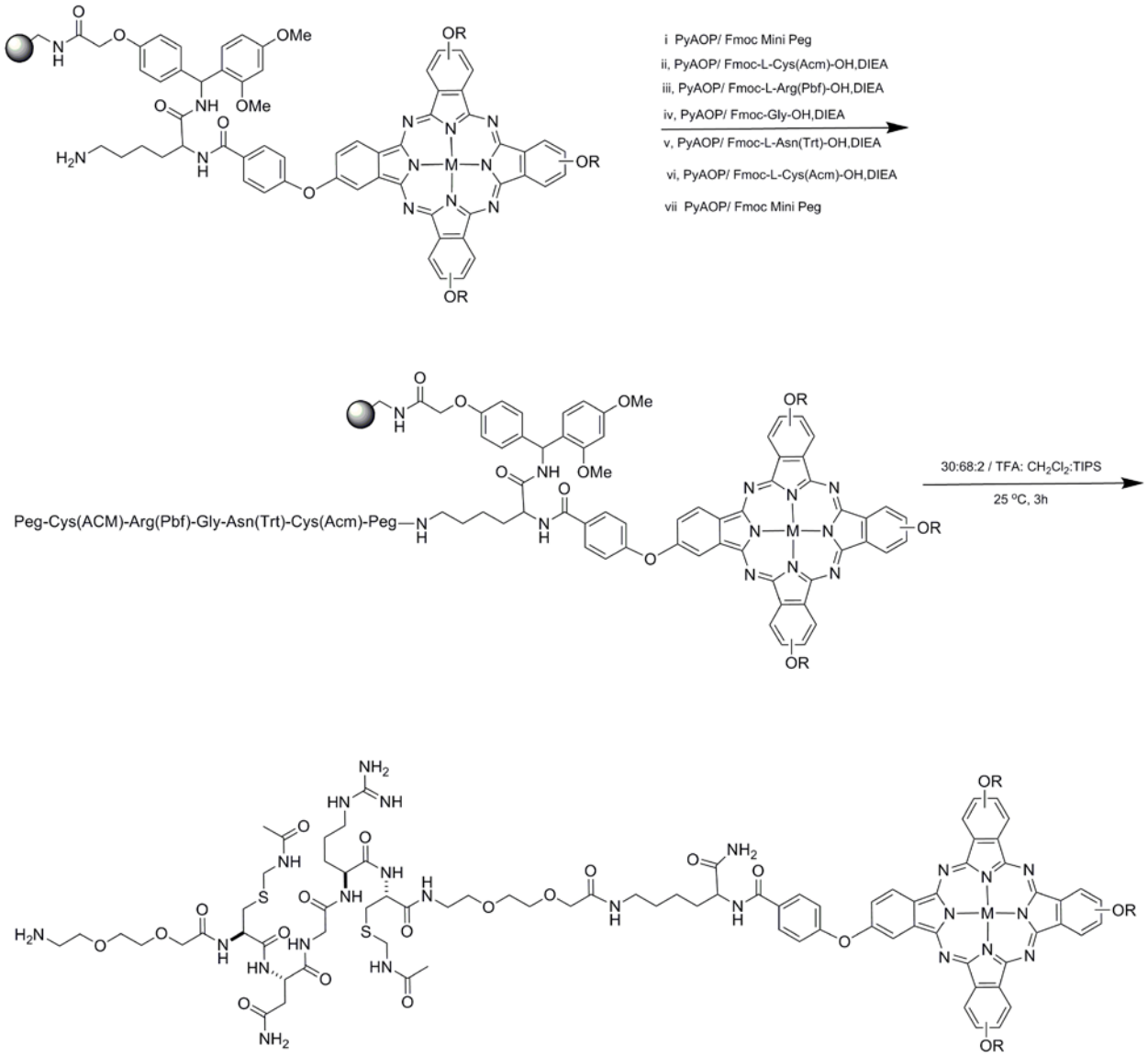

Scheme A.1. Synthesis of CNGRC-phthalocyanine (Conjugate 1) where R= $(CH_2CH_2O)_3CH_3$

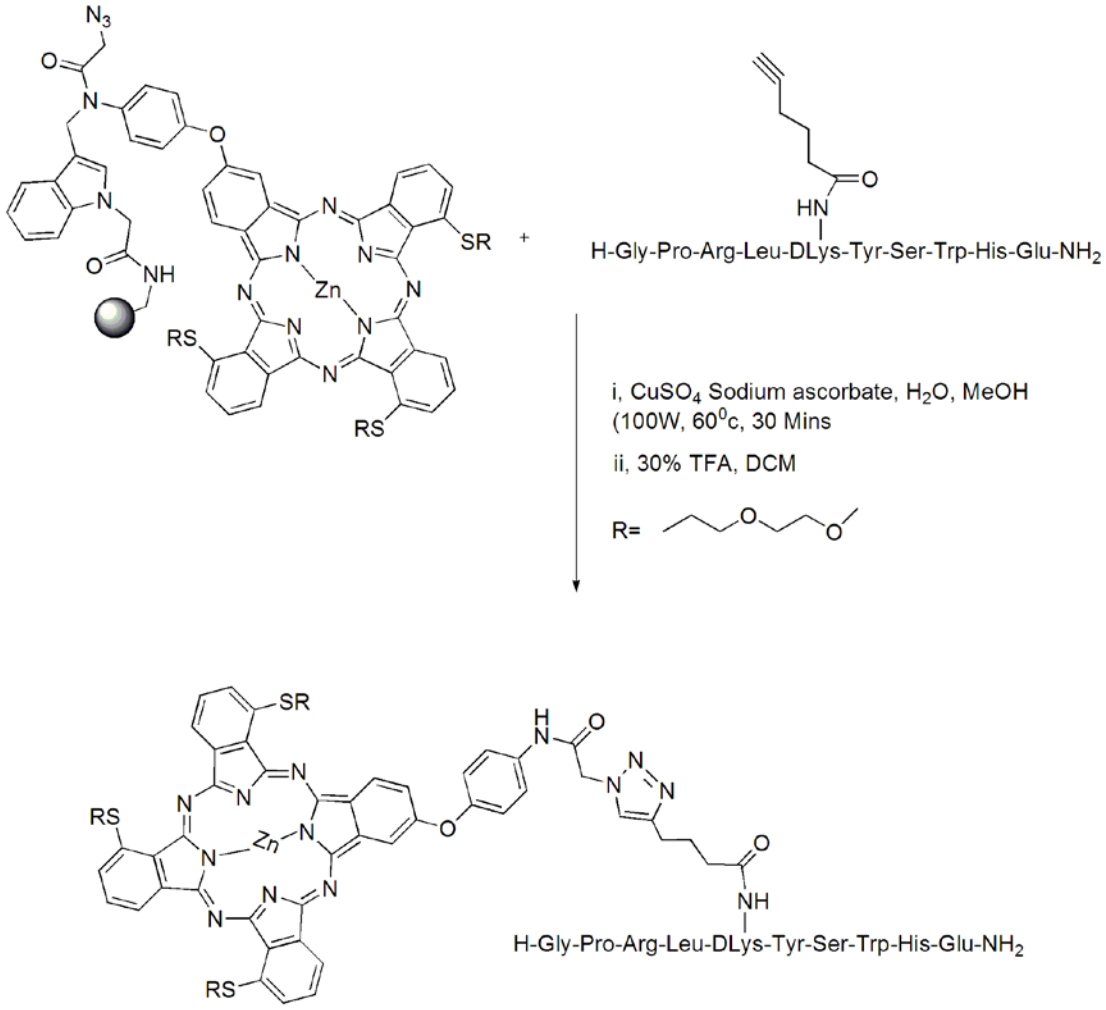

Scheme A.2. Synthesis of LHRH-phthalocyanine (Conjugate 2)

A.3 References

1. Taquet, J.-p.; Frochot, C.; Manneville, V.; Barberi-Heyob, M., Phthalocyanines covalently bound to biomolecules for a targeted photodynamic therapy. *Current Medicinal Chemistry* **2007,** *14* (15), 1673-1687.

2. Henderson, B. W.; Dougherty, T. J., How does photodynamic therapy work? *Photochemistry and Photobiology* **1992,** *55* (1), 145-57.

3. Dougherty, T. J.; Marcus, S. L., Photodynamic therapy. *European journal of cancer (Oxford, England : 1990)* **1992,** *28A* (10), 1734-42.

4. Sharman, W. M.; Allen, C. M.; van Lier, J. E., Photodynamic therapeutics: basic principles and clinical applications. *Drug Discovery Today* **1999,** *4* (11), 507-517.

APPENDIX B. SUPPLEMENTARY MATERIAL FOR CHAPTER 2

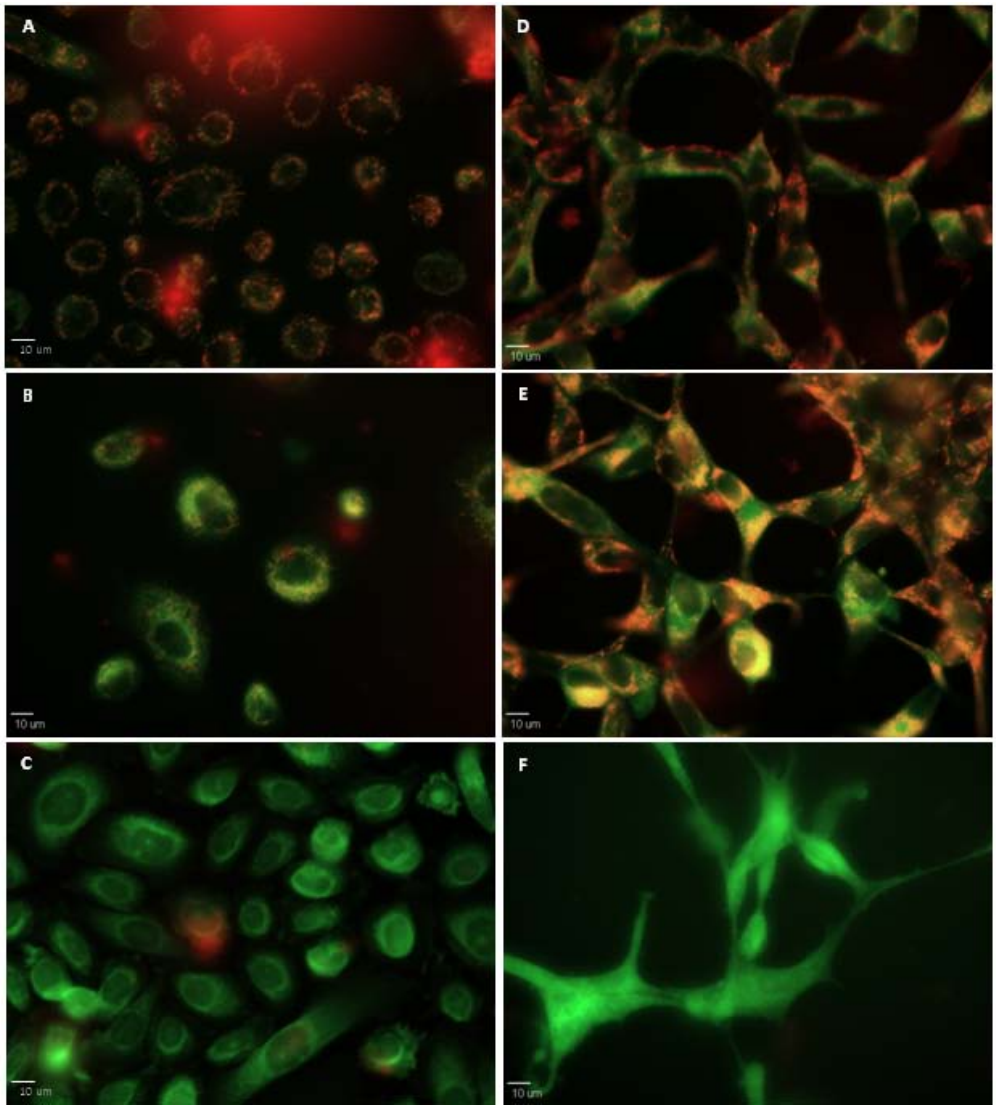

Figure B.1. Fluorescence microscopy of cells that have been treated with various compounds, incubated for 48 h at 37°C and then imaged by JC-1 staining after a further 30 min of incubation. Images **A** and **D;** PC-3 and LNcap cells, respectively, treated with RPMI media only. Images **B** and **E;** PC-3 and LNcap cells, respectively, treated with 200 μM of Pt-peptide conjugate **7** in RPMI media. Images **C** and **F;** PC-3 and LNcap cells, respectively, treated with 50% DMSO.

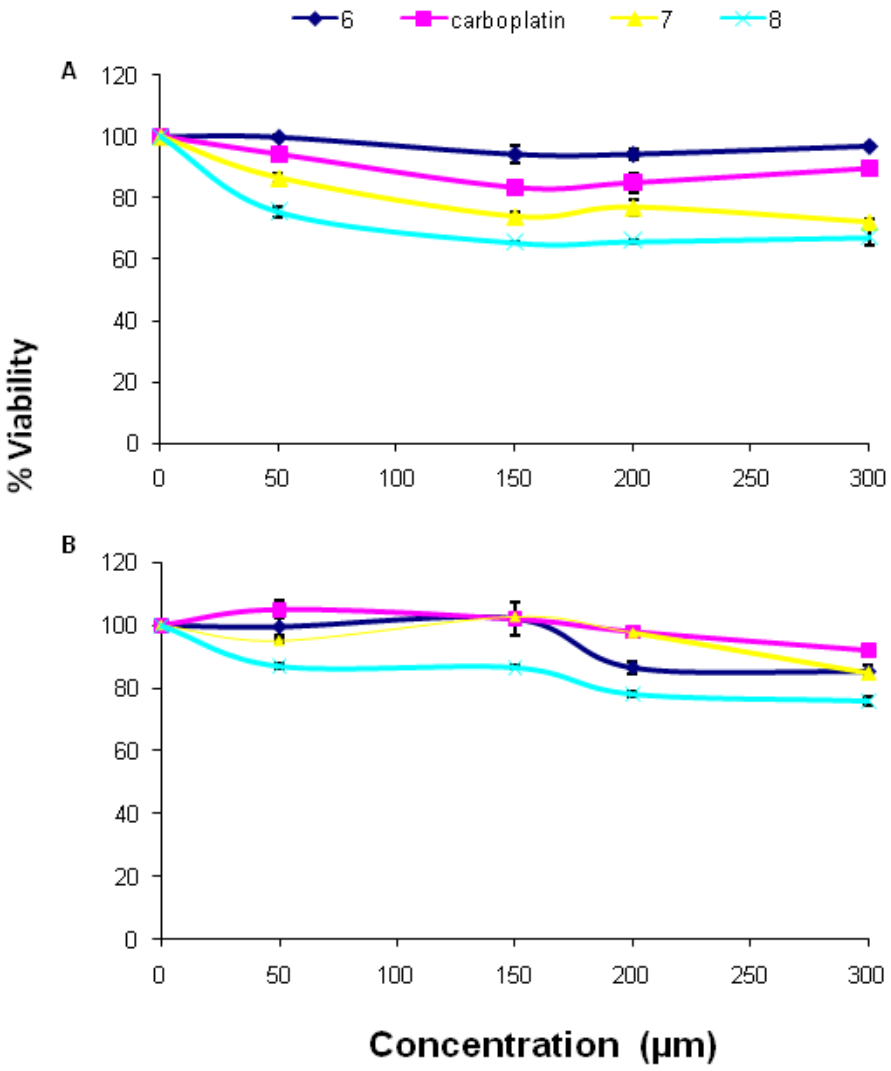

Figure B.2. The effect of carboplatin, cyclic mPeg-CNGRC-mal (**6** free peptide)**,** the mixture of carboplatin and mPeg-CNGRC **(9),** and the Pt-peptide conjugates; cyclic mPeg-CNGRC-Pt (**7**) and cyclic mPeg-CNGRC-Pten (**8**) on the proliferation of prostate cancer PC-3 (CD13 positive) cells and LNcap (CD13 negative) cells. (A) PC-3 cells and (B) LNcap cells were exposed to the compounds listed and incubated for 4 h followed by replacement of the drug medium with the regular cell growth medium and incubation for 48 h at different concentration.

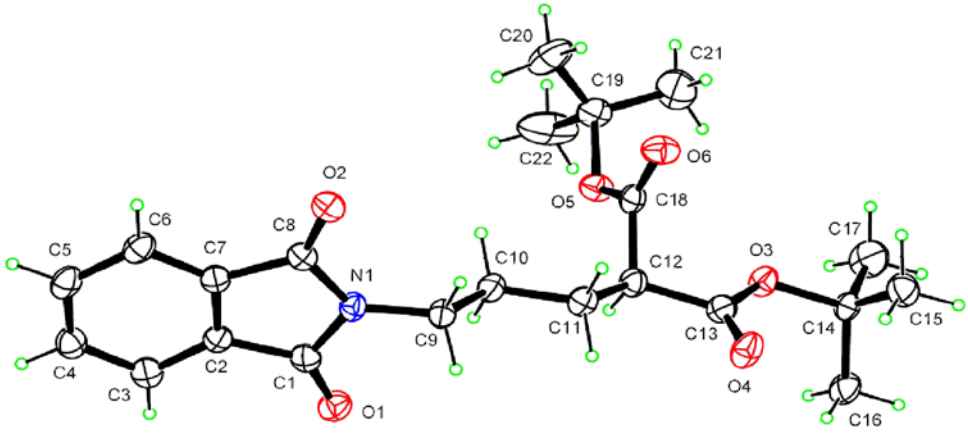

Figure B.3. The structure of di-tert-butyl 2-(3-phthalimidopropyl)malonate with 50% probability

Experimental

Crystal data

$C_{22}H_{29}NO_6$
$M_r = 403.46$
Orthorhombic
$Pca2_1$
$a = 16.373\ (6)$ Å
$b = 8.350\ (2)$ Å
$c = 31.743\ (10)$ Å
$V = 4340\ (2)$ Å^3
$Z = 8$
$D_x = 1.235$ Mg m^{-3}
D_m not measured

Mo $K\alpha$ radiation
$\lambda = 0.71073$ Å
Cell parameters from 4240 reflections
$\theta = 2.5–25.0°$
$\mu = 0.090$ mm^{-1}
$T = 110$ K
Plate
Colorless
0.35 × 0.30 × 0.05 mm
Crystal source: local laboratory

Data collection

KappaCCD (with Oxford Cryostream) diffractometer
ω scans with κ offsets
Absorption correction: none
18711 measured reflections
3880 independent reflections

3025 reflections with $I > 2\sigma(I)$
$R_{int} = 0.038$
$\theta_{max} = 25.0°$
$h = -19 \rightarrow 19$
$k = -9 \rightarrow 9$
$l = -37 \rightarrow 37$
intensity decay: <2%

Refinement

Refinement on F^2
$R[F^2 > 2\sigma(F^2)] = 0.044$
$wR(F^2) = 0.117$
$S = 1.027$
3880 reflections
523 parameters
H-atom parameters constrained

$w=1/[\sigma^2(F_o^2) + (0.0762P)^2]$
where $P = (F_o^2 + 2F_c^2)/3$
$(\Delta/\sigma)_{max} = 0.000$
$\Delta\rho_{max} = 0.34$ e Å^{-3}
$\Delta\rho_{min} = -0.18$ e Å^{-3}
Extinction correction: none
Scattering factors from *International Tables for Crystallography* (Vol. C)

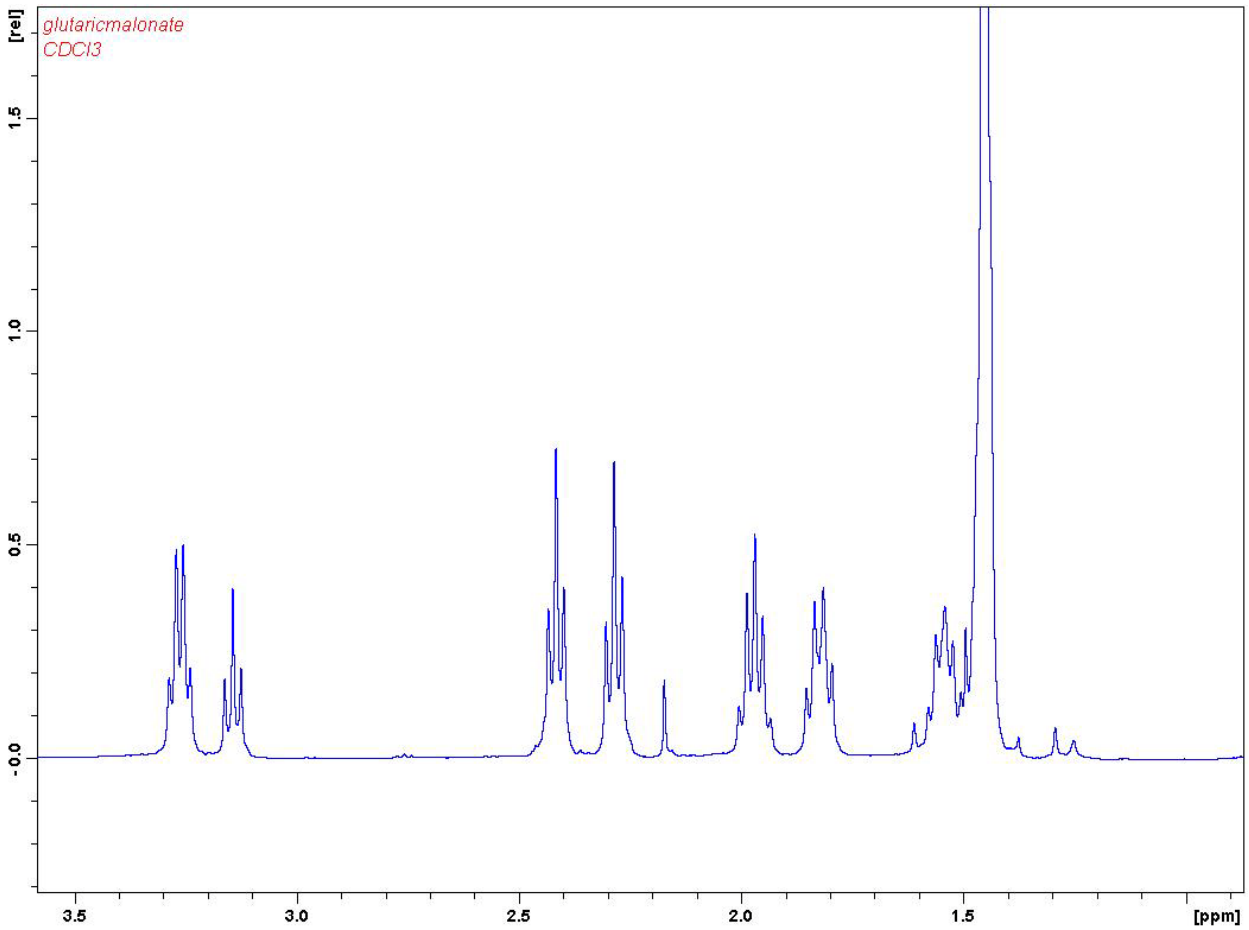

Figure B.4. 1H NMR of Di-tert-butyl 2-(3-glutaricaminopropyl)malonate (**5**).

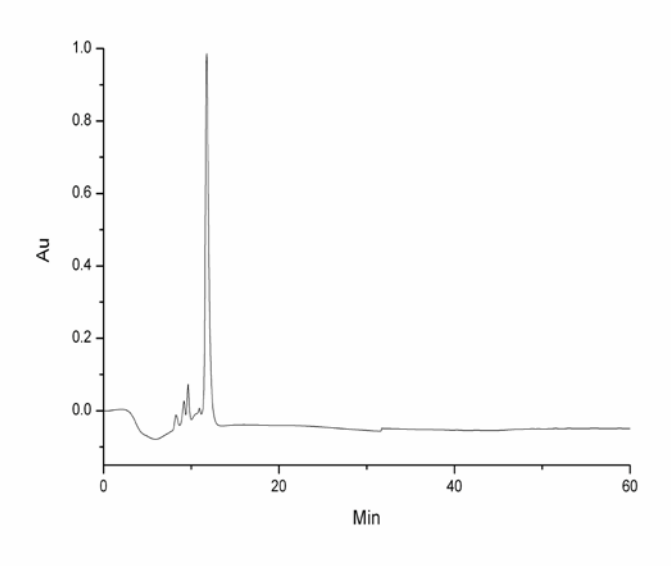

Figure B.5. HPLC chromatogram of linear CNGRC.

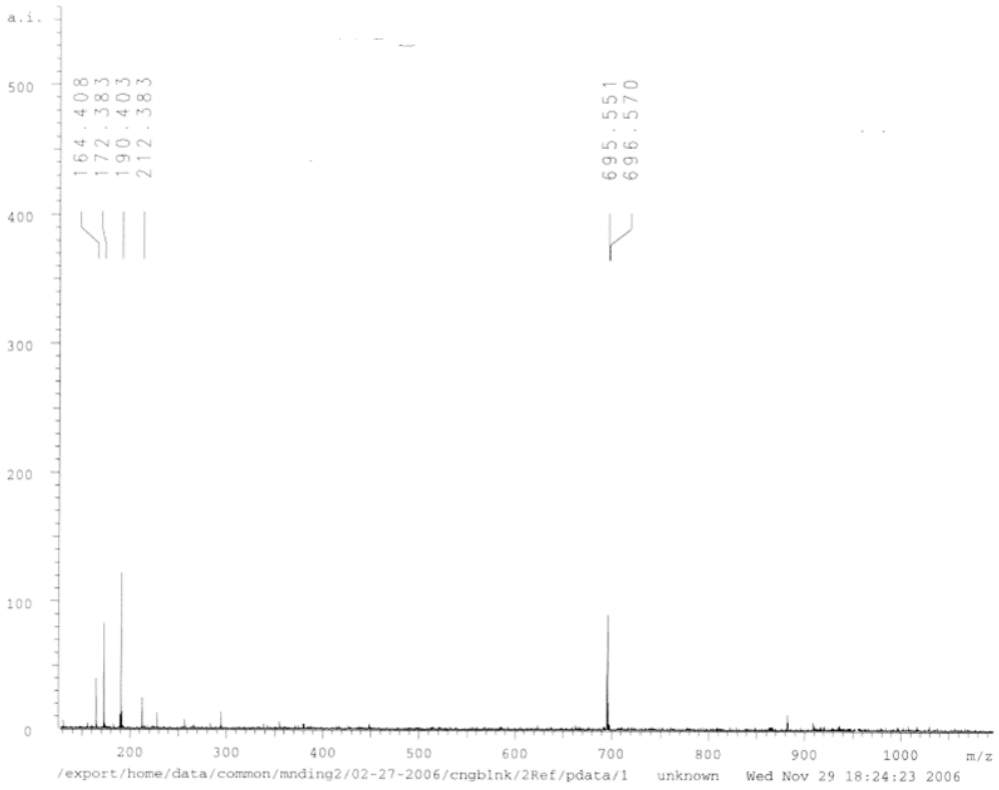

Figure B.6. Mass spectrum of linear CNGRC

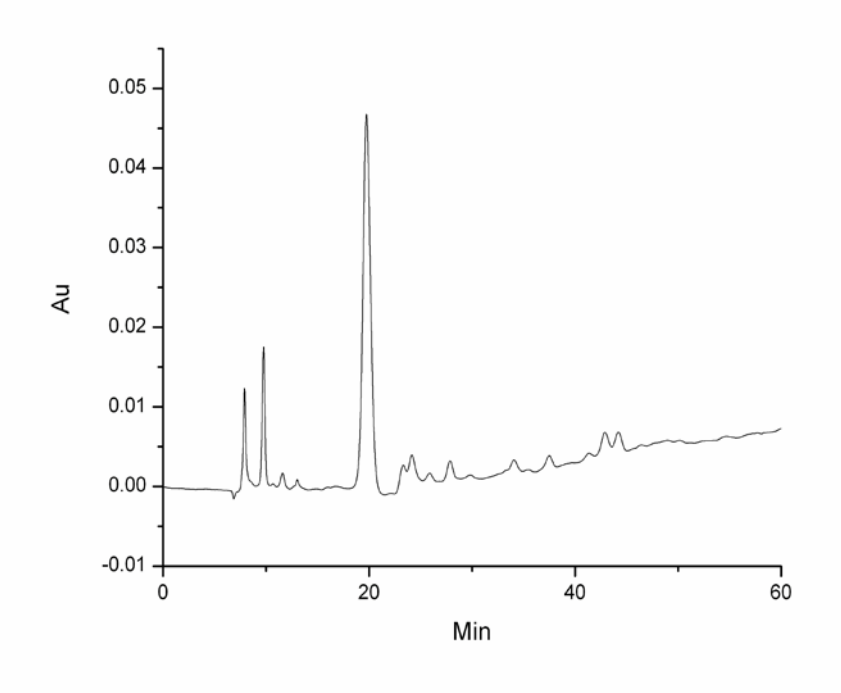

Figure B.7. HPLC chromatogram of cyclic CNGRC

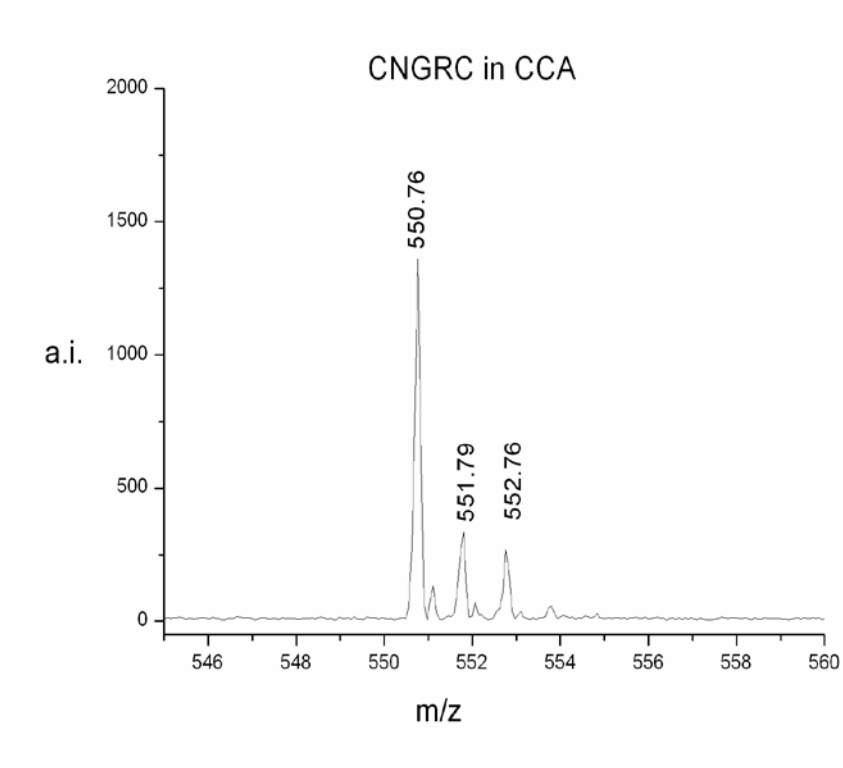

Figure B.8. Mass spectrum of cyclic CNGRC

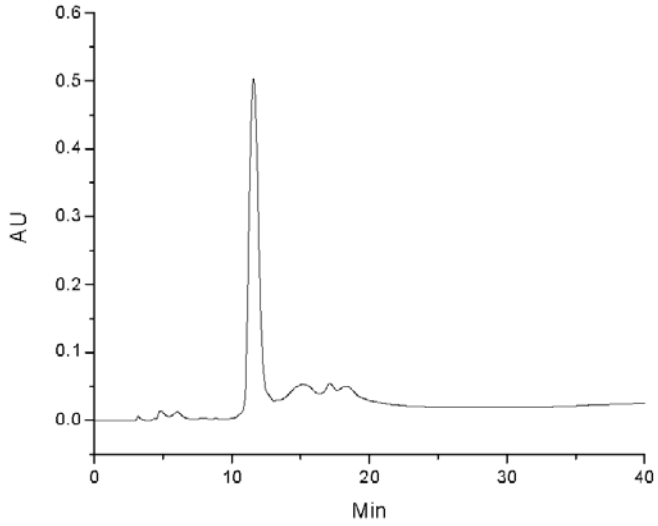

Figure B.9 HPLC chromatogram of conjugate **2** (Mal-Glut-CNGRC)

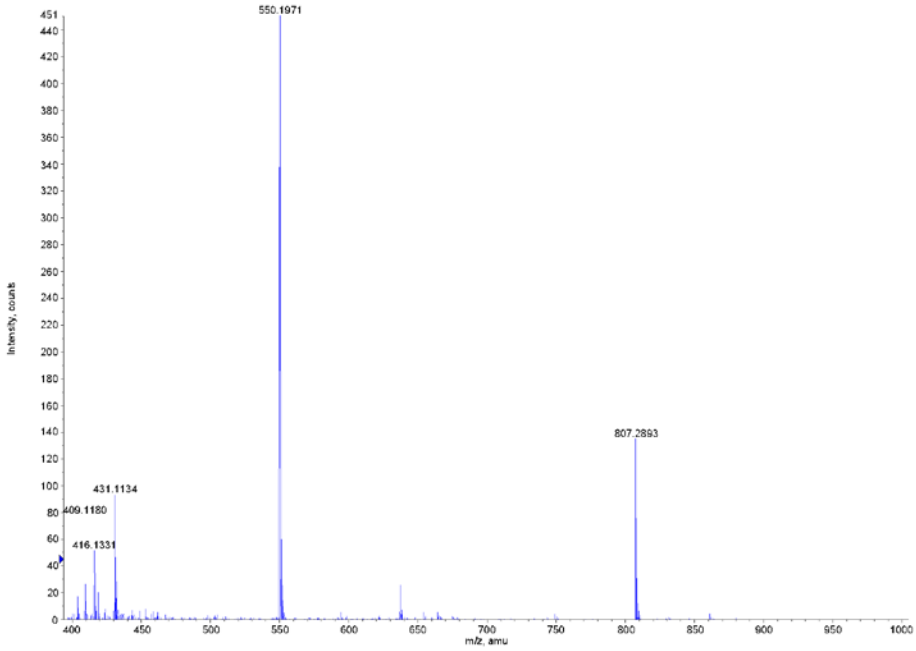

Figure B.10. Mass spectrum of conjugate **2** (Mal-Glut-CNGRC).

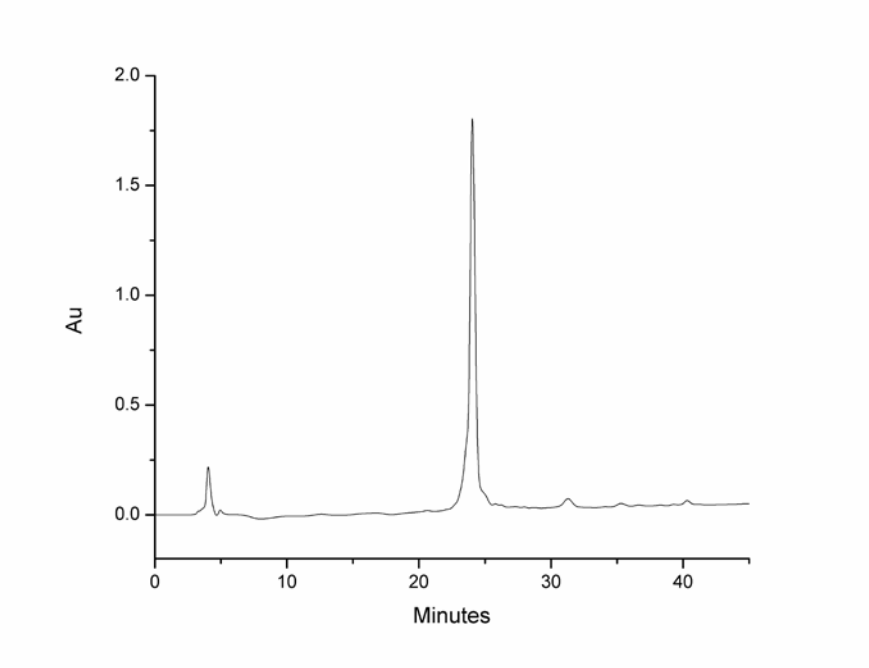

Figure B.11 HPLC chromatogram of linear mPeg-CNGRC-mal

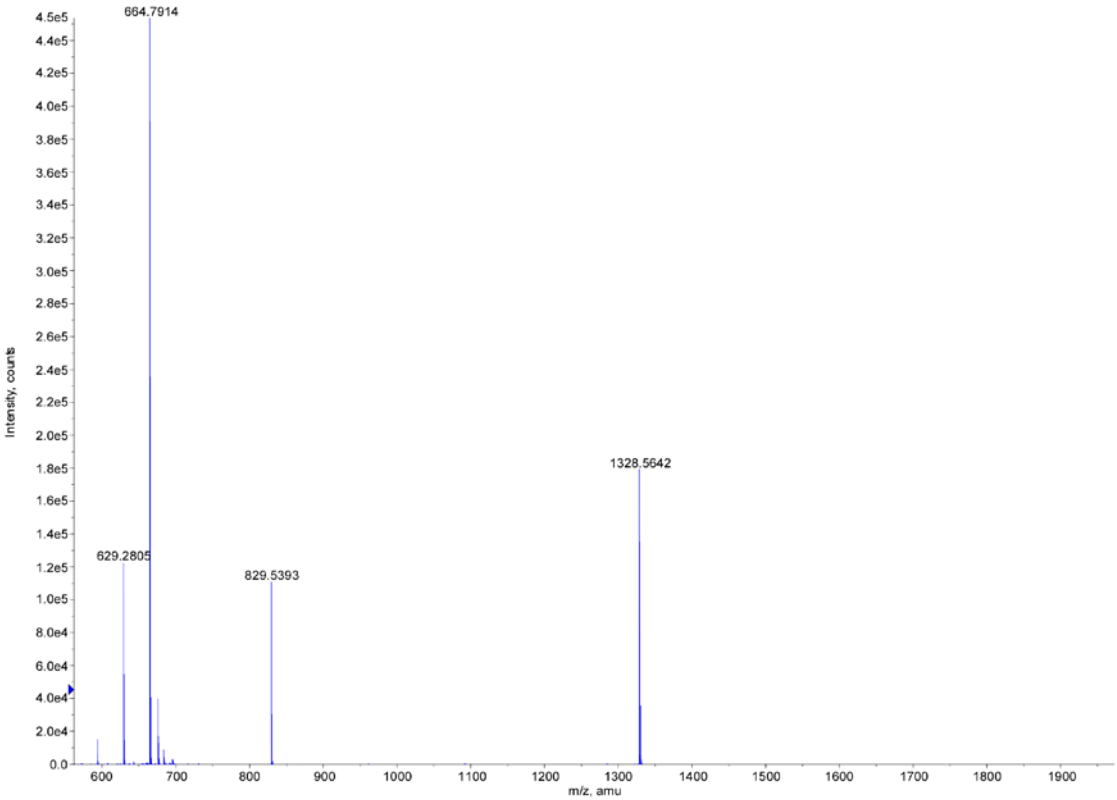

Figure B.12. Mass Spectra of linear CNGRC mPeg-CNGRC-mal

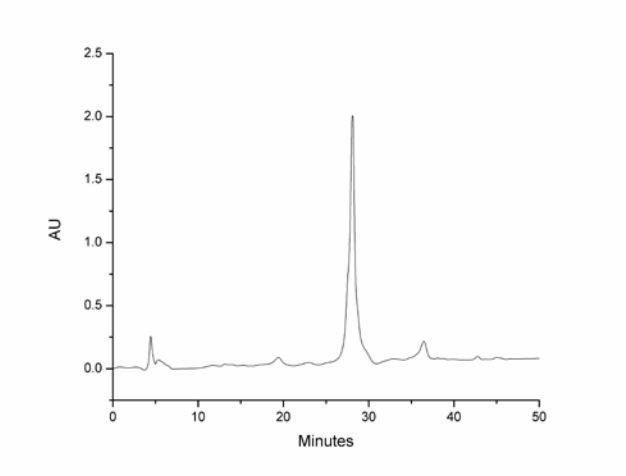

Figure B.13. HPLC chromatogram of conjugate **6** (cyclic mPeg-CNGRC-mal)

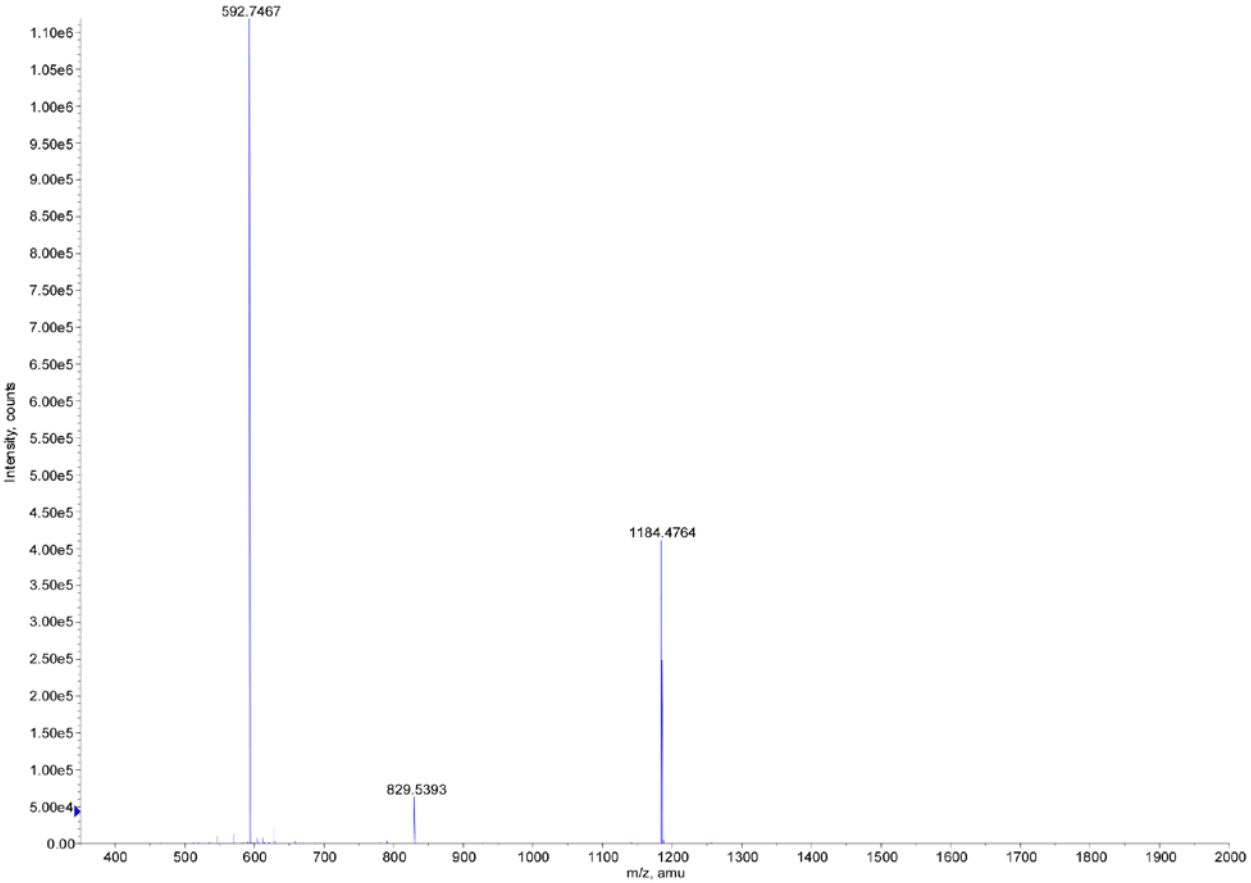

Figure B.14. Mass spectrum of conjugate **6** (cyclic mPeg-CNGRC-mal).

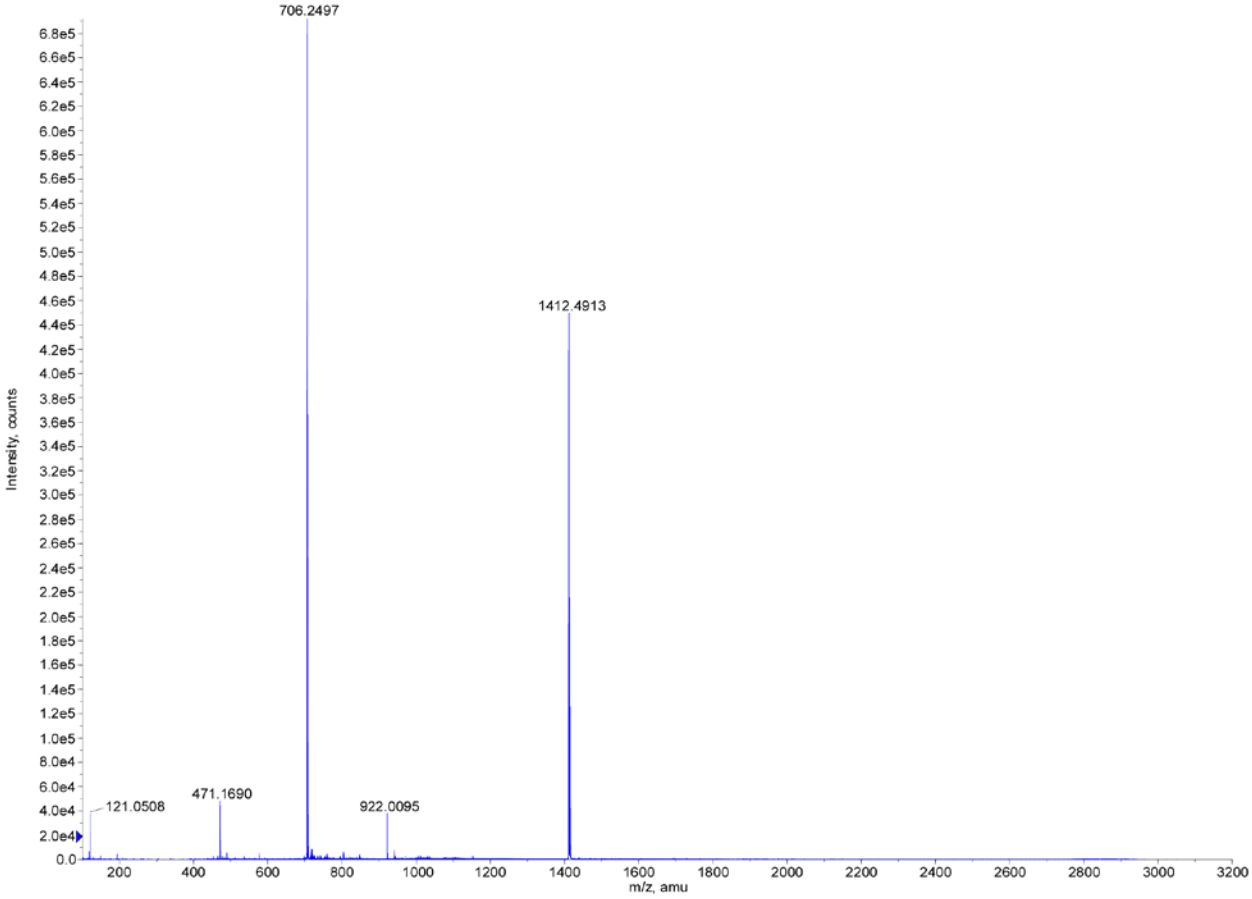

Figure B.15. Mass spectrum of conjugate **7** (cyclic mPeg-CNGRC-Pt).

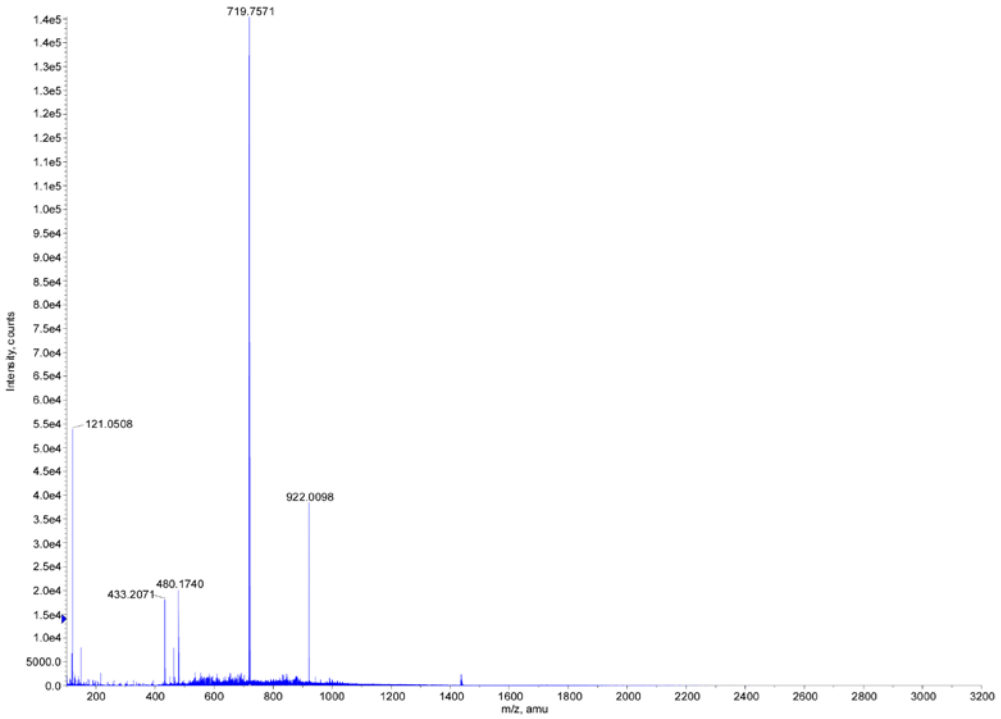

Figure B.16. Mass spectrum of conjugate **8** (cyclic mPeg-CNGRC-Pten).

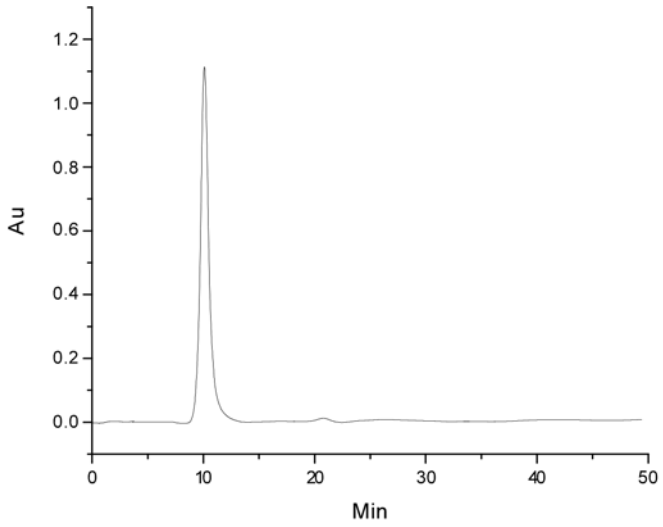

Figure B.17. HPLC chromatogram of free peptide **9** (cyclic mPeg-CNGRC)

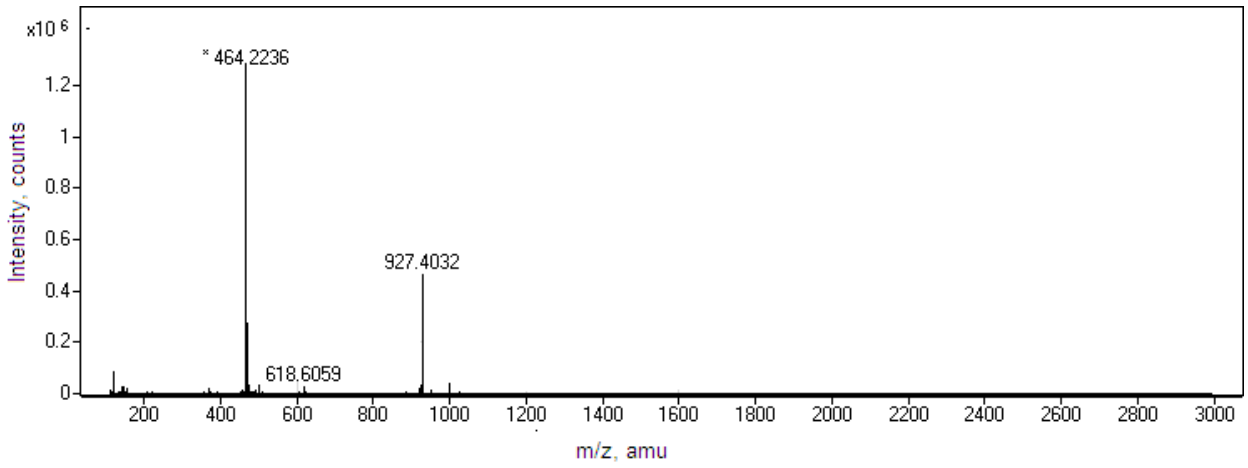

Figure B.18. Mass spectrum of cyclic mPeg-CNGRC (**9**).

VITA

Margaret Wambui Ndinguri was born in Nairobi, Kenya, and is a graduate of Senior Chief Koinage High School, Kiambu and Jomo Kenyatta University, Thika (2001), where she received her Bachelor of Sciences degree in chemistry. After working with Kenya Shell Ltd. for two years she enrolled in the doctoral program of chemistry at Louisiana State University (2003). She will receive her Doctor of Philosophy degree in chemistry during the Summer Commencement 2009.